THE EFFECTS OF MOVING CLOUD SHADOWS ON ELECTRIC

UTILITIES WITH DISPERSED SOLAR

PHOTOVOLTAIC GENERATION

By

WARD THOMAS JEWELL
II
Bachelor of Science in Electrical Engineering
Oklahoma State University
Stillwater, Oklahoma
1979

Master of Science
Michigan State University
East Lansing, Michigan
1980

Submitted to the Faculty of the Graduate College
of the Oklahoma State University
in partial fulfillment of the requirements
for the Degree of
DOCTOR OF PHILOSOPHY
December, 1986

THE EFFECTS OF MOVING CLOUD SHADOWS ON ELECTRIC

UTILITIES WITH DISPERSED SOLAR

PHOTOVOLTAIC GENERATION

Thesis Approved:

R. Ramakumar

—————————————————
Thesis Adviser

Wm. L. Hughes

—————————————————

R. W. Engelbrecht

—————————————————

Donald W Grace

—————————————————

Norman N. Durham

—————————————————
Dean of the Graduate College

ACKNOWLEDGMENTS

I express my sincere thanks to Dr. Ramachandra Ramakumar, my thesis adviser. He was, of course, instrumental in getting this project started, and in all phases of the work. I have learned immensely from my work with Dr. Ramakumar, about the technical subject, about research techniques, and also about life and the world in general.

I thank my committee members, Dr. Daniel Lingelbach, Dr. William Hughes, and Dr. Donald Grace, for their time, support, and suggestions throughout the project. Thanks also to Dr. Charles Bacon, who was Head of the Department of Electrical and Computer Engineering when I began my program, Paula Satterfield, the department's supervising secretary, and Dr. James Baker, who is now Head. They made possible my position on the electrical engineering faculty, and made my time at OSU easier in many ways.

iii

TABLE OF CONTENTS

LIST OF TABLES

LIST OF FIGURES

CHAPTER I

INTRODUCTION

Central-station solar photovoltaic (PV) generators have now been successfully supplying power to utilities for several years [1-5]. If the cost of PV systems continues to decrease, and their efficiency continues to increase [6, 7], individual utility customers may begin to install small residential PV systems in increasing numbers. Such a system could provide all or part of the owner's electric energy needs. A necessary part of a residential PV system is a backup energy system to provide energy when the sun is not shining.

Backup energy can be provided by energy storage, such as batteries, or by simply drawing energy from the electric utility grid when needed. Energy storage systems, however, are not expected to drop in price as rapidly as the rest of the PV system components [8]. Many residential PV systems will therefore be connected to the electric utility grid as allowed by the Public Utilities Regulatory Policies Act (PURPA) [9].

These small systems will be dispersed throughout the utility's service area, and most will be connected to the distribution system at 240 volts, the low voltage side of a residential step-down transformer. When a PV system is not supplying enough energy to meet the owner's

1

loads, the loads will draw energy from the utility. Similarly, the PV system will supply energy to the utility when it is generating more than the owner needs.

This work discusses in detail one aspect of the interaction between the utility and these small PV generators. When clouds move over a PV array, its power output is reduced. It resumes full production when the clouds move away. The utility must follow these changes with its own generation and energy imports just as it now follows the normal variations in customer loads.

To determine what the fluctuations in dispersed PV generation can be, and what PV penetrations might be noticeable by the utility, a computer simulation of PV systems dispersed throughout a service area was developed. It simulates actual cloud patterns and their effects on the output of each PV system located within the area. The PV generation is then aggregated as needed to estimate the effects on the utility. The effects of various weather patterns over service areas of several sizes were intially assessed. The worst weather patterns were then simulated over the Public Service Company of Oklahoma (PSO) service area and power flow studies were performed. The results of this study are presented.

This work begins with a literature survey of utility-interactive PV systems in Chapter I. Chapter II then describes the important differences between PV generation and conventional utility generators. Chapter III then describes the problem addressed in detail and presents

the approach used in this research. Modeling and simulation development are discussed in the next four chapters, insolation modeling in Chapter IV, distribution feeder modeling in Chapter V, and model verification in Chapter VI. The final simulation programs and their use is then outlined in Chapter VII. Chapter VIII contains the results of the project. Conclusions drawn from these results are presented and further work identified is described in Chapter IX.

<center>Literature Survey on Utility-Interactive

Photovoltaic Generation</center>

The photovoltaic effect, through which light is converted directly to electricity, was first observed by Edmond Becquerel in 1839. In 1954 a solar cell with efficiency of 6% was developed at Bell Laboratories, and these cells saw their first application on Vanguard I, a U.S. satellite launched in 1958. The Vanguard I cells were made by hand and cost over $1000 per watt [10]. In 1986 the cost of mass-produced cells has dropped to $4-5 per watt [6], and they are now economical for a number of terrestrial applications.

Until the mid-1970s there was very little talk of using photovoltaic (PV) generation outside the space program. However, with the rapidly rising cost of fossil fuels, as well as the increasing environmental concerns about their use, interest developed in terrestrial uses of PV. The first mention of grid-connected PV generation in the IEEE Transactions on Power Apparatus and Systems (IEEE-TPAS) came in 1974 [11]. This general discussion of possible utility use of PV cited rapidly accelerated fossil fuel costs, concern

over environmental quality, and U.S. Government support as reasons for considering PV. It predicted, however, that there would be no central-station solar power generators before the year 2000. Subsequent events have proved otherwise. Several such generators are operating in the U.S. and around the world in 1986 [1-6].

A design for a central-station solar thermal generator was published in 1975 [12]. Concentrated sunlight heats boilers to produce steam, which then powers a conventional steam turbine/rotating generator unit. Although there was no mention of PV in this paper, it did, along with another paper out of Oklahoma State University [13], confirm the prospects for large-scale use of solar energy. National Science Foundation interest was also formally discussed in 1975 [14], and at the University of Delaware an experimental residential application of PV was documented [15].

The University of Delaware "Solar One" home had a very small array of PV cells that were used to study the correlation of solar energy with typical daily residential electrical loads. Energy from the PV array was used to charge batteries that supplied energy to dc loads within the home. When battery charge levels dropped too low, or when the PV generation was not sufficient, a transfer switch allowed charging by the electric utility. While this was not a true utility-interactive PV application, it seems to be the first major experimental study of the interaction between PV generation and an electric utility.

Battery charging was again the topic in a 1976 paper [16] discussing battery charge controllers. PV technology was covered in detail for an electric utility audience in an IEEE tutorial that same year [17]. Neither of these, however, mentioned the possibility of utility-interactive PV operation.

Utility-interactive operation was first described in IEEE-TPAS in 1978 [18]. The authors discussed PV and solar thermal generation in both utility-interactive and stand-alone applications, but even the utility-interactive systems still included some energy storage. The analysis was mainly economic, and did not discuss possible technical problems of the utility interconnection.

Another economic analysis was also published in 1978 [19]. Simple designs and economic analyses of several utility-interactive solar energy systems, including residential, intermediate, and central-station PV, were included. Interconnection problems were not discussed, although the authors did recognize that "in the case of utility connection, issues relating to the customer/utility interface such as rate structure, ownership, energy feedback to the utility, and safety and control require further definition [19]." This further definition began in a reliability assessment that looked at the load carrying capability of PV [20], and how the utility might see PV generation in terms of its conventional generators.

Discussion of interconnection issues continued in a detailed 1979 assessment of using PV generation to reduce utility peak generation needs [21]. The system studied, however, was not a true

utility-interactive system. The authors envisioned battery energy storage and a transfer switch to the utility, so no PV power actually flowed to the utility. It was, however, a useful discussion of correlation between utility and PV peaks. It also recognized the "trade-off between maximizing efficiency of the dc array for the user and minimizing the generation capacity requirements of the utility [21]," an early indication of the impending debate over "avoided cost." The fact that some terrestrial remote-power applications of PV were then economical was pointed out in another 1979 paper [22], and an overall strategy of solar energy development was outlined [23].

Details of interconnection issues began to come out at the 1980 PV Specialists Conference [24]. The general concerns of personnel safety, equipment and utility system protection, and power quality were discussed. One specific problem mentioned was the possibility of distribution transformer overloads caused by residential PV generation.

In the early 1980s the interconnection of PVs to the electric utility began to receive a great amount of attention. The debate over buy/sell rates and avoided cost grew. A detailed production cost model of an electric utility with intermittent dispersed generation was used to "calculate the rates for buying and selling power so that ... neither the utility or any customer gains or loses with the inclusion of distributed generators" [25]. This study contributed greatly to the knowledge of the utility effects of uncontrolled, intermittent generation. It did not address the effects of short-term,

minute-to-minute power changes of such generation. It used a probabalistic model for PV availability and implicitly assumed that the swings in PV generation would be no greater than normal load changes.

Another study addressed the issues of load reduction, harmonic distortion, and protection coordination with dispersed PV generation [26]. In another, the authors performed power flow studies on utility systems with simulted dispersed generation and concluded [27]:

1. Power generated by dispersed PV generation may overload distribution equipment and lines under light load conditions.

2. PV energy may interfere with voltage regulators and load tap changers under light load conditions.

3. Reactive power consumed by line-commutated PV system inverters increases as voltage decreases. This reactive power will reduce the capacity of the distribution lines.

4. Residential PV systems may cause unbalanced conditions on three-phase systems.

5. PV generation may interfere with fault clearing.

6. Personnel safety problems may arise from dispersed PV generation.

The short-term changes in dispersed generation, such as those caused by cloud shadows moving over PV systems, and the resulting utility load following and spinning reserve requirements were first addressed in a 1981 paper by S.T. Lee and Z.A. Yamayee [28]. In this

paper the authors provided a detailed model for calculating the load following and spinning reserve requirements of a utility with intermittent generation. This established a framework for calculating production costs once the data on dispersed generation power changes are available. However, the authors noted that "the lack of data on short-term variation of the intermittent resources and their spatial diversity is especially notable [28]." This lack of data still exists today, and is specifically addressed in this work.

Load following and spinning reserve were also addressed in two other papers [29,30], although neither included any quantitative analysis. Both confirmed, however, that these costs would be important to a utility with dispersed PV generation.

In 1982 the intermittent, unpredictable nature of PV and other dispersed generation was again recognized, but this time in a long-term sense. Three papers discussed such "non-dispatchable" generation as decision variables in generation expansion models [31], general utility planning models [32], and distribution planning models [33]. Standards development began with a list of functional dispersed storage and generation requirements for effective utility integration [34]:

Control and Monitoring

Power Flow and Quality

Communications and Data Handling

Operations: Normal, Abnormal, Emergency

Failure Detection and Correction

Special Control Functions

Under the power quality heading, an experimental study of harmonic distortion and reactive power consumption by line commutated PV inverters was published [35]. The author concluded that the one isolated inverter studied would not have noticeable effects on the utility. The effects noted, however, were significant enough to suggest further study of high penetrations of such inverters. But at the same time new inverter designs were becoming available that had none of the power quality problems of the line commutated inverter [36].

Power quality of a line commutated inverter was studied further in a computer simulation of an inverter connected to a distribution feeder [37]. The results correlated well with the previous experimental results [35]. The power quality effects of high penetrations of line commutated inverters were then simulated [38]. A proposed subdivision with close to 100% penetration of residential PV systems was studied. The results indicated that if the PV designers and the utility were careful to avoid harmonic amplification, there should be no significant harmonic distortion or reactive power problems for this subdivision.

Utility interest in central-station PV generation was growing and two conceptual designs were published. The first of these was to use thin-film amorphous silicon cells [39], which have only recently become commercially available. The other used conventional cells and concentrated on the balance-of-system costs, such as site purchase and preparation, installation, and utility interface equipment [40].

PV reliability was the focus of two other studies published in 1983. In one, hourly insolation data were used to determine how much PV capacity is needed to replace one kW of conventional capacity [41]. This study implicitly includes all interface and other costs in the PV capital cost. There is no discussion of the technical effects or their costs. A combined PV-hydroelectric system with energy storage was the subject of the other reliability study. The conclusion here was that very small generation reserves are needed with such a system. The short-term PV power changes, however, were not considered in reaching this conclusion [42].

Research into reducing the cost of PV power conditioners resulted in the design of a conditioner that needs no isolation transformer [43]. Such a transformer has been necessary for grounding and protection, and is a significant part of the cost and weight of the utility interface equipment.

The line commutated inverter continued to receive attention. Harmonic distortion and reactive power consumption were addressed in three studies [44-46]. These power quality issues, however, were shown to be "completely alleviated with self-commutated high frequency switching converters [47]" that are now commercially available. In addition, these new inverters were shown to provide "appropriate response to utility disconnects and faults." Voltage flicker caused by sudden changes in PV generation due to moving clouds was ruled out in this study. The changes were said to be too gradual to cause such

visible changes in voltage. The authors did not address the effects of such changes on utility power flows or system protection.

This optimism over technical issues continued into 1985 with the publication of performance data from the 1 MW central-station PV generator located on the Southern California Edison Co. Lugo Substation in Hesperia, California [3]. The plant was termed "reliable," with capacity factors ranging from 12% in a "very overcast" January 1983 to 37% in July 1983. Low operation and maintenance costs and no water usage contributed to the conclusion that the limits to future PV use would be strictly economic, and not technical.

This same conclusion was echoed in a panel discussion [7] that concluded reduced PV module cost would be the key to increased use of PV. The panelists also agreed that increased module efficiency is also necessary to allow lower balance-of-system costs. A description of the Tennessee Valley Authority's PV projects confirmed these conclusions by focusing exclusively on economics, with little mention of technical issues [48].

The issue of short-term changes in PV generation caused by moving clouds, however, arose again in a study of central-station PV generation [49]. The authors looked at the possible changes, caused by moving cloud shadows, in the output of a central-station PV generator. An automatic generation control (AGC) simulation was then used to find PV penetrations and weather conditions that would cause area control error (ACE) in excess of National Electric Reliability Council (NERC) guidelines.

General conclusions of this study were:

* "As PV penetrations exceed the range of 5% or greater of the system load, the conventional generation has difficulty in tracking rapid PV changes."

* "When PV generation changes are made there is a possibility that NERC guidelines will be exceeded temporarily."

* "A utility that has an uncontolled large PV plant may wish to make accommodations in the dispatch of regulating units to assure adequate positive and negative regulating margins, distributions, and rates."

* "The system operator would benefit by having metered information from concentrated PV generators as well as good forecasts of cloud location, type, and movement."

The literature seems to indicate that these problems, which are caused by the unpredictable changes in PV generation as cloud shadows pass over the arrays, may be the only remaining technical limitations to large-scale use of utility-interactive PV generation. These are addressed in detail in the following chapters of this work.

CHAPTER II

EFFECTS OF SMALL UTILITY-INTERACTIVE

PHOTOVOLTAIC SYSTEMS ON A UTILITY

Small dispersed PV generators represent a significant change in the way electric utility systems have operated in the past. This chapter discusses the major differences between PV and conventional utility generation and the relevance of these differences to the utility.

Dispersed Generation

Conventional central-station generation feeds very large amounts of power, up to 2000 MW or more at a single point, to a few points on the high voltage transmission system. Residential PV systems, in contrast, feed relatively small amounts of power, for example 5 to 10 kW at one interconnection point, to many points on the low-voltage distribution system.

Operating a utility that receives a significant part of its energy from residential PV systems will be quite different from operating one with only central-station generation. The interactions of many small generators on the distribution system with the rest of the utility system will be quite different from that of a few large generators.

Interactions among the many dispersed generators must also be considered.

Power flows throughout the system will certainly change. Because the power flows change, existing system protection practices may no longer be appropriate [50]. Personnel safety procedures may have to change because it will be much more difficult to guarantee that a line is dead before servicing. While these issues have been addressed in proposed standards [51,52] for low penetrations, any problems will be multiplied for high penetrations, and the solutions for low penetration may not be practical, sufficient, or appropriate.

Inertialess Generation

The second difference between PV and rotating generators is in the type of generation. Utilities have almost exclusively used rotating generators to supply electric energy to the utility grid. These rotating machines have mechanical inertia, which allows the utility system to continue operating through changes in load and other disturbances. The energy stored in the rotating generator mass provides instantaneous response to the continuous changes in load connected to the system. When additional load is connected the needed energy comes from the generator inertia until the generator controls can adjust to the new load. The system frequency decreases slightly. Similarly, when system load decreases, the excess energy is absorbed by the generator mass, increasing its speed and the system frequency. This ability to adjust to continuous load changes is an inherent characteristic of rotating generators.

Electronic power converters, which convert the dc output of a PV array to ac, have no moving parts and thus no inertia. They cannot contribute to the support of continuous load changes in the way rotating generators do [53], or help compensate for the loss of another PV system. The response of an electronic converter, if any, to changes in the utility system, will depend on how the converter is controlled.

Electronic converters, however, are highly controllable. A converter's power output can be adjusted almost instantaneously. Thus, for example, a PV converter might be controlled to reduce power output when utility frequency increases, and to increase output when frequency decreases. PV generation can also be reduced to zero within a few cycles of a major loss of load on the utility. Power might also be modulated rapidly during transients to improve stability. Proper control may therefore overcome the problems caused by inertialess generation.

Economics, however, may limit the available control methods for dispersed PV systems. Economics of residential PV systems are usually evaluated assuming that all possible PV power is output at all times [10]. If converter controls force the PV system to operate at less than full possible output, the PV economics will be degraded.

Other philosophical issues may also influence the control question. Customer resistance to utility control of their systems must be weighed against the utility's need and desire for control. The

importance of proper maintenance must also be considered. It may be simpler, albeit more costly, for the utility to adjust its system, for example by increasing spinning reserves, to account for the inertialess generation. These issues must all be considered when choosing a control method.

Variable Generation

Possibly the most important difference between PV and conventional generation is the uncontrollability and variability of the PV generation power output. Present utility practices assume controllable and extremely reliable generation. PV generation, however, can vary continuously, and may be very difficult to predict days, hours, and even minutes in advance [53].

This variability results from the variable nature of sunshine. First, of course, the sun will shine only during a certain number of daylight hours, which are entirely predictable. Second, however, during those potential daylight hours, the sun may or may not shine because of cloud cover. Clouds may entirely block the sun, or may only reduce the available sunlight. Partial cloud cover moving across the sky will cause the sunlight, and therefore the PV generation, to vary continually.

The lack of PV generation on cloudy days may affect utility economics. Maintaining capacity to use only on cloudy days could be very costly. The minute-to-minute power variations caused by broken,

moving clouds can have a variety of effects on the utility. Mentioned earlier was the need for the utility to follow the changes in PV generation with its own generation, as it now follows changes in loads. Large swings in PV generation may force changes in existing operating procedures [54,55].

Because the PV output can disappear abruptly at any time, transient and dynamic stability may be degraded. Sufficient spinning reserve and load shedding capability must be available to offset the loss of PV generation. Voltage control becomes more difficult when power flows swing wildly. System protection can also be affected. Various utility system controls, including Automatic Load Frequency Control (ALFC, or Automatic Generation Control, AGC) and tie line power flow controls may not function well. The magnitude of these effects will depend on how much PV generation is operating on a utility system, and how much it can change over time.

Consequences for the Electric Utility

Much work has been done to determine the effects of utility-interactive PV generation on a utility [32,33,38,50,56,57]. A preliminary standard for connecting residential PV systems to the utility grid has been issued by the Institute of Electrical and Electronics Engineers (IEEE) [51]. Public Service Company of Oklahoma (PSO) has also proposed standards for small PV interconnection [52]. The purpose of these standards is to protect both the customers and the utility, and to minimize the effects of interconnected PV systems on the utilities.

These standards address the performance of the dc-to-ac power converter used to connect the dc PV modules to the ac utility system. Rules about the quality of the converter output waveform, the amount of reactive power the converter can consume, and the protection and safety functions it will have are examples of the issues addressed. Inverters are available now that can meet all the requirements [36], so the standards are intended to guarantee compatibility with the utility systems, and not to limit the use of residential PV systems.

These existing standards, however, may be sufficient only for a small number of dispersed PV systems, or for a low "penetration" of PV connected to the utility. "Penetration" is the ratio of PV capacity to the total generating capacity on the utility system. A low penetration of residential PV systems, with each meeting the proposed standard, should have insignificant effects on the utility. As the penetration increases, however, any detrimental effects of PV generation will also increase. At some point, these effects will have significant operational or economic consequences to the utility.

Two different definitions of penetration are important in discussing at what penetration the problems discussed above may occur. "Installed penetration" is the ratio of installed PV capacity to total installed generating capacity on a utility system. Installed penetration changes only when new conventional or PV generation is installed or when generation is removed from service. "Operating

penetration" is the ratio of installed PV capacity to total capacity in operation at a specific time. This therefore changes continuously as load and insolation change. Also note that because the utility's load is usually much lower in spring and fall than in summer, the operating penetration of PV generation will be much higher in the spring and fall.

At the penetration where PV generation becomes significant, the PV systems can no longer be thought of as small, individual generators. Instead, their combined effects must be considered. This is particularly important on those partly cloudy days when broken, moving clouds cause the output of each PV system to vary unpredictably over time. Following the power fluctuations of a few small PV generators is equivalent to normal load following, and will be unnoticed by the utility. As the number of small PV generators increases, however, the fluctuations in power become more significant. At some penetration they will exceed the normal load fluctuations and the utility will then have to consider their effects. The effects may appear in several ways. Larger than normal variations in generation or in tie line flows into an area may be seen. The utility may also experience unusual power flows throughout its system as PV generation changes. Over-and undervoltages and currents may occur, and control and protection equipment may malfunction.

A utility should look at the possible technical and economic consequences of fluctuating PV generation. It might be possible to have swings in PV generation so large that the utility simply cannot follow them, causing loss of service to some loads. Before this occurs,

however, the utility will most likely notice the economic effects of the power fluctuations. Increased generation ramping and changes in tie line and other power flows can all increase operating costs for the utility.

These effects would be the worst if all PV generation in a service area were lost simultaneously. The utility would then need to have spinning reserves equal to the total PV capacity. Fortunately, this does not occur because of the diversity that arises from the geographical separation of the small PV systems. A cloud that reduces the insolation on one PV system will affect one at a different location at another time or not at all. The fluctuations a utility should consider will therefore be only that fraction of the PV generation that can be lost or added in a given time.

CHAPTER III

STUDY METHODOLOGY

To determine what fluctuations moving cloud shadows can cause in dispersed PV generation and how PV systems dispersed throughout a large geographical area interact, time-varying incident solar radiation (insolation) data at many points within that area are needed. A source for such data was not found during this study. To provide this information a physically-based computer simulation of insolation over a large geographical area was developed. The simulation accounts for day of the year, time of day, location, and moving clouds. It simulates actual cloud patterns and their effects on the output of each PV system located within the area.

Interaction of Dispersed PV Systems

This simulation was initially used to study two factors that influence the cumulative effects of dispersed PV systems within an area. First, as the area increases more PV systems can be located within it, and the PV capacity that can be lost or added becomes greater. Mitigating this, however, is the fact that the geographical diversity increases as the size of the area increases; in other words, a PV system's output will correlate much better with one that is a few meters

away than with one a few kilometers away. One isolated PV system can be lost entirely as clouds move over, but because one system represents such a small penetration on the utility grid, its loss will not be noticed. As more systems are added, the penetration increases, but because of the physical distance between them, they cannot all be lost or regained at once.

For a given geographical area, then, only a certain percentage of the PV generation within that area can be lost or added during a certain period. To provide an estimate of these values, five service areas of size ranging from 10 to 100,000 square kilometers, all square in shape, were simulated. PV systems were uniformly dispersed throughout the areas and cloud patterns were passed overhead. The outputs of the PV systems were summed and recorded. This resulted in estimates, presented in Chapter VIII, of the possible changes in PV generation for a service area of a given size.

Effects on the Electric Utility

Once the possible changes in PV generation were known, the effects of these changes on the electric utility were studied. One of the main tools of utility system analysis, the power flow (load flow) program, was used for this. The power flow study begins with models of the utility's generation, transmission, and distribution systems and load and generator data. Loads are estimated from historical load data and forecasts of future load. The utility's own generation and energy purchases from other utilities are set to meet the load demand in the

most economical way. The output of the power flow program estimates voltages, currents, and real and reactive power flows at various locations throughout the utility system.

For steady-state analysis the power flow program is run once, with the input and output data corresponding to one instant. For analyses of slowly-varying system parameters over time the program can be run repeatedly, with the appropriate changes made to the system model for each time increment. The results then describe changes in the system over the period of the simulation. Such a time-varying power flow study was used in this study.

Power flow studies, however, assume that all generators are controlled by the utility. Small dispersed PV generators, however, are not within the utility's control. Their outputs will be determined primarily by the amount of solar radiation (insolation) falling on the PV arrays at any time. To estimate these outputs for power flow studies, therefore, the insolation simulation is used to compute the output of each PV generator.

Because the power flow program models only the utility system between the generators and the distribution substations, the PV generation on each feeder had to be aggregated to the distribution substation. A study described in Chapter V revealed that the "negative load" model was most appropriate for this. The power generation of all PVs on each feeder were summed and subtracted from the normal feeder load. This was then used as load data for the power flow program. The

power flow results then describe the operation of the utility system with dispersed PV.

PV Distributions and Insolation Patterns

The penetration and location of PV systems, the time of day and season, and the cloud patterns used in these simulations were chosen to provide the worst realistic cases for the utility. The location of the PV systems was chosen through discussions with PSO personnel and study of other utilities' experience with dispersed generation. Realistic cloud patterns were identified through the verification process, described in Chapter VIII, of the insolation model, and by a literature study of cloud patterns. The worst cases were then identified in the PV interaction study described above. The PV interaction results also allowed estimates of what penetrations can be considered significant to the utility. Season and time of day were chosen to provide the worst case for the utility.

Location of PV Generation

Because of its present high cost, almost all existing dispersed PV in the U.S. is located in affluent urban or suburban areas. As noticable penetrations begin to come on-line they will almost certainly follow this pattern until the technology is better known and costs become significantly lower. For this reason the PV generation is simulated in southeast Tulsa, PSO's most affluent area.

Seasons

The utility will be most affected by dispersed PV generation during spring and fall, the light load seasons. A given capacity of installed PV generation will represent a much higher operating penetration during these light load periods. PSO's peak daily load during these seasons can drop to as low as 40% of its peak summer load. The light load model will therefore receive the most detailed study. Planners at PSO made available a light load model for Spring 1988 for this study.

The other important season for study is the peak summer season. PV generation, as well as PSO's load, are at their peaks in the summer. PSO's planning power flow model for Summer 1989 was used for peak load study.

Insolation Patterns

During the verification of the insolation model several actual cloud patterns from the recorded insolation data were studied. These patterns were employed during the PV interaction study to determine the worst cases for the utility in terms of changes in PV generation. Others not verified but which are known to occur, such as a squall line that totally obscures the sun, were also studied. The worst cases were then used in the power flow studies of southeast Tulsa.

The worst case patterns turned out to be one cumulus cloud pattern, fast-moving, broken, well-defined clouds with clear sky between

the clouds, and the squall line, a solid line of dark clouds that moves across a clear sky. These cases were therefore used in the power flow studies. However, the results of the PV interaction study indicated that the cumulus pattern would probably not be significant during summer because of low operating PV penetration, so the cumulus pattern was simulated only for spring.

Penetration of PV Generation

The PV interaction study indicated that significant effects from dispersed PV generation might be noticed by the utility when operating penetrations reach the 30% - 50% levels. This corresponds to installed penetrations of 10% - 15% in the spring, and 30% - 50% in the summer. For the power flow study, then, spring installed penetrations of 15% and 30%, and summer installed penetrations of 30% and 50% were used. The results indicate that these were good choices.

Time of Day

Because insolation peaks at solar noon, the greatest possible changes in PV generation also occur at this time. To provide worst case analysis all simulations were run for solar noon conditions.

CHAPTER IV

INSOLATION MODELING FOR DISPERSED

PHOTOVOLTAIC SYSTEMS SIMULATION

The insolation model used in this study provides simulated insolation data over a large utility service area for a specified period. The insolation data will depend on the location of the service area, time of the year, time of day, and on the characteristics of the clouds passing overhead. The model is based on actual meteorological data.

The Effects of Clouds on PV

Descriptions of Clouds

Meteorologists have identified ten main types of clouds. They are described in the International Cloud Atlas [58] in the following way.

1. Cirrus: Detached clouds in the form of white, delicate filaments or white or mostly white patches or narrow bands. These clouds have a fibrous (hair-like) appearance, or a silky sheen, or both.

2. Circocumulus: Thin, white patch, sheet or layer of cloud without shading , composed of very small elements in the form of grains, ripples, etc., merged or separate, and more or less regularly arranged; most of the elements have an apparent width of less than one degree.

3.   Cirrostratus: Transparent, whitish cloud veil of fibrous (hair-like) or smooth appearance totally or partly covering the sky, and generally producing halo phenomema.

4.   Altocumulus: White or grey, or both white and grey, patch sheet or layer of cloud, generally with shading, composed of laminae, rounded masses, rolls, etc., which are sometimes partly fibrous or diffuse and which may or may not be merged; most of the regularly arranged small elements usually have an apparent width of between one and five degrees.

5.   Altostratus: Greyish or bluish cloud sheet or layer of striated, fibrous or uniform appearance, totally or partly covering the sky, and having parts thin enough to reveal the sun at least vaguely, as through ground glass. Altostratus does not show halo phenomena.

6.   Nimbostratus: Grey cloud layer, often dark, the appearance of which is rendered diffuse by more or less continuously falling rain or snow, which in most cases reaches the ground. It is thick enough throughout to blot out the sun. Low ragged clouds frequently occur below the layer, with which they may or may not merge.

7.   Stratocumulus: Grey or whitish, or both grey and whitish, patch, sheet, or layer of cloud which almost always has dark parts, composed of tessellations, rounded masses, rolls, etc., which are non-fibrous (except for virga) and which may or may not be merged; most of the regularly arranged small elements have an apparent width of more than five degrees.

8.   <u>Stratus</u>: Generally grey cloud layer with a fairly uniform base which may give drizzle, ice prisms or snow grains. When the sun is visible through the cloud, its outline is clearly discernible. Stratus does not produce halo phenomena except, possibly, at very low temperatures.

Sometimes Stratus appears in the form of ragged patches.

9.   <u>Cumulus</u>: Detached clouds, generally dense and with sharp outlines, developing vertically in the form of rising mounds, domes or towers, of which the bulging upper part often resembles a cauliflower. The sunlit parts of these clouds are mostly brilliant white; their base is relatively dark and nearly horizontal.

Sometimes Cumulus is ragged.

10.   <u>Cumulonimbus</u>: Heavy and dense cloud, with a considerable vertical extent, in the form of a mountain or huge towers. At least part of its upper portion is usually smooth, or fibrous or striated, and nearly always flattened; this part often spreads out in the shape of an anvil or vast plume.

<u>Cloud Characteristics of Importance to the Utility</u>

Any of these ten different clouds will reduce the output of a PV system when they pass between the sun and the PV system. While the physical descriptions of the clouds are important to understanding how

they affect the PV output, the specific characteristics of the variations in PV generation are more important to the utility. The severity of the effects on the utility can be described by the following four characteristics of the insolation pattern:

1. Frequency of variation: How often does the sunlight vary?

2. Magnitude of variation: How large is the variation in sunlight?

3. Duration of each variation.

4. Relative variations among dispersed PV systems.

Each of these changes the way the utility is affected by the interconnected PV systems.

Frequency of Variation

Each time the incident sunlight, and thus the PV systems' output, varies, the utility system must adjust for the changing energy input. The more frequent the variations, the more often the utility must adjust, so more frequent variations are not good for the utility. Frequency of variation depends on the size of the clouds in the cloud pattern, the percentage of the sky covered by the pattern, and the speed of the cloud movement. Smaller clouds, greater percentage cover, and higher speed all contribute to greater frequency of variation.

Magnitude of Variation

The effects on the utility increase also with increasing

magnitude of variation in insolation. The magnitude of variation depends on the optical transmission properties of the clouds. A greater amount of light transmitted through the cloud means a smaller variation. The utility must adjust more for a greater variation, so greater variation is worse than smaller for the utility. The amount of light transmitted is determined by the thickness and density of the clouds, and whether the cloud is made of water vapor, ice crystals, or other material.

Duration of Variation

How quickly the insolation changes from full sun to the minimum magnitude for a particular cloud is determined by how the cloud's optical properties vary from the edge to the center of the cloud. There will usually be a gradual change from the cloud's maximum density at its center to a minimum density at the edge. This will result in a slower, less abrupt change in insolation when the cloud passes between the sun and the PV system. How gradual the change is will depend on the optical properties and how fast the cloud is moving.

Relative Variations Among PV Systems

The final cloud pattern characteristic of importance to the PV/utility interconnection is the relative variation in power generated among PV systems dispersed throughout the utility service area. The worst case for the utility would be for the outputs of all PV systems to change simultaneously. However, because of the geographic separation among the PV systems and the finite rate of cloud movements, this worst

case cannot occur. There will always be some diversity; the variations in the output will occur for each system when a cloud passes between that PV array and the sun, and this will be at a different time for each PV system. This diversity will reduce the effects of the variations on the utility. The relative variations among the dispersed PV systems are determined by the relative locations of the PV systems and the relative locations and movements of the clouds in the sky.

Specific Cloud Characteristics

In the previous discussion of the four insolation pattern characteristics, six specific features of clouds have been mentioned:

1. Size of individual clouds.

2. Shape of individual clouds.

3. Percent of sky covered by clouds.

4. Speed and direction of cloud movement.

5. Optical transmission of clouds.

6. Changes in optical transmission from the center to the edge of clouds.

These six cloud characteristics completely define the four insolation parameters, and fully describe the clouds from the utility point of view.

For the simulation of dispersed PV systems within a utility service area an insolation model is therefore needed that provides realistic simulated data for all six of these cloud characteristics. These characteristics have been studied for various reasons by others. The next section will review existing literature on relevant models and characteristics of clouds.

Literature Review of Cloud Models

The most relevant cloud modeling work is modeling that has been done specifically for the simulation of PV systems. Unfortunately, very little has been done for this purpose. However, much work has been done for other purposes, such as weather forecasting and aviation, and some of this work is applicable to PV simulation. This review will therefore cover both types of cloud research. An enormous amount of work has been done on clouds. Only the work that is relevant to this study will be discussed.

General Cloud Models

The only cloud model specifically designed for simulation of PV systems was developed at Arizona State University [59]. The model was used to study the effects of central-station PV generators on the automatic generation control (AGC) systems of an electric utility. Area Control Error (ACE) was obtained from a model of the AGC system, and the ACE values were compared with limits established by the National Electric Reliability Council (NERC) to estimate maximum allowable penetrations of central-station PV generators.

The cloud model used in this study modeled only cumulus and cumulonimbus, or cumuliform clouds. These sharply-defined, dark clouds produce the worst effects on the utility. The shape of the clouds was assumed to be rectangular, and the size was determined stochastically from models developed in another study [60]. Constant speed of cloud movement was assumed.

The cloud model was based on the more general model developed by the Aerospace Corporation [60]. The complicated trigonometric relationships that determine the relations between the clouds and their shadows are developed in this model. The stochastic models for size and distribution of clouds are obtained from cloud observations [61-63].

These two models provide much useful information for modeling cumuliform clouds for this study. Neither model, however, considers the optical transmission properties of the clouds. Both assume a complete shadow, or no insolation, beneath the cloud. Nor is information about modeling clouds other than cumuliform provided. Because these may be important in this study, other research was reviewed for the needed data.

Cloud Size and Shape

There is some information available on size and shape of clouds other than cumuliform. Such clouds have been studied extensively for meteorological purposes. For example, data on Cirrus clouds are available in the literature [64]. Stochastic descriptions suitable for computer modeling would have to be developed from the available data.

Optical Transmission Properties

To provide a realistic simulation of clouds the optical transmission characteristics should be modeled. There are several ways to do this.

In the 1940s an attempt was made [65] to relate the insolation reaching earth through a cloudy sky to the type of clouds present. A simple exponential formula,

$$T = (a/m) \exp(-bm)$$

relates insolation T to airmass m, a function of the distance the sunlight passes through air, and two constants "a" and "b", which are empirically determined for various cloud types. The paper provides values for "a" and "b" for several types of clouds. Lack of data forced omission of several cloud types, including cumuliform, which are most important for the simulations of this study.

Another study [66] relates the insolation to the amount and type of clouds present. This study used hourly insolation and cloud data for a ten-year period at Hamburg, Germany, to derive the necessary constants. These constants and graphs relating insolation to the amount and type of clouds are presented, but again, certain types of cumuliform clouds are omitted.

Two other papers [67,68] take this same approach of relating insolation to cloud type. The model developed in these papers, however,

presents cloud transmittance coefficients for all important cloud types. The coefficients in these papers were also determined empirically.

One other study employed a different method to estimate the optical transmission of a cloud pattern [69]. These estimates use values of cloud base height and percent coverage, which are commonly reported hourly for aviation purposes. Transmission coefficients are given for a number of cloud base heights and for overcast and broken-cloud patterns. This provides an alternative to estimating optical transmission as a function of cloud type.

Cloud Speed

Cloud movement was studied near Saporro, Japan, from 1969 to 1971 [70]. Two cameras were used in a "stereophotogrammetric" analysis of cumuliform clouds. The results indicated that for cumuliform clouds at heights greater than 700 meters, the direction of cloud movement was the same as the direction of the prevailing wind at the height of the clouds. The speed of movement was somewhat slower than that of the prevailing winds, with speeds becoming increasingly slower as the height of the clouds decreased. However, the results of this study showed the assumption that the moving velocity of cumuliform clouds is equal to the velocity of the prevailing winds at the cloud height to be reasonable.

Studies performed at the Goddard Space Flight Center [71] extended these results to other types of clouds. Using High Resolution Infrared Radiometer recordings from two Nimbus satellites, cloud direction and speed were compared at various heights for various types of clouds. The

results showed that the direction of movement and the speed of movement for any clouds can be assumed to be the same as that of the prevailing winds at the cloud base height.

Cloud Model Development

In order to arrive at a model that most accurately addresses the important cloud characteristics for the PV/utility interconnection studies, portions of several of these models will be assembled and used. This is discussed in more detail in this section.

The six cloud pattern characteristics previously discussed will be used to describe a cloud formation in this model:

1. Size of individual clouds.

2. Shape of individual clouds.

3. Percent of sky covered by clouds.

4. Speed and direction of cloud movement.

5. Optical transmission of clouds.

6. Variations in optical properties from the center to the edge of clouds.

These six are sufficient to completely describe the clouds' effects on PV systems and, in turn, on the utility.

Only cumuliform clouds will be addressed, although at a later time, the model and simulations developed as a result of this project may be used to simulate other types of clouds. The justification for this is that cumuliform clouds will cause the greatest variations in power output from PV systems, and are thus the worst case for the electric utility. Therefore, cumuliform clouds will be simulated first.

Cloud Size and Shape

To estimate the size of individual clouds, a stochastic model is developed. This model is based on cloud size statistics derived by the Aerospace Corporation [60] from observed data on cumuliform clouds [61-63]. Cloud sizes and their frequencies of occurrence in the total cloud pattern were observed and recorded for small, large, and stormy-weather cumuliform clouds. Regression analysis was then performed on this data, resulting in the following equations.

$$p = 16.086 - 16.256 \ln A; \quad 0.100 < A < 2.690 \qquad (4-1)$$

$$p = 14.754 - 6.363 \ln A; \quad 0.100 < A < 10.163 \qquad (4-2)$$

$$p = 10.500 - 3.061 \ln A; \quad 0.100 < A < 30.884 \qquad (4-3)$$

These equations are plotted in Figures 1 and 2.

Equations 4-1, 4-2, and 4-3 represent the discrete probability "p", in percent, of a cloud of area "A" square nautical miles occuring for, respectively, small, large, and stormy-weather cumuliform clouds. They are valid only over the range of areas noted. Outside this range the probability is zero.
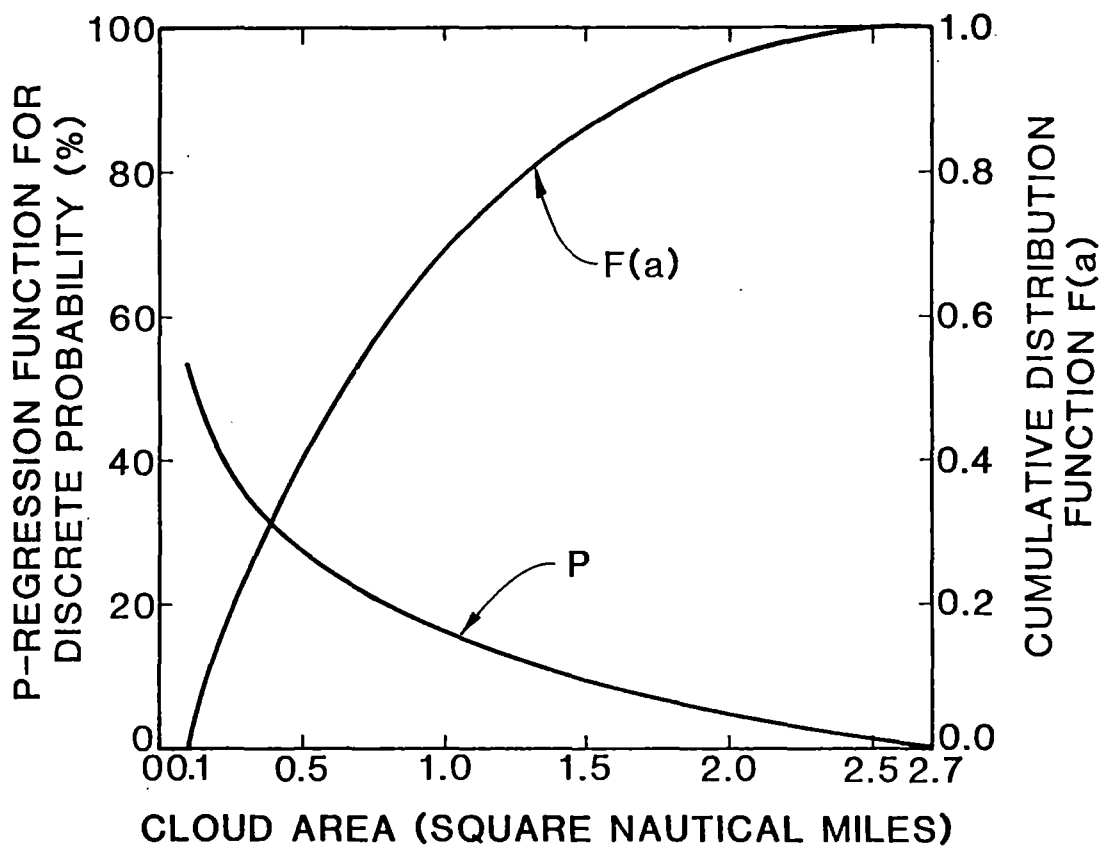
Figure 1. Probability functions for small cumulus clouds.
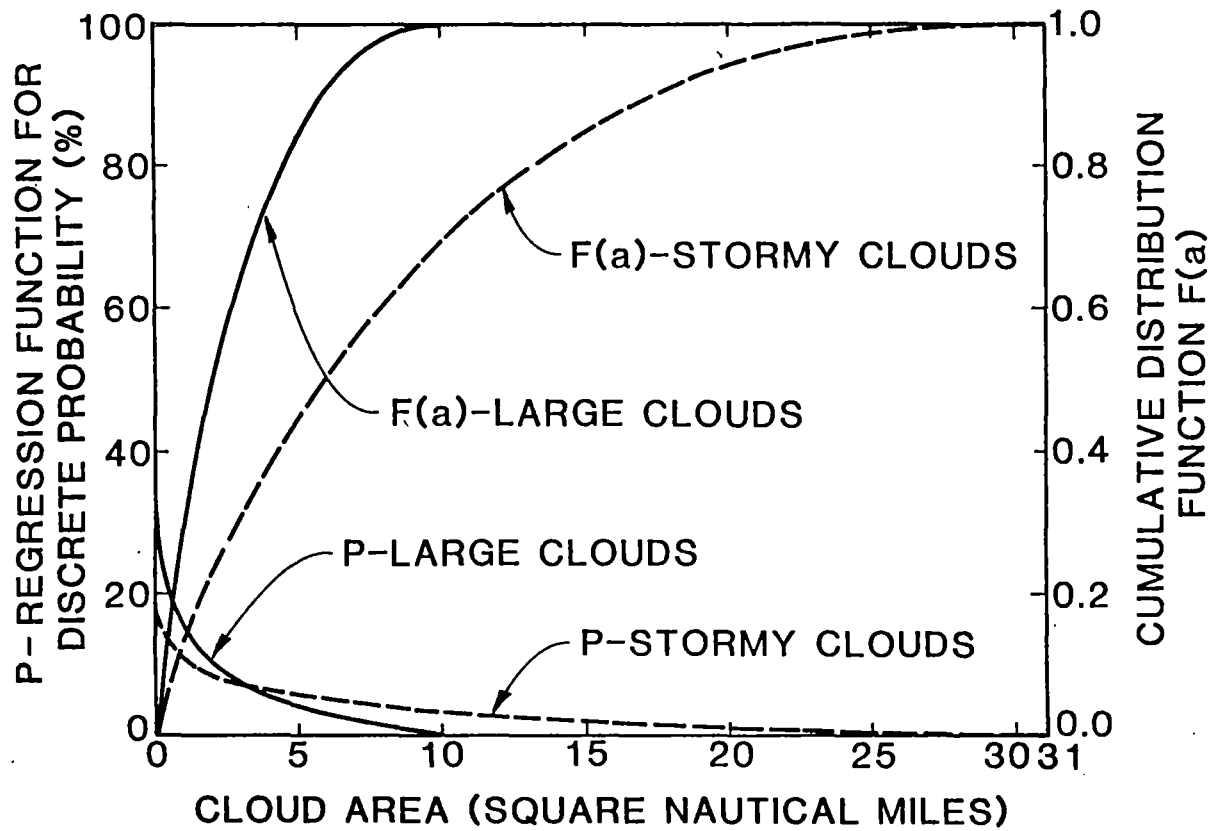
Figure 2. Probability functions for large and stormy cumulus clouds.

In the stochastic cloud size model a cloud area will be generated for each cloud simulated. To do this a cumulative distribution function (cdf) is needed for each cloud type. This can be obtained by integrating equations 4-1, 4-2, and 4-3 over their applicable ranges and normalizing the resulting functions to range from zero to one. Mathematically, this is stated in equation 4-4, which gives the probability F(a) of a cloud of size equal to or less than a.

$$F(A') = \frac{\int_{0.1}^{A'} p \, dA}{\int_{0.1}^{2.69} p \, dA} \qquad (4-4)$$

For small cumuliform clouds, represented by equation 1, the derivation of the cdf proceeds as follows.

$$\int_{0.1}^{A'} p \, dA = 16.086 \, A - 16.256 \, (A \ln A - A) \Big|_{0.1}^{A'}$$

$$= A \, (32.342 - 16.256 \ln A) \Big|_{0.1}^{A'}$$

$$= A' \, (32.342 - 16.256 \ln A') - 6.977$$

$$\int_{0.1}^{2.69} p \, dA = 43.729 - 6.977 = 36.752$$

$$F(A') = \frac{A' \, (32.342 - 16.256 \ln A') - 6.977}{36.752}$$

$$F(a) = a \, (0.880 - 0.442 \ln a) - 0.180; \quad 0.100 < a < 2.690 \qquad (4-5)$$

Equation 4-5 is the cdf for small cumulus clouds. This function is plotted in Figure 1. Similar derivations provide the cumulative distribution functions for large and stormy cumulus clouds, equations 4-6 and 4-7, respectively. These are shown in Figure 2.

$$F(a) = a (0.346 - 0.104 \ln a) - 0.059; \quad 0.100 < a < 10.163 \qquad (4-6)$$

$$F(a) = a (0.147 - 0.033 \ln a) - 0.022; \quad 0.100 < a < 30.884 \qquad (4-7)$$

A random number generator will provide a random value between 0 and 1 that will be substituted for F(a) in the appropriate equation, either 4-5, 4-6, or 4-7, for each cloud. The equation will be solved iteratively for the area a, which will be the size of the cloud simulated. The cloud sizes generated will thus conform to the probabilities represented by equations 4-1, 4-2, and 4-3.

Once the cloud area is defined, the shape of the cloud must be chosen. All clouds in this model will be assumed to have rectangular shape. The purpose of the model is to produce representative power output distributions for small PV systems dispersed throughout a utility service area. For this purpose the assumption of rectangular cloud shape should have very little effect on the power output distribution, and on how the PV systems affect the utility. Rectangular clouds will be much simpler to simulate by computer. Rectangular clouds were assumed in the studies of references [59,60] also. The equation

$$W = 0.582 L$$

will determine the length to width ratio for each cloud [60].

Percent of Sky Covered

The percent of sky covered by clouds in the model will be varied from very low - a few broken clouds - to 100% - completely overcast. Any value can occur in nature. The desired percent coverage will be input to the simulation program and will limit the generation of clouds described above.

Cloud Speed

Speed of cloud movement will also be varied over the range of possible values. This range will be estimated from data on wind speed at cloud height, as suggested in references [70,71]. Such data have been obtained from the Oklahoma Climatological Survey, which records wind speed at various altitudes twice daily for the Oklahoma City area.

Optical Transmission

The optical transmission properties of the clouds will be estimated from the data in references [67,68]. This will provide a range of possible insolation available in the shadow area of a certain type of cloud. The mean transmittance of clouds of type i is given as

$$\text{Transmittance} = x(i)' + y(i)'m$$

where $x(i)'$ and $y(i)'$ are given in Table I, taken from reference [67], and m is the airmass, which is determined by the angle of the sun at the time of the simulation.

The airmass m is given by:

$$m = \frac{35}{(1224 \cos^2 Z + 1)^{1/2}}$$
(4-8)

"Z" is the zenith angle of the sun. The clear sky insolation is then multiplied by the transmittance to give a value of insolation within the shadow area.

The final cloud characteristic, the variation in optical properties from the edge of the cloud to its center seems to have received little attention. There are no data available on how this transition should be modeled. The conservative assumption of instantaneous transition from full sun to full cloud attenuation at the edge of the clouds will therefore be made. This assumption is conservative and will produce homogeneous clouds. This should have little effect, if any, on the usefulness of the model.

Summary of the Insolation Model

The model developed in this study will simulate the insolation on a number of small PV systems geographically dispersed throughout a utility service area [72]. It will do this by providing a realistic simulation of cloud patterns passing over the service area. Combining this with conventional models of clear-sky insolation will provide a two-dimensional time-domain model of insolation for the service area.

Only cumuliform clouds will be modeled in this study. Cumuliform clouds are distinct, sharply-defined clouds that can be quite dark and fast-moving. They therefore will cause the greatest variation in PV

TABLE I

CLOUD TRANSMITTANCE COEFFICIENTS

Cloud Type	x'	y'
Fog	0.163	0.005
Stratus Nimbostratus	0.268	0.101
Stratocumulus	0.366	0.015
Cumulus	0.366	0.015
Cumulonimbus	0.236	0.015
Altostratus	0.413	0.001
Altocumulus	0.546	0.024
Cirrostratus	0.905	0.064
Cirrus	0.872	0.018

system output and represent the worst case for the utility receiving the PV energy.

The model will completely define the cloud pattern in terms of the following five characteristics.

(1) Size of individual clouds. This will be generated stochastically from data obtained from cloud observations.

(2) Shape of individual clouds. For ease of programming, and because it should have very little effect on the usefulness of the final results, all clouds are assumed to be rectangular.

(3) Percent of sky covered by clouds. This will vary from very low to completely overcast, because any value can realistically occur.

(4) Speed and direction of cloud movement. The clouds will be assumed to be moving at the prevailing wind speed and direction at the cloud altitude. This has been shown to be accurate for cumuliform clouds.

(5) Optical transmission of clouds. Typical values will be used for each cloud type.

A sixth characteristic, the change in optical transmission from the edge of the cloud to the center, will not be modeled. The cloud transmission will be assumed to be homogeneous. This is a conservative assumption, and should have little effect on the accuracy of the model.

The five characteristics of the cloud pattern will provide the necessary information to determine the following four insolation

characteristics, which will determine how much the variations in PV output will affect the utility:

(1) Frequency of variation.

(2) Magnitude of variation.

(3) Duration of the variation.

(4) Relative variations among dispersed PV systems.

The output of the insolation program will be the time-varying insolation at each PV system site within the service area. This data will be used to generate PV energy output data, which will be used in the analysis of dispersed PV interaction and utility effects. In the latter case the PVs on each feeder within the study area must be aggregated. This is discussed in Chapter V.

CHAPTER V

DISTRIBUTION FEEDER MODELING FOR

UTILITY SYSTEM POWER FLOW ANALYSIS

When electric utility engineers perform a power flow analysis of a utility system, it is impractical to use an exact model of the system. Most utility systems consist of many generators, transmission and distribution lines and equipment, and thousands of customers. Furthermore, almost all parts of the U.S. power grid east of the Rocky Mountains are interconnected, as are all parts west. An exact model would be impossibly and unneccesarily large and complex.

Approximate equivalent models are therefore used to represent parts of the utility system that are not under direct study. External equivalents at a utility's ties to other systems are almost always employed to model the interconnected system outside the one being studied. Moreover, instead of modeling each individual customer, lumped equivalents of the low voltage parts of the distribution system are used. Where these models begin and end and what form they take, are decided by the utility engineers based on the problem under study and the nature of their system.

The Public Service Company of Oklahoma (PSO) power flow distribution equivalents begin at the high voltage (transmission) side of each distribution substation. They include all feeder and distribution lines and all loads connected to that substation. The model consists of real and reactive power flows through the substation. Values for these are obtained by recording currents and power factors at the substation. In this way different equivalents for various load levels can be easily obtained for existing lines and loads.

One of the objectives of power flow analysis, however, is to evaluate the effects of changes to the existing system. To do this, it is necessary to develop appropriate models for the changes. When changes are small, simply adding or subtracting the changes in load from the known values at the substation may suffice. For more significant changes, however, the addition of a new feeder, for example, more detailed models may be needed for accurate simulations.

The addition of customer-owned dispersed PV generation represents another significant change that can occur in an electric utility system. One of the problems in including this change in power flow studies is that much of this type of generation is expected to be connected to that part of the system that is now represented only by aggregate equivalents.

In the few studies of dispersed generation that have already been done, the dispersed generation is usually modeled as a "negative load"; it is simply subtracted from the load existing on the feeder. This implies that the effects of intervening distribution lines,

transformers, and other equipment are negligible. In other words, all the dispersed generators are assumed to be connected directly to the high voltage side of the substation.

No documented effort is available verifying the accuracy of this negative load model. Similarly, there is very little documented study of appropriate models for adding new feeders or other similar changes in the utility system. As is shown in the next section, however, there are several models that may be used.

Feeder Models

The terminology to be used in discussing feeder models is illustrated in Figure 3. The feeder is assumed to be radial, with the substation considered an infinite bus. Node 0 is the point of feeder connection to the substation. Nodes 1 through n represent locations of either loads or generators connected directly to the feeder, or a feeder lateral containing multiple loads and generators. The complex voltage at node i is assumed to be V_i.

At node i the complex power flow $(P_i + jQ_i)$ is defined positive for lagging power factor loads. Generator real power and capacitor reactive power flows will therefore be negative. The sum of load, generation, and capacitor complex powers is the total power leaving the feeder at each node:

$$P_i + jQ_i = (P_{li} + P_{gi}) + j(Q_{li} + Q_{gi} + Q_{ci}) \qquad (5-1)$$

$P_0 + jQ_0 \rightarrow$ NODE 0 $P_{01} + jQ_{01} \rightarrow$ NODE 1 $P_{12} + jQ_{12} \rightarrow$ NODE 2 $P_{i-1,i} + jQ_{i-1,i} \rightarrow$ NODE I $P_{n-1,n} + jQ_{n-1,n} \rightarrow$ NODE n

$\underline{V}_0$ LINE 01 $\underline{V}_1$ LINE 12 $\underline{V}_2$ LINE 23   LINE I-1,I $\underline{V}_I$ LINE I,I+1   LINE n-1,n $\underline{V}_n$

$P_1 + jQ_1$ $P_2 + jQ_2$ $P_I + jQ_I$ $P_n + jQ_n$

I_{L1} I_{g1} I_{C1} I_{L2} I_{g2} I_{C2} I_{LI} I_{gI} I_{CI} I_{Ln} I_{gn} I_{Cn}

| LOAD 1 $P_{L1} + jQ_{L1}$ | GEN. 1 $P_{g1} + jQ_{g1}$ | CAP. 1 jQ_{C1} | LOAD 2 $P_{L2} + jQ_{L2}$ | GEN. 2 $P_{g2} + jQ_{g2}$ | CAP. 2 jQ_{C2} | LOAD I $P_{LI} + jQ_{LI}$ | GEN. I $P_{gI} + jQ_{gI}$ | CAP. I jQ_{CI} | LOAD n $P_{Ln} + jQ_{Ln}$ | GEN. n $P_{gn} + jQ_n$ | CAP. n jQ_{Cn} |
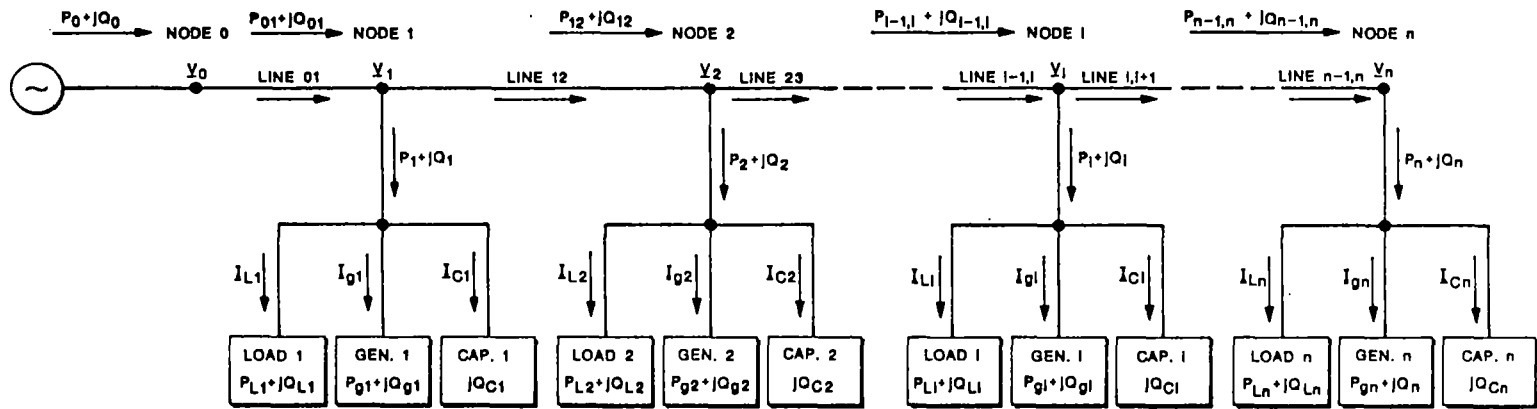
Figure 3. Feeder Representation.

Variables with double subscripts represent line sections between nodes. Line 12, for example, connects nodes 1 and 2. I_{12} is the complex current, and $(P_{12} + jQ_{12})$ the complex power, flowing into node 2 through line section 12.

Figure 4 shows how parallel feeder sections can be represented. Instead of only being connected to node i+1, node i is now connected also to node j+1. Such a parallel connection could exist at any node, and more than two parallel sections can emanate from any node.

The four feeder models considered in this work are actually different only in their representations of the line sections. The most exact of the four models is shown in Figure 5. Each line section consists of series inductance and resistance and shunt admittance and capacitance. Note that C includes only line capacitance, not capaitors connected to supply reactive power. While this model is useful for representing transmission systems, the values of G and C for a distribution feeder section are negligible. This model is therefore more detailed than necessary.

The shunt elements can therefore be neglected, resulting in three possible series models. The first, shown in Figure 6, includes both resistance and inductance. Neglecting the series resistance results in the model of Figure 7. Finally, the simplest model of all is that of Figure 8, an "ideal" feeder section. This means that the section has zero series impedance and infinite shunt impedance. This will be called the "zero impedance" model.
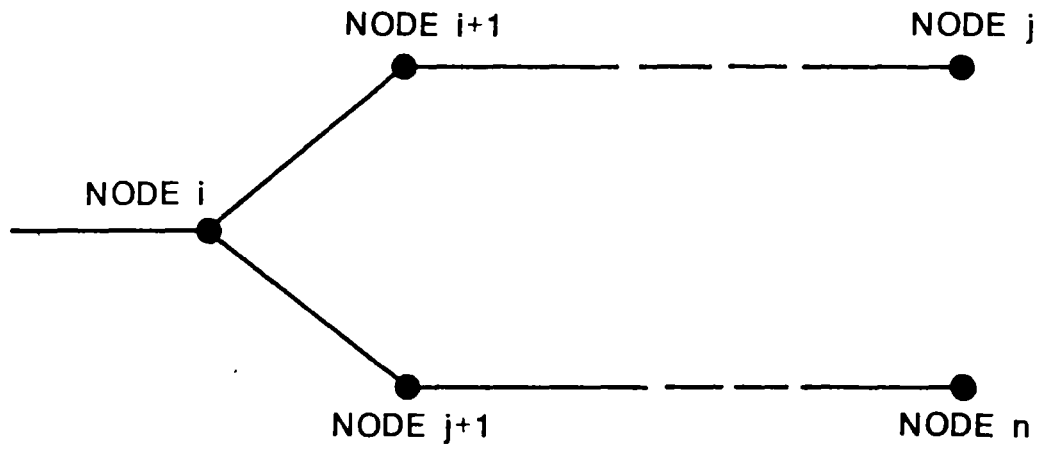
Figure 4.   Parallel Feeder Sections.
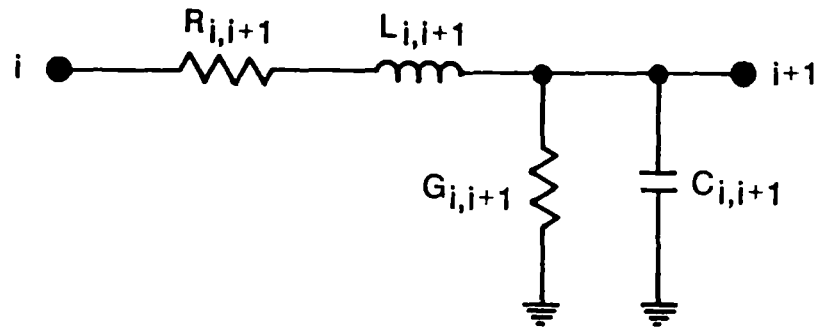
Figure 5.   Series/Shunt Model.
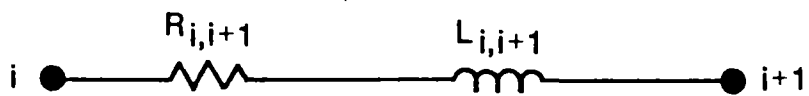
Figure 6. Series Impedance Model.
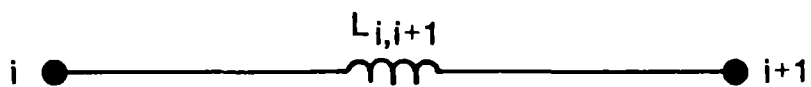
Figure 7. Series Inductance Model.
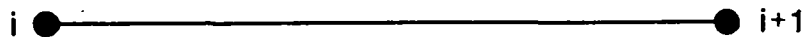
Figure 8. Zero Impedance Model.

The negative load model mentioned earlier is equivalent to the zero impedance model of Figure 8. Because this is the most widely-used model, it was studied. Because the shunt model of Figure 5 is unnecessarily complicated it was not considered further. The series L, R, however, is a more accurate model than the zero impedance model, so it was analyzed. Neglecting the resistance reduces the complexity of this model only slightly because of the similarities between series L and series R analysis, so the resistance term remains. The rest of this analysis focuses on the series impedance model of Figure 6 and the zero impedance model of Figure 8.

Series Impedance Model

The analysis of feeder models will be done in terms of real and reactive power because the models are needed for power flow analysis. The simplest feeder that can be represented by the series impedance model is the one bus system shown in Figure 9.

The voltages of buses 0 and 1 are related by:

$$V_0 = V_1 + R_{01}I_{01} + jX_{01}I_{01}$$

Because this is a simple series system,

$$I_{01} = I_0 = I_1$$

$$P_0+jQ_0 \quad \underline{V}_0 \qquad\qquad\qquad P_{01}+jQ_{01} \quad \underline{V}_1$$

SUBSTATION $\quad \underline{I}_0 \qquad X_{01} \quad \underline{I}_{01} \quad R_{01} \qquad \underline{I}_1$

$$P_1+jQ_1$$
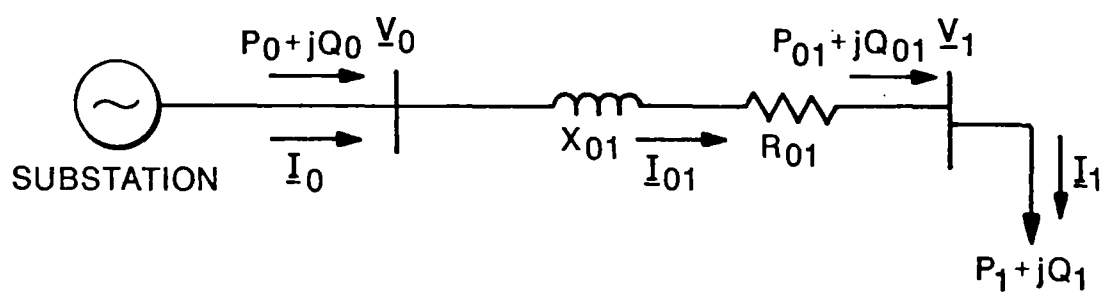
Figure 9. One-bus Feeder.

The complex power flow from the substation is therefore

$$P_0 + jQ_0 = V_0 I_0^* =$$

$$= (V_1 + R_{01} I_1 + jX_{01} I_1) I_1^* = \qquad (5\text{-}2)$$

$$= P_1 + R_{01} I_1^2 + j(Q_1 + X_{01} I_1^2)$$

Separating this into real and reactive power results in:

$$P_0 = P_1 + R_{01} I_1^2$$

$$\qquad (5\text{-}3)$$

$$Q_0 = Q_1 + X_{01} I_1^2$$

This same method of analysis can be extended to the 2-bus system of Figure 10.

The objective again is to define the substation complex power, $(P_0 + jQ_0)$, in terms of the powers leaving the two nodes and the current magnitudes along the lines.

$$P_0 = P_1 + P_2 + R_{01} (I_1 + I_2)^2 + R_{12} I_2^2$$

$$\qquad (5\text{-}4)$$

$$Q_0 = Q_1 + Q_2 + X_{01} (I_1 + I_2)^2 + X_{12} I_2^2$$
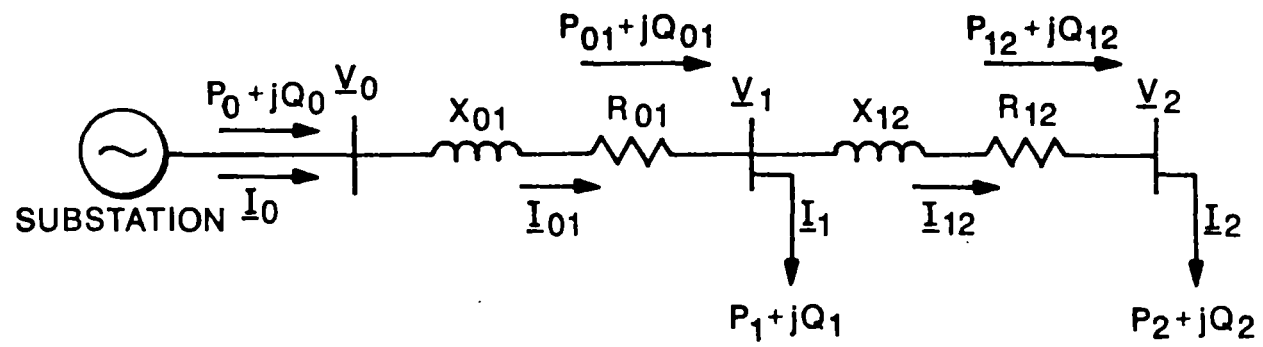
Figure 10. Two-bus Feeder.

The pattern is now becoming obvious, and the equations for a three-bus system can be written:

$$P_0 = P_1 + P_2 + P_3 + R_{01} (I_1 + I_2 + I_3)^2$$
$$+ R_{12} (I_2 + I_3)^2 + R_{23} I_3^2$$

(5-5)

$$Q_0 = Q_1 + Q_2 + Q_3 + X_{01} (I_1 + I_2 + I_3)^2$$
$$+ X_{12} (I_2 + I_3)^2 + X_{23} I_3^2$$

Finally, for an n-bus system, the power equations are:

$$P_0 = P_1 + P_2 + \ldots + P_n + R_{01} (I_1 + I_2 +$$
$$\ldots + I_n)^2 + R_{12} (I_2 + I_3 + \ldots + I_n)^2 + \ldots$$
$$\ldots + R_{n-1,n} I_n^2$$

(5-6)

$$Q_0 = Q_1 + Q_2 + \ldots + Q_n + X_{01} (I_1 + I_2 +$$
$$\ldots + I_n)^2 + X_{12} (I_2 + I_3 + \ldots + I_n)^2 + \ldots$$
$$\ldots + X_{n-1,n} I_n^2$$

Shunt capacitors are often used on distribution feeders for voltage support. These are therefore included in the final model shown in Figure 11.

The addition of capacitors affects only the reactive power equation:

$$Q_0 = Q_1 + Q_2 + \ldots + Q_n + X_{01} (I_1 + I_2 +$$
$$\ldots + I_n)^2 + X_{12} (I_2 + I_3 + \ldots + I_n)^2 + \ldots$$
$$\ldots + X_{n-1,n} I_n^2 - Q_{c1} - Q_{c2} - \ldots - Q_{cn}$$

The amount of reactive power supplied by a capacitor depends on the bus voltage to which it is connected:

$$Q_{ci} = C_i V_i^2$$
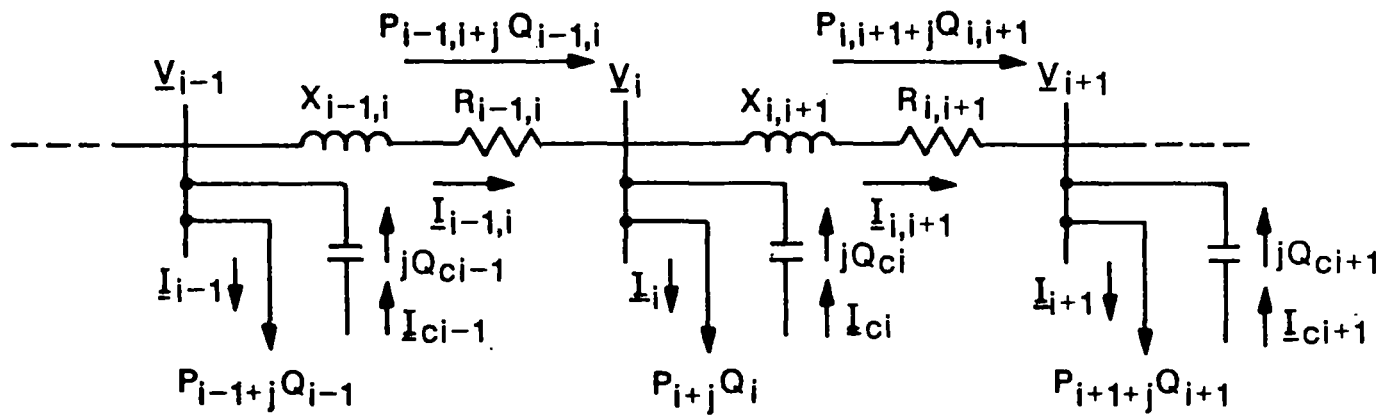
Figure 11. General Feeder Model.

The final equations for the most general n-bus model of Figure 11 are:

$$P_o = P_1 + P_2 + \ldots + P_n + R_{o1} (I_1 + I_2 + \ldots + I_n)^2 + R_{12} (I_2 + I_3 + \ldots + I_n)^2 + \ldots \\ \ldots + R_{n-1,n} I_n^2$$

(5-7)

$$Q_o = Q_1 + Q_2 + \ldots + Q_n + X_{o1} (I_1 + I_2 + \ldots + I_n)^2 + X_{12} (I_2 + I_3 + \ldots + I_n)^2 + \ldots \\ \ldots + X_{n-1,n} I_n^2 - Q_{c1} - Q_{c2} - \ldots - Q_{cn}$$

Zero Impedance Model

The zero impedance model is much simpler than the series impedance model. Calculating the complex power flow at the substation involves only summing all real and reactive powers on the feeder. For the n-bus feeder, then:

$$P_o = P_1 + P_2 + \ldots + P_n$$

(5-8)

$$Q_o = Q_1 + Q_2 + \ldots + Q_n - Q_{c1} - Q_{c2} - \ldots - Q_{cn}$$

Comparison of Series Impedance and
Zero Impedance Feeder Models

A modified power flow program was developed to compare the series impedance and zero impedance feeder models. The program uses the equations for the models to determine power flows and voltages along a feeder. Beginning with an assumed voltage at the far end of the feeder, it calculates iteratively the complex power flowing into the bus, the

current flowing into the bus, and then the voltage at the previous bus. When it reaches the substation bus, the voltage is compared with the nominal feeder voltage, the starting voltage at the end of the feeder is adjusted accordingly, and the iterative process is repeated.

Inputs to the program are nominal substation feeder voltage, loads, generation, and capacitors at each feeder bus, and resistance and inductance of each feeder line section. Program output includes the feeder voltage profile and complex power flow at the substation. To obtain realistic results a typical PSO distribution feeder was used in the simulation.

The PSO feeder known as ZM-6 serves about 2 MVA of load in south Tulsa at 7620 V. The primary feeder is 6.5 miles long, with laterals about every one-half mile. Loads served include single- and multi-family residences and some commercial customers. Table II lists the characteristics of the primary feeder. Table III provides recorded data on peak power flows at the substation.

Only the feeder primary was simulated using the power flow program. The model is shown in Figure 12. Loads and generation were distributed evenly along the line at one-half mile intervals. Power flow analysis was done at peak, half-peak, and zero load, with generation beginning at zero and increasing until either 100% dispersed generation penetration or the feeder MVA limit was reached.

TABLE II

PRIMARY FEEDER DATA FOR PSO FEEDER ZM-6

Beginning location		Length	Conductor
Substation	(S. 76th St.)	158 feet	1000AX
1813-11-9948	(S. 76th St.)	4.5 miles	477AS
1713-02-9999	(S. 121st St.)	1.0 miles	4/0AS
1713-12-0199	(S. 131st St.)	1.0 miles	2AS
1713-12-0106	(S. 141st St.)	(end of feeder primary)	

TABLE III

CONDUCTOR DATA FOR PSO FEEDER ZM-6

Conductor	R (ohms/Mft)	X(ohms/Mft)
477AS	0.037	0.082
4/0AS	0.084	0.110
2AS	0.267	0.126

NORTH ←

TULSA STREET (SOUTH) →	76th	81st		91st		101st		111th		121st		131st		141st
MILES FROM → SUBSTATION	0	$\frac{1}{2}$	1	$1\frac{1}{2}$	2	$2\frac{1}{2}$	3	$3\frac{1}{2}$	4	$4\frac{1}{2}$	5	$5\frac{1}{2}$	6	$6\frac{1}{2}$
MODEL BUS → NUMBER	~	1	2	3	4	5	6	7	8	9	10	11	12	13

CONDUCTOR →

|←————————————————— 477 AS —————————————————→|←— 4/0 AS —→|←— 2 AS —→|
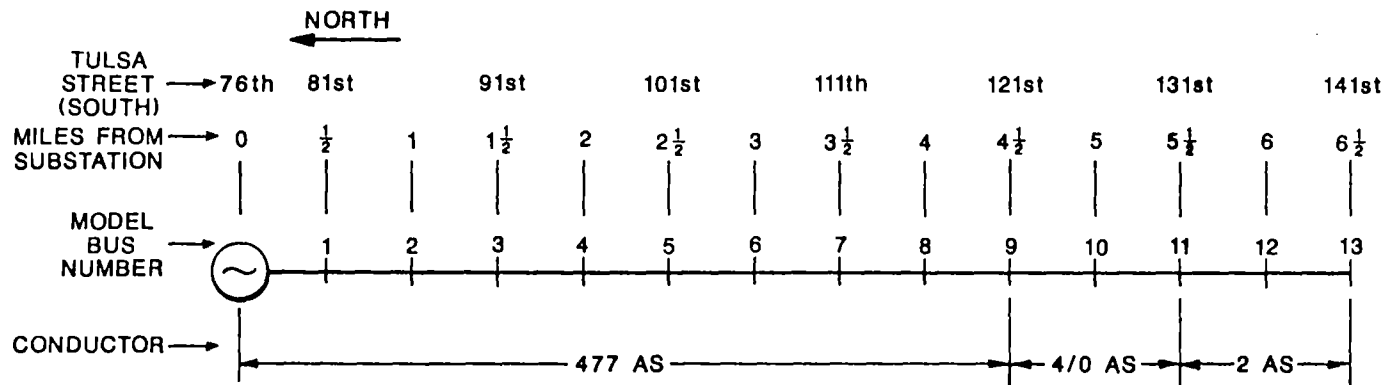
Figure 12. PSO Feeder ZM-6.

64

Results of Model Comparisons

The results of the model comparisons are shown in Figures 13 through 18. Figures 13 to 15 represent the feeder at no load, one-half peak load, and peak load, respectively. The PV generation power factor at each feeder bus is assumed to be 1.0. The same feeder loads are used in Figures 16 to 18, but the dispersed generation is now assumed to be operating at a power factor of 0.707 lagging. The curves shown are:

P_{si} - Real power calculated by the series impedance model.

Q_{si} - Reactive power calculated by the series impedance model.

$Q_{si, with\ o}$ - Reactive power calculated by the series impedance model. The dispersed generators in this case operate at a power factor of 0.707, but shunt capacitors are used to correct the power factor to approximately 1.0. (Figures 13 to 15 only).

Q_{zi} - Reactive power calculated by the zero impedance model.

Q_{v} - Another model of reactive power, which is discussed in the next section.

MVA - The MVA loading of the feeder at the substation, as calculated by the series impedance model.

Visual inspection of all 6 figures indicates that the values for real and reactive power calculated by the zero impedance model follow closely those of the more exact series impedance model. To quantify the

REAL POWER(MW), REACTIVE POWER(MVAR), MVA LOADING AT SUBSTATION
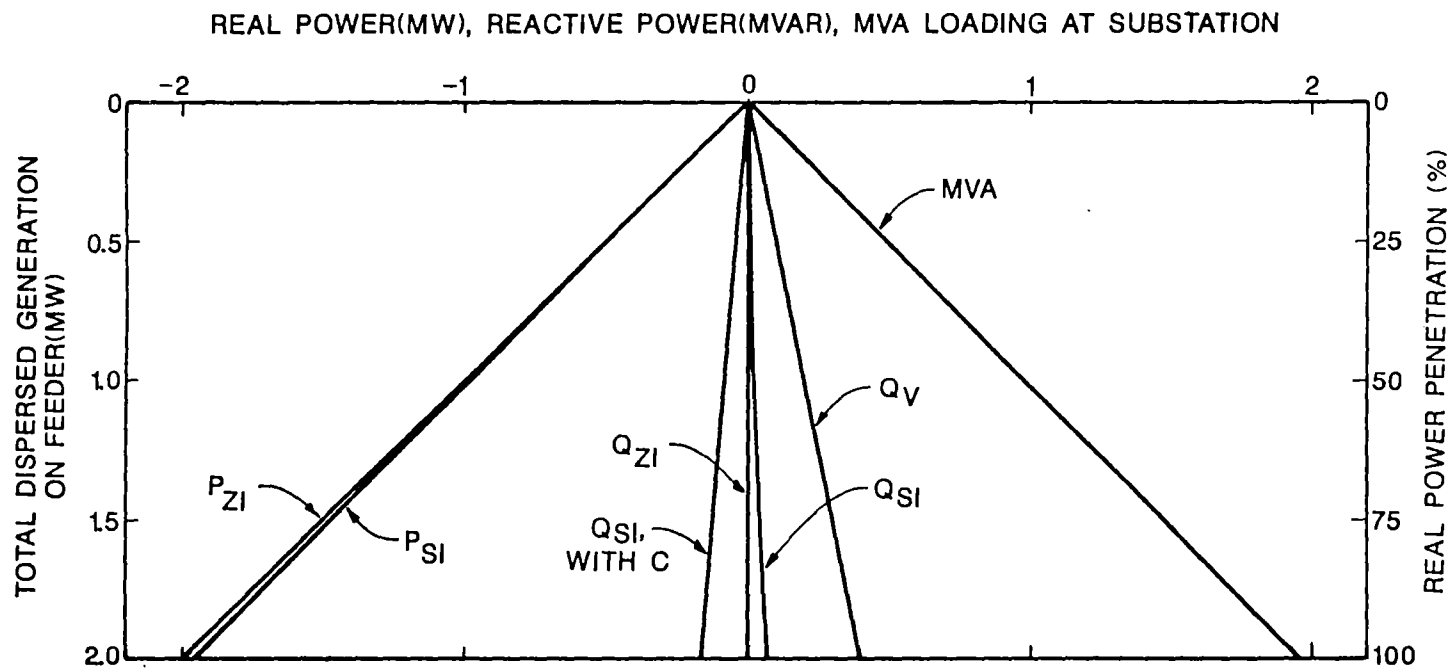
Figure 13. Feeder Power Flows: No Feeder Load.
PV Generation Power Factor = 1.0

REAL POWER(MW), REACTIVE POWER(MVAR), MVA LOADING AT SUBSTATION
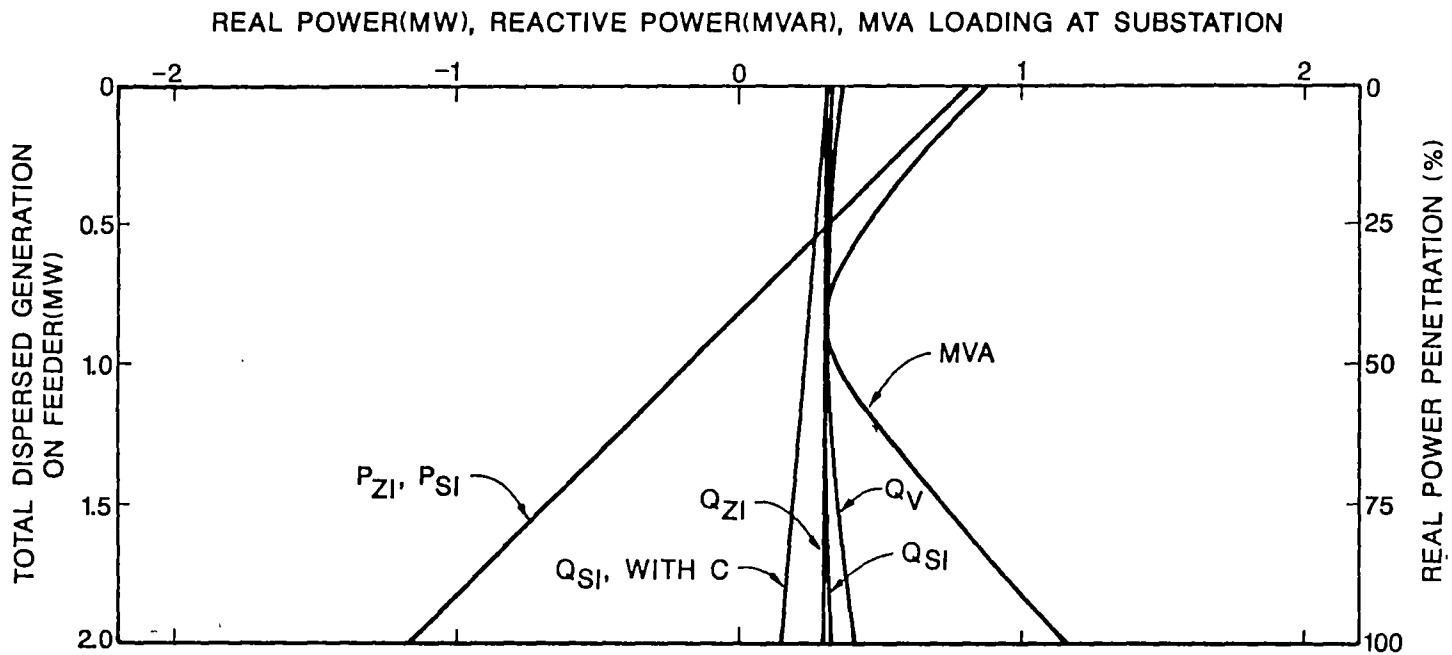
Figure 14. Feeder Power Flows: Half-Peak Feeder Load.
PV Generation Power Factor = 1.0

REAL POWER(MW), REACTIVE POWER(MVAR), MVA LOADING AT SUBSTATION
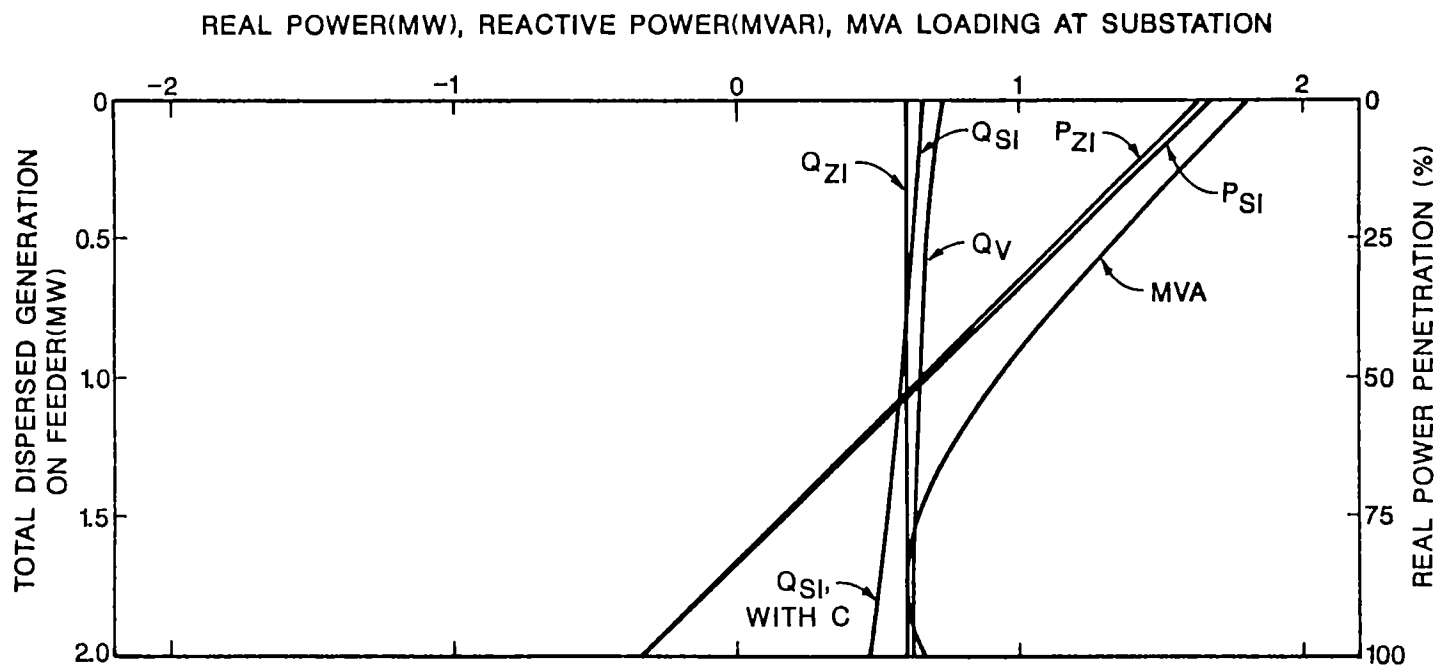
Figure 15.   Feeder Power Flows: Peak Feeder Load.
PV Generation Power Factor = 1.0

REAL POWER(MW), REACTIVE POWER(MVAR), MVA LOADING AT SUBSTATION
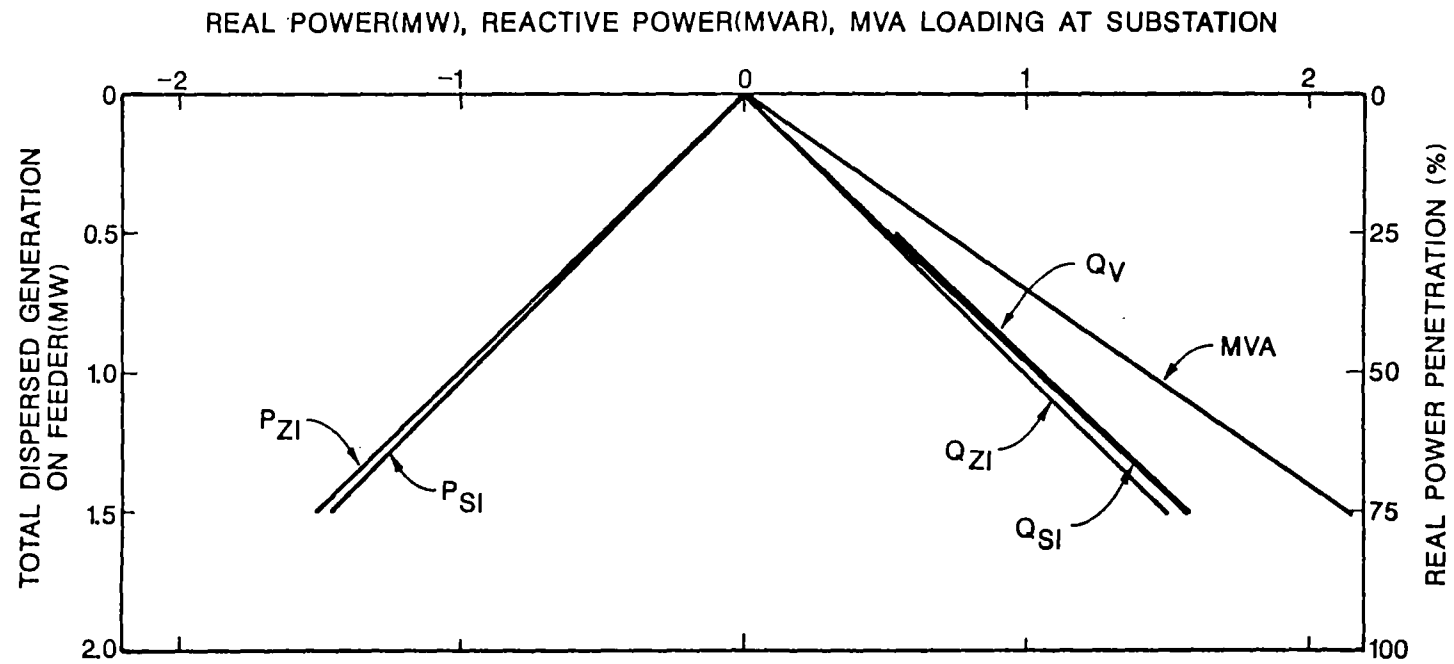
Figure 16.   Feeder Power Flows: No Feeder Load.
PV Generation Power Factor = 0.707

REAL POWER(MW), REACTIVE POWER(MVAR), MVA LOADING AT SUBSTATION
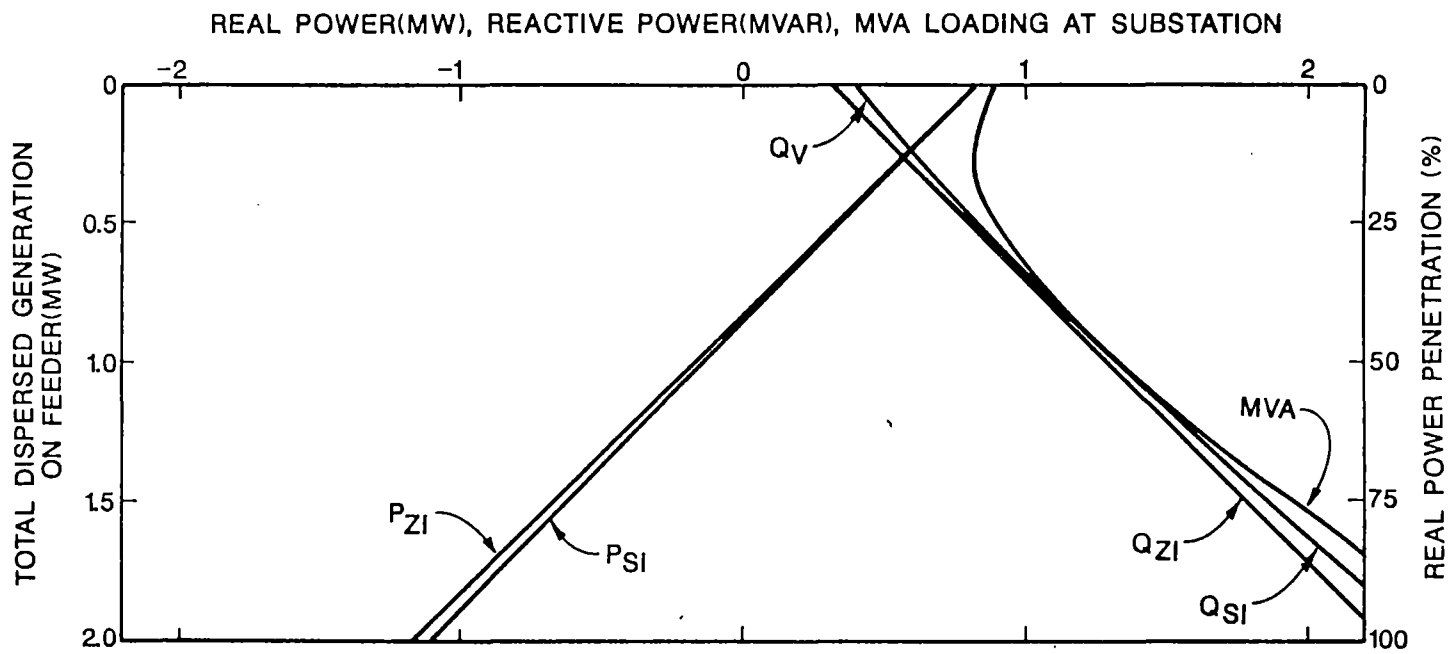
Figure 17.   Feeder Power Flows: Half-Peak Feeder Load.
PV Generation Power Factor = 0.707

REAL POWER(MW), REACTIVE POWER(MVAR), MVA LOADING AT SUBSTATION
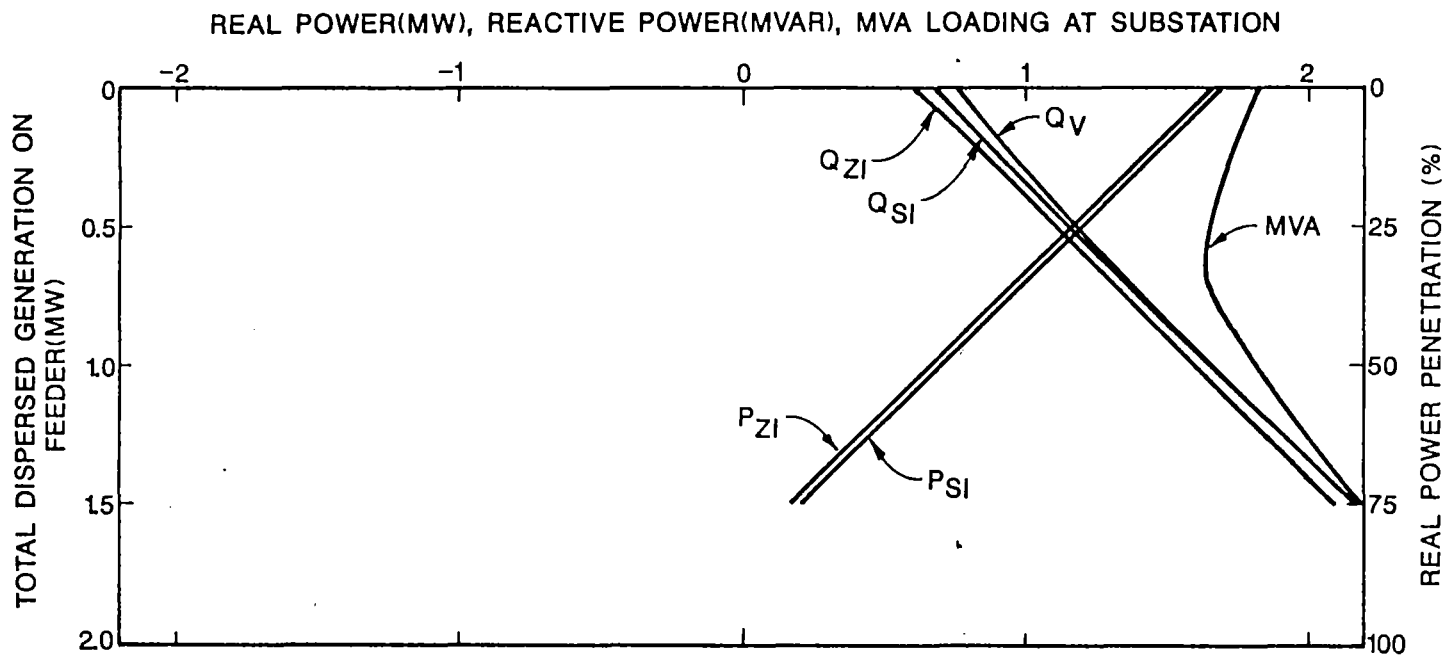
Figure 18.   Feeder Power Flows: Peak Feeder Load.
PV Generation Power Factor = 0.707

accuracy of the zero impedance model, an error value is calculated:

$$\text{Error} = \frac{Q_{s_i} - Q_{z_i}}{\text{MVA Loading}} \times 100$$

This gives the percentage difference between the zero impedance model and the more exact series impedance model in relation to the MVA loading of the feeder. The worst-case values for the six different feeder loadings are presented in Table IV.

The values in the third column of Table IV confirm the visual inspection results that the zero impedance model is a very good approximation to the more exact series impedance model. In a power flow simulation of a small part of a utility system in which only one or a few feeders are modeled, the more exact series impedance model may be useful. Simulation of a large utility system, however, must include hundreds or even thousands of feeders. In this case it is not necessary or even realistic to model each feeder with the series impedance representation.

Voltage Drop Model

Another possible simple feeder model relies on the fact that the voltage drop along the feeder is limited to a certain value. PSO uses a limit of ± 5%. When the load and generation on the feeder are known, and the voltage drop is assumed equal to the maximum allowable drop, the power flow from the substation can be computed.

TABLE IV

MODEL COMPARISONS
BASE CASE: SERIES IMPEDANCE MODEL

| Feeder Loading | | Error (%) | |
| | Dispersed Generation | | |
Load	Power Factor	Zero Impedance Model	Voltage Drop Model
0	1.0	3.6	16.8
0	0.7	3.9	3.9
Half Peak	1.0	2.2	7.2
Half Peak	0.7	3.6	0.7
Peak	1.0	1.3	1.8
Peak	0.7	4.0	1.4

This "voltage drop" model is demonstrated for a one-bus system in Figure 19. X_{o1} is unknown, and for the purposes of this example resistance is neglected. $P_1 + jQ_1$ is the feeder load minus any generation on the feeder. V_1 is assumed equal to 95% of the voltage at the substation. The voltage equations can then be written:

$$P_1 + jQ_1 = V_1 \angle 0 \; I_{o1}^*$$

$$I_{o1}^* = \frac{P_1 + jQ_1}{V_1 \angle 0}$$

$$I_{o1} = \frac{P_1 - jQ_1}{V_1}$$

$$\underline{V}_o = V_1 \angle 0 + jX_{o1} I_{o1} = V_1 + jX_{o1} \frac{P_1 - jQ_1}{V_1}$$

$$\underline{V}_o = V_1 + j\frac{X_{o1}P_1}{V_1} + \frac{X_{o1}Q_1}{V_1} = (V_1 + \frac{X_{o1}Q_1}{V_1}) + j\frac{X_{o1}P_1}{V_1}$$

$$V_o = \sqrt{(V_1 + \frac{X_{o1}Q_1}{V_1})^2 + (\frac{X_{o1}P_1}{V_1})^2} \qquad (5\text{-}9)$$

The only unknown value in this equation is X_{o1}. Solving for X_{o1} gives:

$$X_{o1} = \frac{-2Q_1 + \sqrt{4Q_1^2 - 4(\frac{Q_1^2 + P_1^2}{V_1^2})(V_1^2 - V_o^2)}}{2(\frac{Q_1^2 + P_1^2}{V_1^2})} \qquad (5\text{-}10)$$
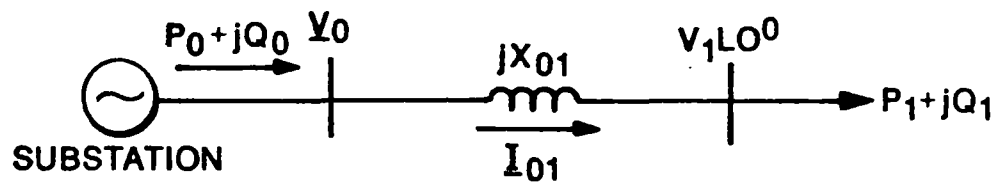
Figure 19. Voltage Drop Model.

This value of reactance is then used to compute the power flow from the substation:

$$Q_0 = Q_1 - X_{01} I_{01}^2 \qquad\qquad (5-11)$$

$$I_{01} = \frac{P_1 - jQ_1}{V_1^*} \qquad\qquad (5-12)$$

The advantage of this analysis over the series impedance model is that, just as in the zero impedance model, the only change from feeder to feeder is the load and generation. The necessary assumption, however, is that the voltage drop is the same for all lines.

This analysis can be used in the same type of iterative procedure used in the load flow analysis done previously. A computer program was written to do this, and an approximate model of the PSO feeder ZM-6 was created. The results of this analysis are shown as Q_v in Figures 13-18. The corresponding error values are listed in Table IV.

Referring to the figures and Table IV it is seen that the voltage drop approximation is in some cases better than the short circuit model, but in others it is not as good. The zero impedance model is consistently closer to the series impedance model. The problem with the voltage drop approximation is in the assumption that the voltage drop is always the same, 5% in this case. This is only correct when the feeder is loaded to near its 2 MVA limit. This is a poor assumption, and it results in large errors in the computed reactive power under light load conditions.

Summary of Feeder Models

The zero impedance model is the best model to use in power flow simulation of a large system. For the feeder and the loading cases studied, the worst error between this model and the more accurate series impedance model is only 4%. To simulate each feeder of a large system using the series impedance model would require enormous amount of information and time to develop the individual feeder models. This extra cost and effort are simply not necessary. The voltage drop model, while more accurate in some cases, is not consistent.

The zero impedance model works well because of the required voltage drop constraint on a distribution feeder. The PSO limit of 5% voltage drop from the substation to the end of the feeder is common in the utility industry. To limit the drop to this value, relatively large conductors are needed. The conductors needed to maintain the voltage are larger than are needed to efficiently transmit the power. This results in the conductor impedances having very little effect on the power flow. Neglecting the conductor impedance, as in the zero impedance model, changes the power flow values very little.

The voltage drop model fails to provide a reliable estimate of power flow because of the assumption that the voltage drop is always exactly 5%. This is only a good assumption when the feeder is heavily loaded. This explains why the error values in Table IV decrease as feeder loading increases. When the voltage drop is not near 5%, however, this model is inaccurate.

The feeder loading cases in which the dispersed generation power factor is assumed to be 0.7 are probably not realistic. Although line commutated inverters do operate at about this power factor, a utility will certainly require that power factor correction capacitors be used to supply the reactive power. This case was also simulated, and Figures 13-18 indicate that the zero impedance model, with power factor of 1.0 assumed, is again a good model for this case.

Finally, the popular "negative load" model for dispersed generation is confirmed for large system power flow analysis by this study. The negative load model and zero impedance model are equivalent. As the number of feeders included in a power flow simulation decreases, however, the accuracy of this model will also decrease. At some point, or for certain types of simulations, it may be necessary to use the series impedance feeder model.

CHAPTER VI

DISPERSED PV SIMULATION PROGRAMS

The insolation and utility distribution feeder simulations described in Chapters IV and V were combined to constitute a final simulation of dispersed PV systems. The insolation simulation provided insolation data for each PV system dispersed throughout a geographical area. The feeder model then aggregates all the PV systems on each feeder.

To use the insolation model, the service area is first defined as shown in Figure 20. The area must be rectangular in shape, and its four borders are defined in terms of latitude and longitude. PV systems are located within the area in terms of latitude and longitude also.

The simulation is demonstrated using the city of Stillwater, Oklahoma. This provides a service area of just over 100 km^2, as shown in Figure 21. The rectangular area shown encompasses the entire city.

The northern and southern borders are at latitudes of 36.17° N and 36.08° N, respectively. These borders are divided into 100 equal increments of distance and time for the simulation. Choosing equal numbers of distance and time increments simplifies the simulations by
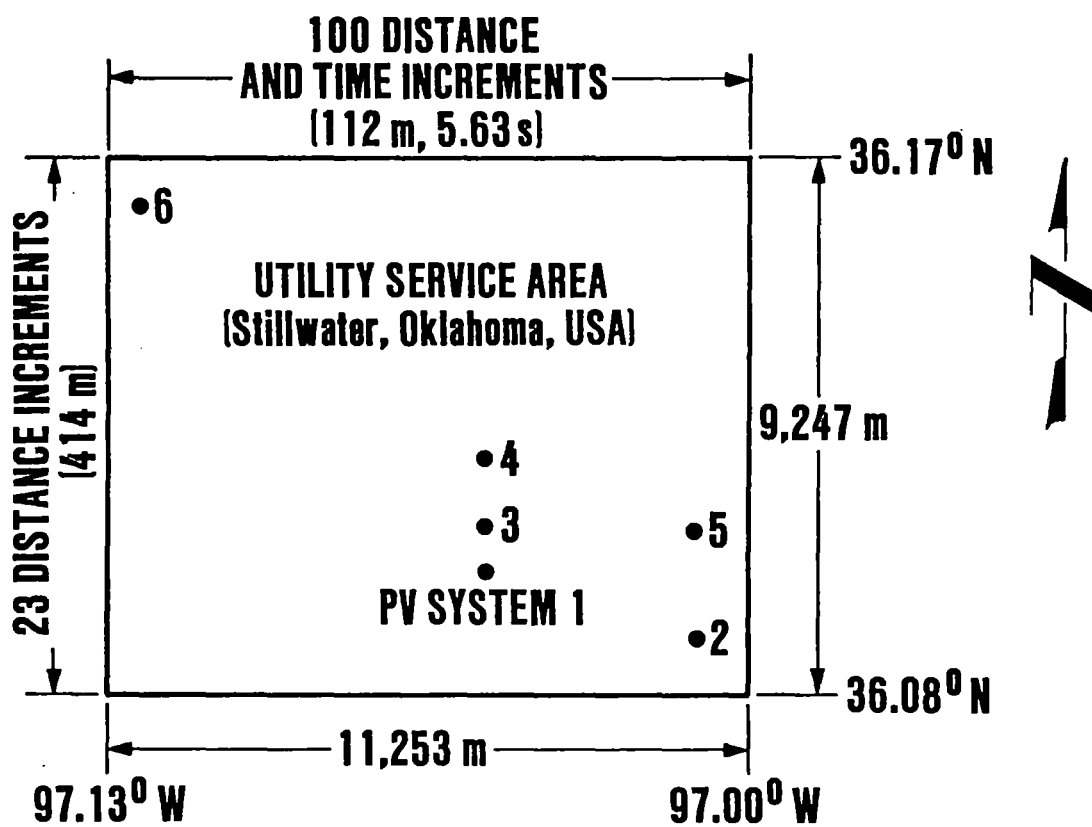
Figure 20. Simulation Service Area.
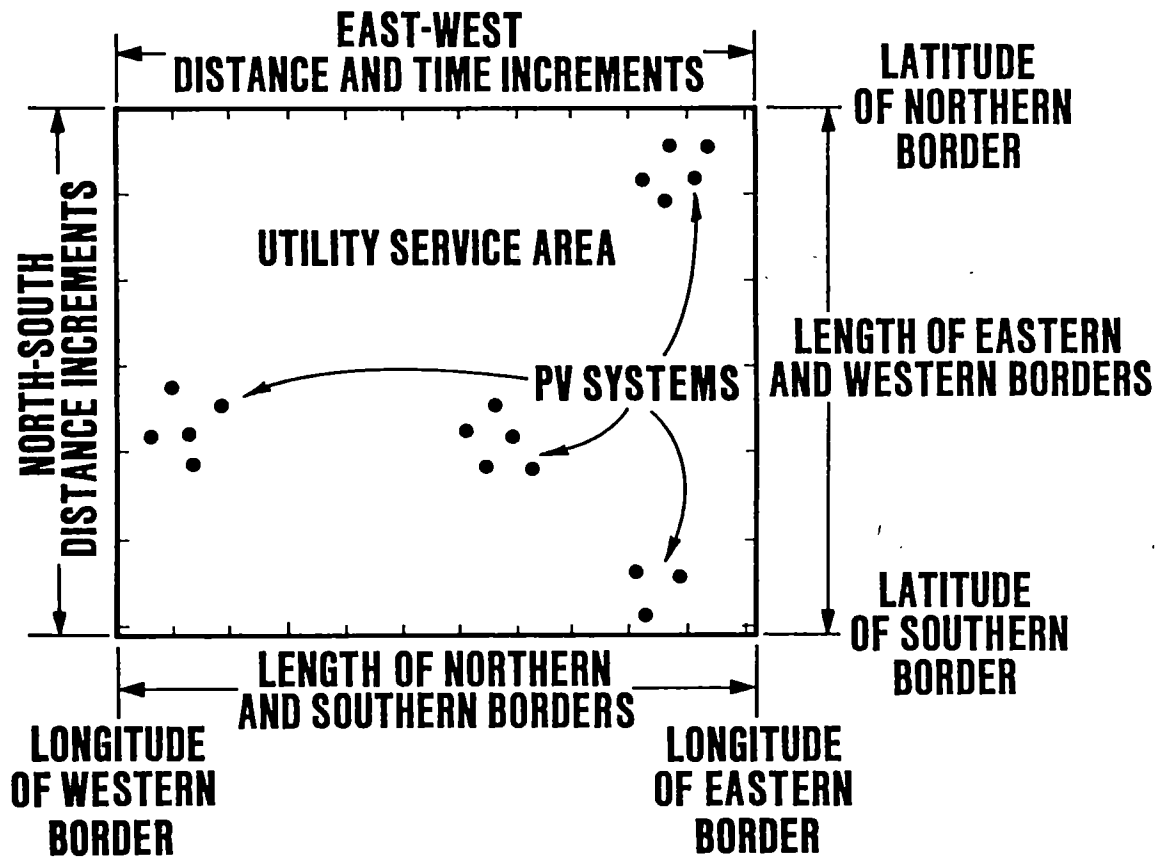
Figure 21. Simulation Service Area for Stillwater, Oklahoma.

allowing the cloud pattern to move exactly one distance increment at each time step. For a cloud speed of 20 m/s, 100 increments give a time increment of 5.63 s and a distance increment of 112.53 m. The number of increments can be changed depending on the size of the service area and the speed of cloud movement.

The eastern and western borders, with latitudes of 97.00° W and 97.13° W, respectively, were divided by the program into 23 distance increments of 414 m each. This is the width of the smallest cloud simulated by the insolation model, and is therefore the smallest increment needed. Keeping all increments as large as possible minimizes simulation costs.

Six locations, shown in Figure 21, were chosen within the service area for dispersed PV systems. Twenty-four minutes of insolation data, beginning at solar noon on April 24, were generated for these six locations. The cloud pattern, consisting of small cumuliform clouds moving west to east at 20 m/s produced the shadows depicted in Figure 22. This shadow pattern, represented by the shaded areas, covers about 50% of the service area. The time at which the increment reaches the western border is shown at the bottom. It was later learned that cumulus clouds of this type usually move south to north, and the simulation was thus corrected.

Insolation at each PV system location varies because of these moving shadows. Plots of the insolation at three locations (1, 3, and 6 in Figure 21) are provided in Figure 23. Notice the correlation between

ONE EAST-WEST DISTANCE INCREMENT
ONE TIME INCREMENT

DIRECTION OF
CLOUD MOVEMENT

— NORTHERN BORDER

ONE NORTH-SOUTH
DISTANCE INCREMENT

— SOUTHERN BORDER

12.0922 12.0766 12.0610 12.0453 12.0297 12.0141 12.000

TIME AT WHICH SHADOW FALLS ON WESTERN BORDER
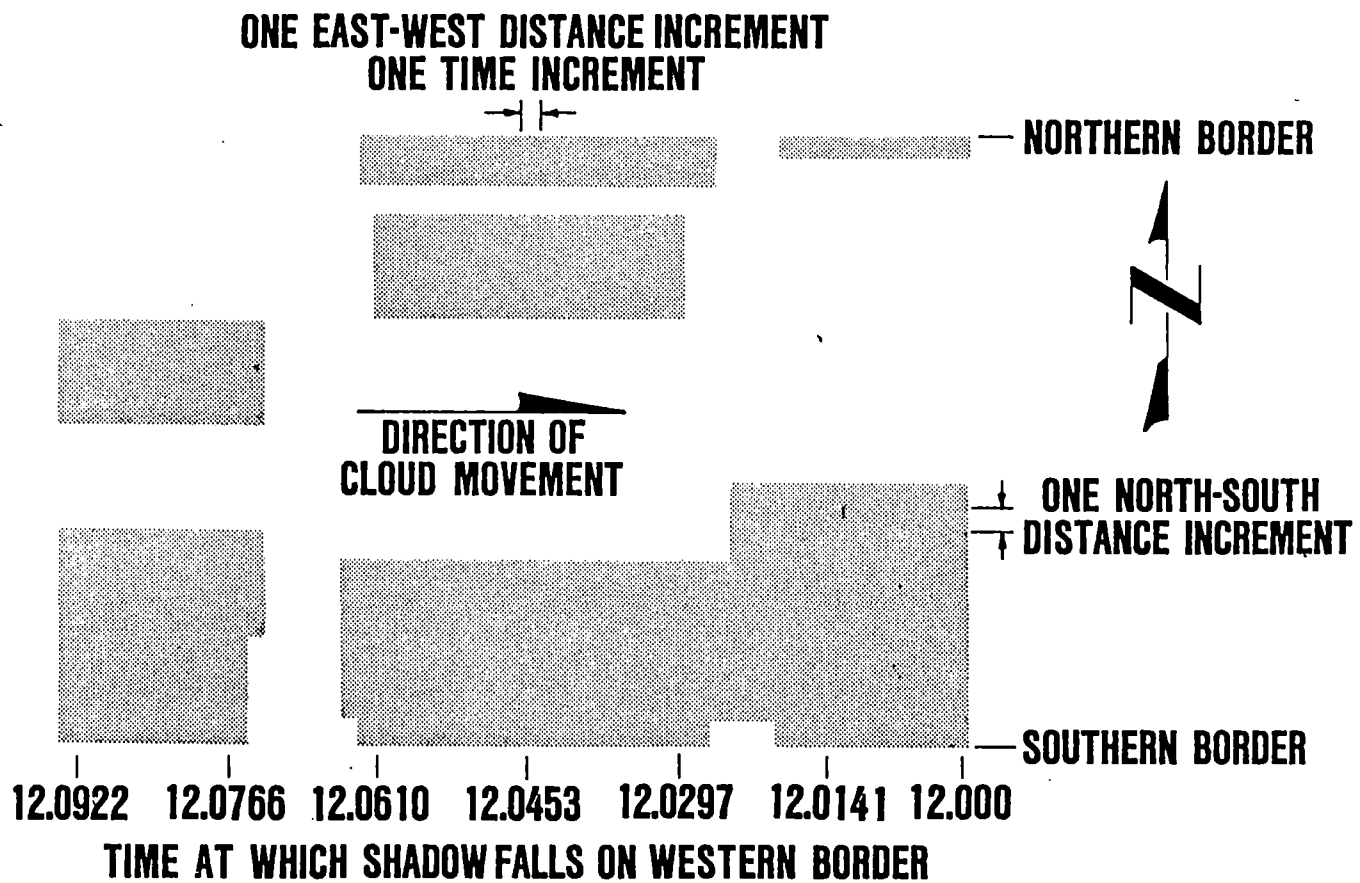
Figure 22. Simulated Cloud Pattern for 50% Shadow Cover.
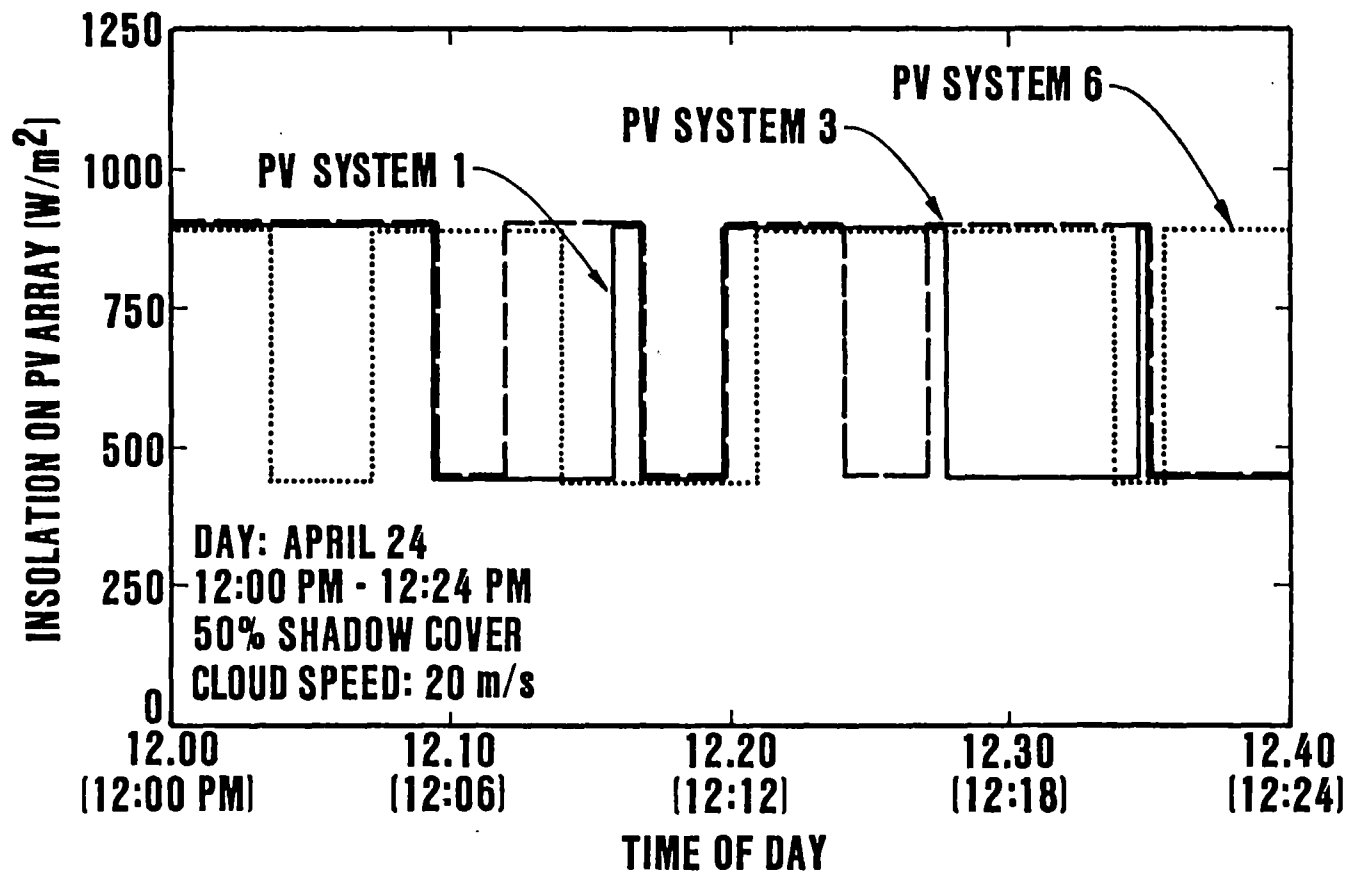
Figure 23. Insolation on PV Arrays Resulting from 50% Shadow Cover.

the insolation on systems 1 and 3, which are geographically close together. System 6, however, has a significantly different insolation characteristic. It is this constantly varying PV systems' output that may cause problems for the electric utility to which these are connected.

Figure 24 shows another cloud pattern over Stillwater that covers 90% of the service area. The resulting insolation for PV systems 1, 3, and 6 is shown in Figure 25. Notice again the correlation between systems 1 and 3. Also, the periods of full insolation are shorter and less frequent because of the greater cloud cover.

Versions of the Simulation Program

The output of the insolation and feeder simulations are processed in one of several ways to provide the needed output for each application. There are therefore several versions of the main program for different aplications. They are all written in FORTRAN and run on the Oklahoma State University School of Electrical and Computer Engineering VAX Computer. The five existing versions, included in Appendix I, are described below.

Insolation only

This is the original program that provides insolation at each PV system location for each simulation time increment. The insolation on each PV array is output for each time increment. This program was used to verify the insolation models. It could also be used as the basis for other simulations needing dispersed insolation data.

ONE EAST-WEST DISTANCE INCREMENT
ONE TIME INCREMENT

— NORTHERN BORDER

ONE NORTH-SOUTH
DISTANCE INCREMENT

DIRECTION OF
CLOUD MOVEMENT

— SOUTHERN BORDER

12.0922 12.0766 12.0610 12.0453 12.0297 12.0141 12.0000
TIME AT WHICH SHADOW FALLS ON WESTERN BORDER
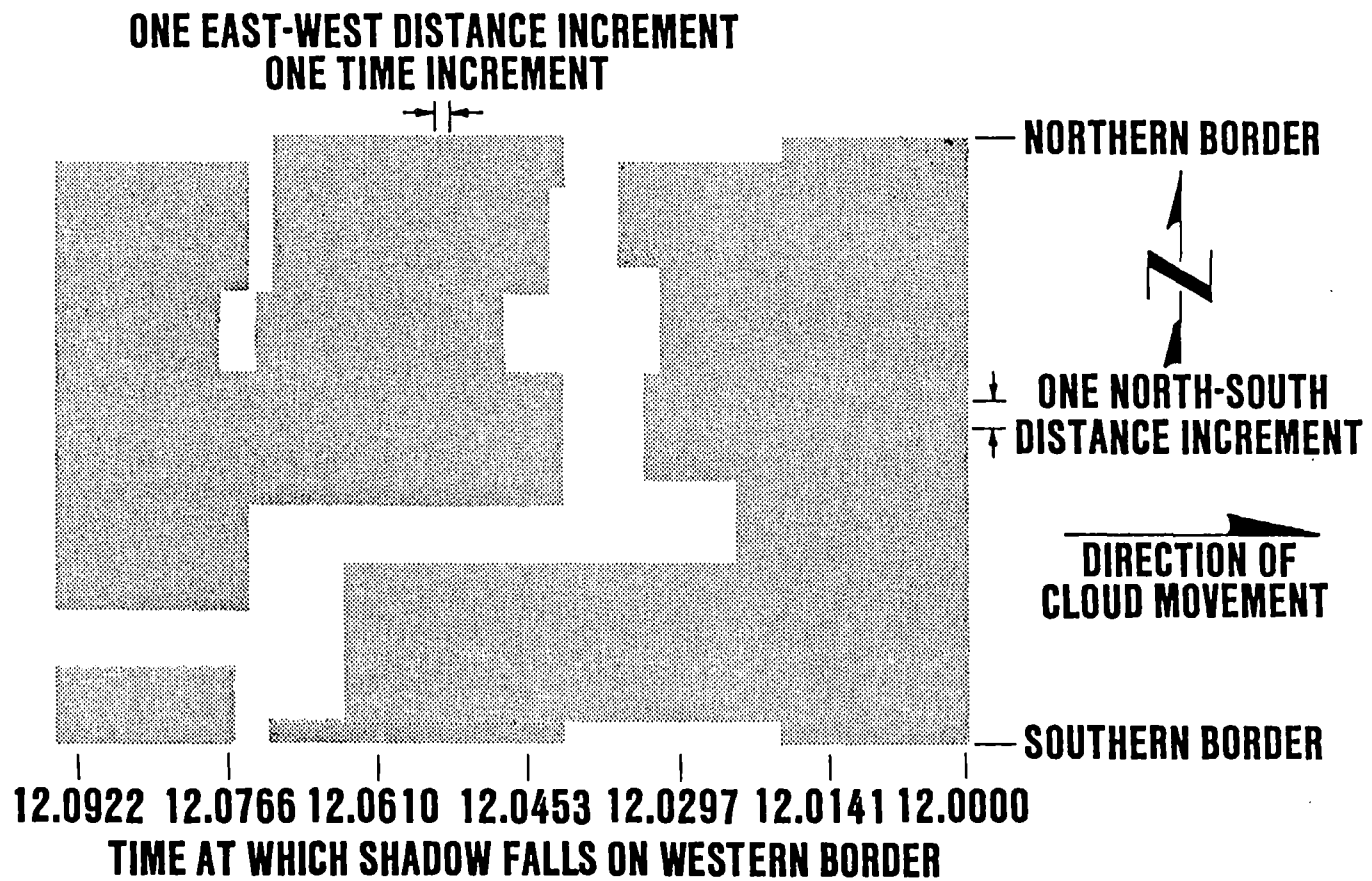
Figure 24. Simulated Cloud Pattern for 90% Shadow Cover.
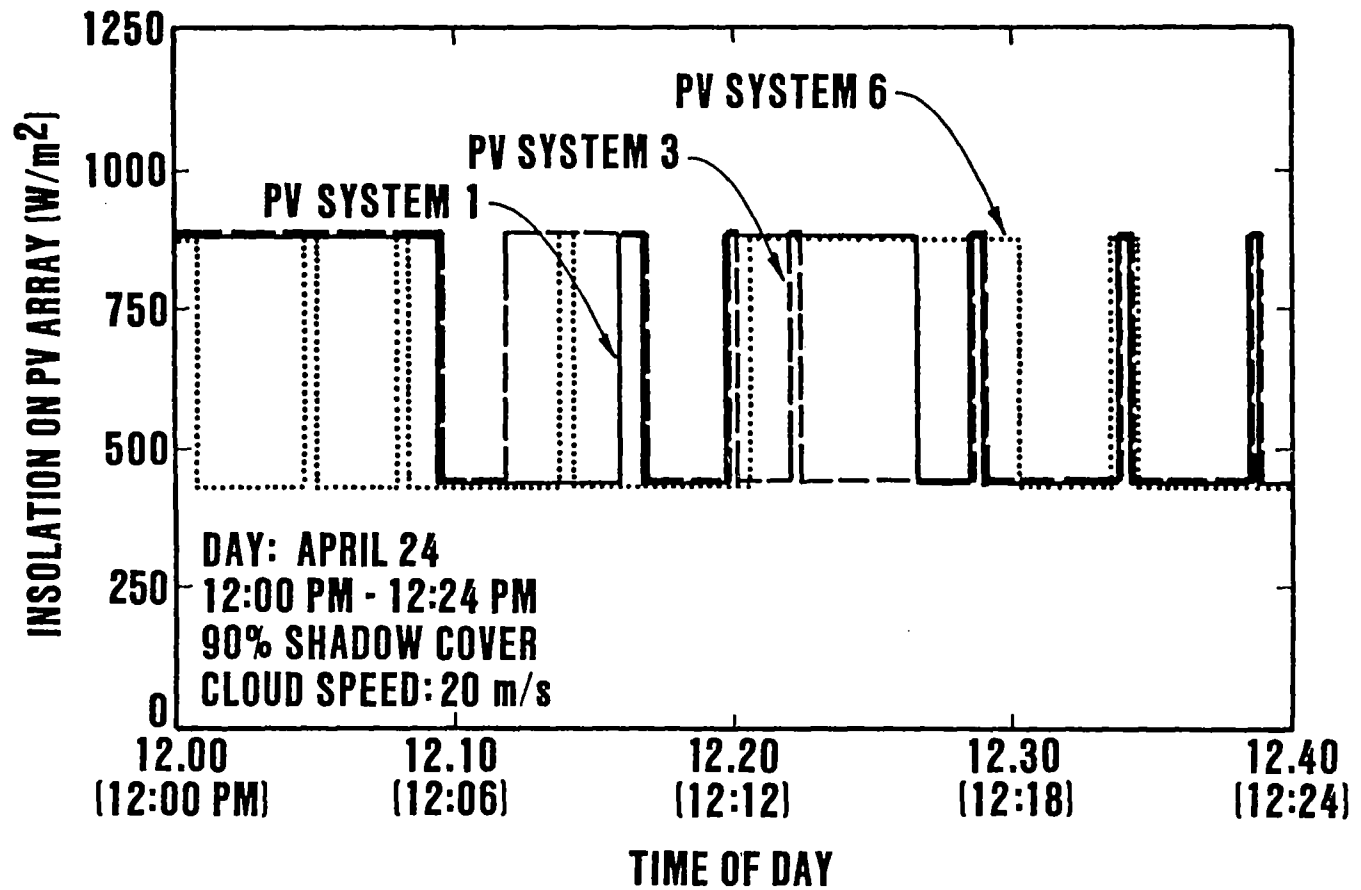
Figure 25. Insolation on PV Arrays Resulting from 90% Shadow Cover.

Cloud Diagrams

This program version generates a graphic display of the simulated cloud pattern. It was used to generate figures, such as Figures 22 and 24 for publications describing the simulation programs. It also was used to demonstrate the simulation.

Insolation Integrated Over 7.5 Minute Period

This program was used to verify the simulation results with the insolation data recorded by the OSU/PSO insolation monitoring station. The output of this version is incident solar energy (kWh/m^2) for 7.5 minute periods. The output is for one PV location only.

Aggregated PV Generation

Output of this version is the aggregated PV generation on each feeder for any time increment specified by the user. This was used to study the interactions of dispersed PV systems. It could also be the basis for other studies needing aggregated energy produced by dispersed PV systems.

Power Flow Input

This is the final version that provides the net load at each substation for power flow program input. The program computes the sum of the power generated by all PV systems on each substation and subtracts this from the normal load at the substation. This output is provided for up to 10 time increments specified by the user.

Data Preparation

Simulation input data is contained in several data files.

Service Area Data (SERVAREA.DAT)

This contains latitude and longitude data for the four sides of the service area. Data are on one line, four real F15.11 values:

<Northern lat.> <Southern lat.> (Eastern long.> <Western long.>

PV Systems Location (PVLOC.DAT)

Describes the location of each PV system. There is one line of data for each system, 3 real F15.11 values followed by one integer I15 value:

<Latitude> <Longitude> <Size> <Substation number>

The size is in rated kW at 1000 W/m² insolation. Substation number is the substation to which the PV system is connected.

Simulation Description (SIMULATE.DAT)

Simulation time and cloud descriptions are contained in this file. There are two lines. The first has 4 real F15.4 values:

<Date> <Begin time> <End time> <Output time increment>

The date is a number from 1 - 365 which represents the day of the year, with January 1 being day 1. Beginning and ending times for the simulation are in decimal hours. The output time increment, also in decimal hours, is the increment at which the "aggregated PV generation" and "power flow input" versions will output PV generation data.

The second line contains cloud data:

<Percent cover> <speed> <transmissivity>

These are real F15.2 values. Percent cover is the percentage of sky covered by clouds. Speed is the speed of cloud movement in m/s, and transmissivity is the percentage of full sunlight that passes through the clouds.

Utility Load Data (LOAD.DAT)

Normal utility bus load data is contained in this file. There is one line for each substation to which PV systems are connected. Data is one integer I10 value and one real F15.5 value:

<Bus number> <Load data (kW)>

This file is needed only for the "power flow input" version.

Not all versions of the simulation program require all the data described here. However, all versions will operate properly with the data files as described.

CHAPTER VII

VERIFICATION OF INSOLATION SIMULATION

The insolation simulation was verified by comparing its output with data recorded at the Oklahoma State University/Public Service Company of Oklahoma (PSO) Insolation Monitoring Station at OSU in Stillwater, Oklahoma. Recording of data began at this station in August 1985. Total solar energy, direct and diffuse, collected on a horizontal surface over 7.5 minute integration periods are recorded in Wh/m^2. The insolation simulation program was modified to provide energy data in these units. Both clear-sky and cloudy-sky models were verified, and results indicated that the clear-sky insolation and the cloud shadow models are valid and realistic.

Verification of clear-sky results was done by simulating insolation for entire days in September, October, December, January, February, and March. These were then compared with data recorded on clear days in each of those months. The results for January are shown in Figure 26. Statistics were calculated for the comparison and are shown in Table V. The residuals calculated are the actual value of energy collected at each increment minus the simulated value. The mean and standard deviation of this series are shown in Table V.

91
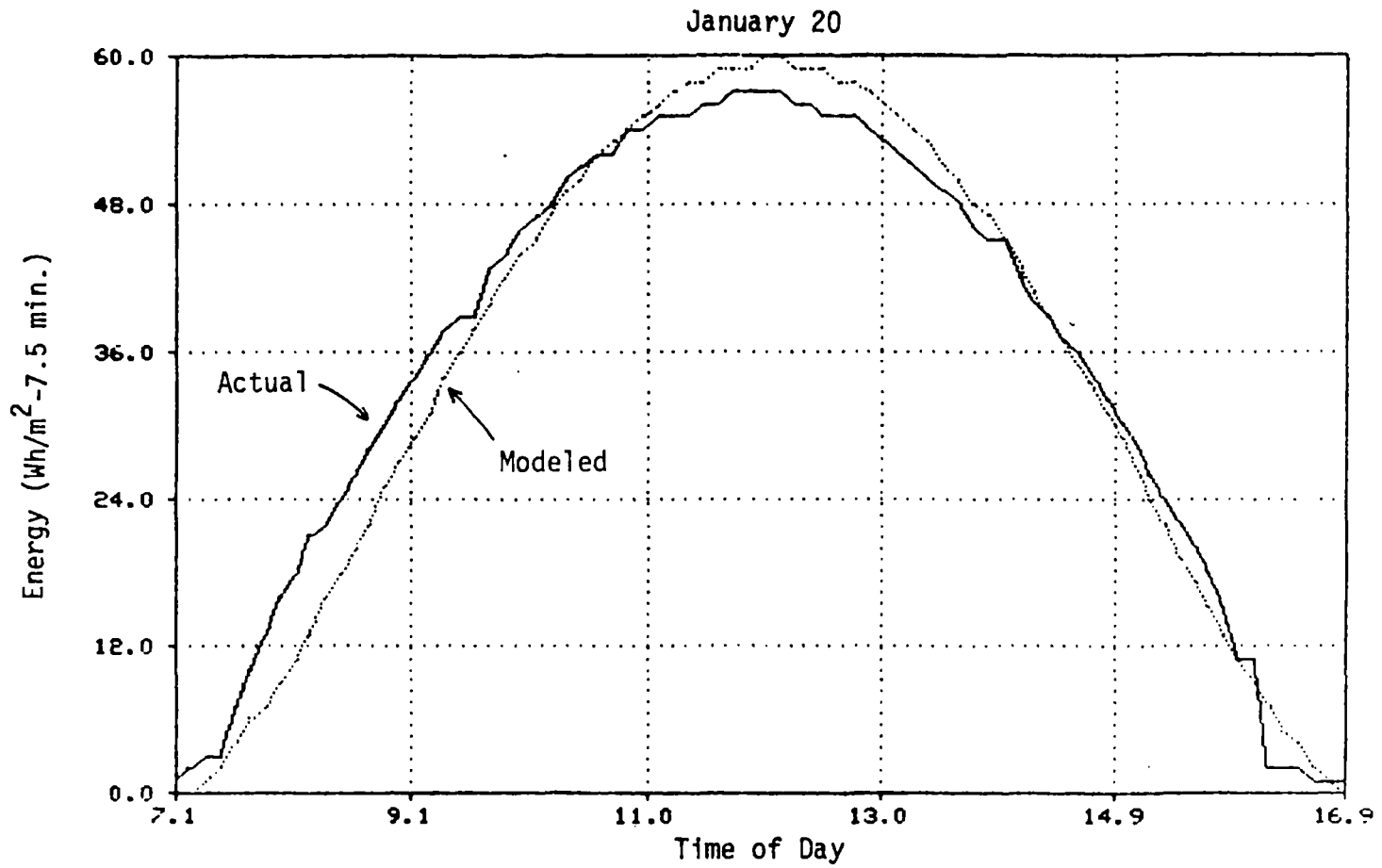
Figure 26. Clear Sky Insolation for January 20.

TABLE V

INSOLATION STATISTICS FOR JANUARY 1986

| | Total Energy (Wh/m²-day) | Peak Energy (Wh/m²-7.5 min) | Residuals (Actual − Simulated) | |
			Mean	Standard Deviation
Actual	2732	57		
Simulated	2678	60		
Difference	2.0%	5.3%	0.68	2.63

These results were typical; for some months the actual and simulated insolation curves matched almost exactly, while for others the correlation was not quite as good as January's. The insolation collected, however, is very sensitive to atmospheric conditions, and with only one year's recorded data to use for comparison the clear-sky simulation correlates very well with recorded data.

Cloudy-sky verification was done in the same way, except that the cloud pattern characteristics had first to be estimated. These were input to the insolation program and the results were compared with the recorded data. Residuals were computed by subtracting simulated clear-sky data from both simulated and actual cloud-sky data. Statistics were computed for the residuals. Several cloudy days were verified in this way.

An example of this process uses recorded data from February 27, 1986, which had fast-moving, broken clouds moving across a relatively clear sky. This was simulated with 50% cloud cover of small cumuliform clouds with 50% optical transmittance moving at 20 m/s. Actual and simulated insolation data and residuals are plotted in Figure 27.

Comparison of the curves indicates the simulation is good from the time shown as 10.0 on the graph, which is 10:00 am solar time, until about the time 14.0, or 2:00 pm solar time. Before 10:00 am the sky was clear, resulting in the monotonically increasing actual insolation. At 2:00 pm some thin high clouds appeared, causing the actual insolation to drop.
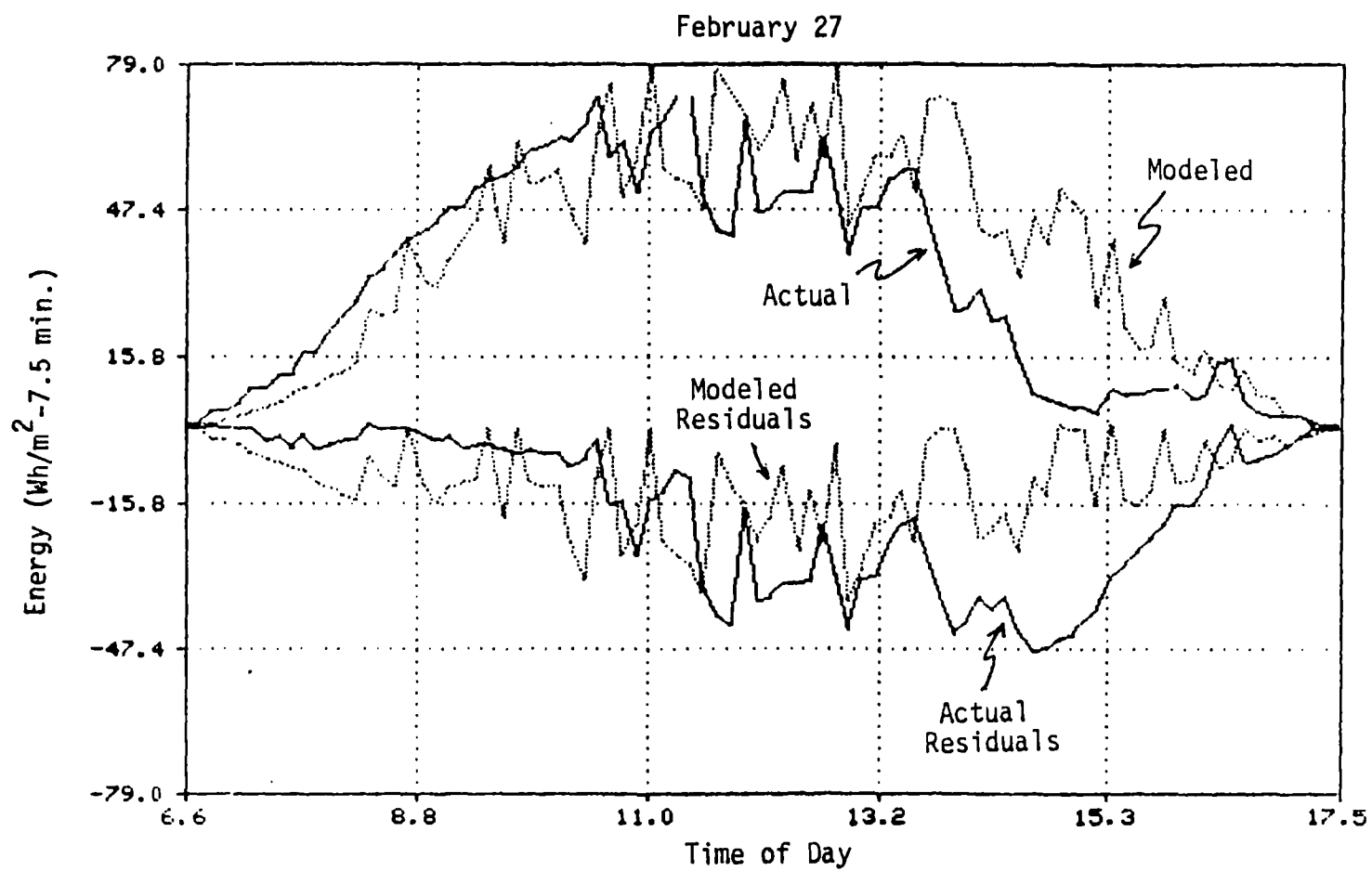
Figure 27. Cloudy Sky Insolation for February 27.

Statistics were therefore calculated for the period over which the simulation might be expected to be valid, 10:00 am to 2:00 pm. The results are shown in Table VI. Negative values for residual means were expected because the residuals represent the difference in cloudy- and clear-sky insolation. The lower value for the simulated mean results from higher values of actual simulation just after 10:00 am. When the clouds first appeared, the coverage was probably not yet 50%. This also explains higher standard deviation and lower total insolation for the simulated data.

The cloud patterns verified with recorded insolation data are listed in Table VII. These were used in the later simulations. Also listed in Table VII is a weather pattern known as a squall line, which is also used in the PV simulations. A squall line is a solid line of dark clouds which moves across a clear sky. Each PV system in the area stops generating as the shadow moves across its array. The squall line will therefore cause the total PV generation in an area to go from full output to zero output in a relatively short time. As this may be a worst case, it is included in the simulations.

TABLE VI

STATISTICS FOR FEBRUARY 27, 1986

	Total Energy (wh/m^2-day)	Residuals (Actual - Simulated)	
		Mean	Standard Deviation
Actual	1532	-24.9	11.4
Simulated	1247	-35.1	15.3

TABLE VII

CLOUD PATTERNS SIMULATED

Type of Clouds	Cover (%)	Speed (m/s)	Direction	Traansmittance (%)
Cumulus	50	20	south to north	50
Cumulus	30	10	south to north	40
Cumulus	10	10	south to north	50
Squall line	100	30	east to west	20

CHAPTER VIII

RESULTS AND DISCUSSION'

Interaction of Dispersed PV Generators

As discussed in Chapter II, to study the interaction of dispersed PV generators, five service areas of size ranging from 10 to 100,000 square kilometers, all square in shape, were used in simulations. Up to 1000 PV systems were uniformly dispersed throughout the areas and the worst case cloud patterns listed in Table VII were passed overhead. The outputs of the PV systems were aggregated and recorded every six seconds for an entire day. This was done five times for each cloud pattern to provide multiple cases for comparison.

The resulting power output data were analyzed for the greatest possible losses in PV generation during periods ranging from 6 seconds to 5 minutes. Consistently, two cases provided the greatest possible loss: (i) the squall line, and (ii) 50% cover, 20 m/s, 50% transmittance cumulus clouds.

Squall Line

The squall line was expected to provide the worst loss of PV generation because as it moves across the area, it causes complete loss

98

of PV generation. How fast this occurs is simply a function of the speed of cloud movement and the size of the service area. The time for 100% loss is shown in Table VIII for each service area studied.

The squall line, however, although it causes complete loss of PV generation, may not be the worst case for the utility. There are several reasons for this. First, the loss is a one-time loss. The PV generation shuts down as the squall line moves over and it does not resume generation until the sun comes back out. This loss is fairly predictable, because the system operators of a large utility monitor the weather conditions constantly and adjust the system accordingly. When a squall line is expected they could prepare for the impending loss of PV generation.

Further mitigating the squall line effects is the reduction in cooling load as the squall line passes through. While no records are kept at PSO, one operator at PSO recalls a load reduction of 200 MW out of a system load of 2700 MW during one hour as a squall line passed through the PSO service area [73]. This may substantially reduce the effects of losing PV generation during summer. During light load seasons, however, when cooling load is very low, this will not help.

Cumulus Clouds

The worst case cumulus clouds, while causing a much lower loss of PV generation than the squall line, may actually pose a more difficult problem for the utility. While the squall line is a one-time, predictable occurrence, PV generation will be continually lost and added

TABLE VIII

LOSS OF PV GENERATION DUE TO A SQUALL LINE

Service area size (square kilometers)	Time for loss of all PV generation (minutes)
10	1.8
100	5.5
1,000	17.6
10,000	55.3
100,000	175.7

under the cumulus pattern. The utility will have to continuously adjust for the changing PV generation. There is no mitigation for these changes, as load will be practically unaffected by the cumulus cloud pattern.

The possible loss of PV generation for each service area size, expressed as a percentage of total PV capacity in the area, is shown in Table IX for time intervals of 1-4 minutes. These worst cases all occurred durng the peak insolation time of day, around noon. Thus for the 10 square kilometer area, the table shows that 15.9% of the total PV generation can be lost during any one-minute period, and 19.1% during a two-minute interval. If, for example, there is 1 MW of dispersed PV generation located in a square area of 10 square kilometers, 159 kW of it can be lost in one minute. The utility must therefore be prepared at any time to increase its power into the area at a rate equal to 15.9% of the total PV generation in the area during a one-minute time interval. In addition, this PV generation can be regained during another one-minute interval.

The geographical diversity causes the possible percentage loss in PV generation to decrease as the size of the service area increases. While 15.9% of the PV generation could be lost during one minute in a 10 square kilometer area, only 5.5% can be lost in the 100 square kilometer area. As the service area size increases to 10,000 and 100,000 kilometers, the maximum loss is about 3%.

TABLE IX

LOSS OF PV GENERATION DUE TO CUMULUS CLOUDS

Service area size (square kilometers)	Maximum loss of PV generation for time interval (% of total PV capacity)			
	1 min.	2 min.	3 min.	4 min.
10	15.9	19.1	19.6	19.6
100	5.5	7.5	7.5	7.5
1,000	2.8	3.1	3.1	3.1
10,000	2.7	2.7	2.7	2.7
100,000	2.7	2.7	2.7	2.7

Simulation of Two PSO Substations

The smallest service area normally of interest to a utility is the area served by one distribution substation. The study performed on the square service areas was therefore repeated on two PSO substation service areas. The substations were chosen by PSO because they serve mostly residential load in southeast Tulsa, Oklahoma, the area that will likely see the first residential PV systems in the PSO service area.

The two service areas are outlined in Figure 28. Area 1 covers about 70 square kilometers, while area 2 covers about 18. Area 2 is oriented in an east-west direction, while area 1 runs about the same distance in each direction.

The corresponding simulation results are presented in Tables X and XI. The squall line results are again a simple function of the east-west length of the service area, because the squall line was simulated as moving west to east, the usual direction of such a pattern. For the cumulus pattern, the possible loss of 6.4% in one minute for area 1 correlates well with the results of the 100 square kilometer area studied previously. The results for area 2, however, are higher than those for the 10 square kilometer area. This is probably because of the area's east-west orientation, with the cumulus cloud pattern moving from south to north. In addition to the service area's geographic location, then, its shape and orientation may also be important in estimating the possible changes in PV generation.

SERVICE AREA 1

SERVICE AREA 2

1 MILE
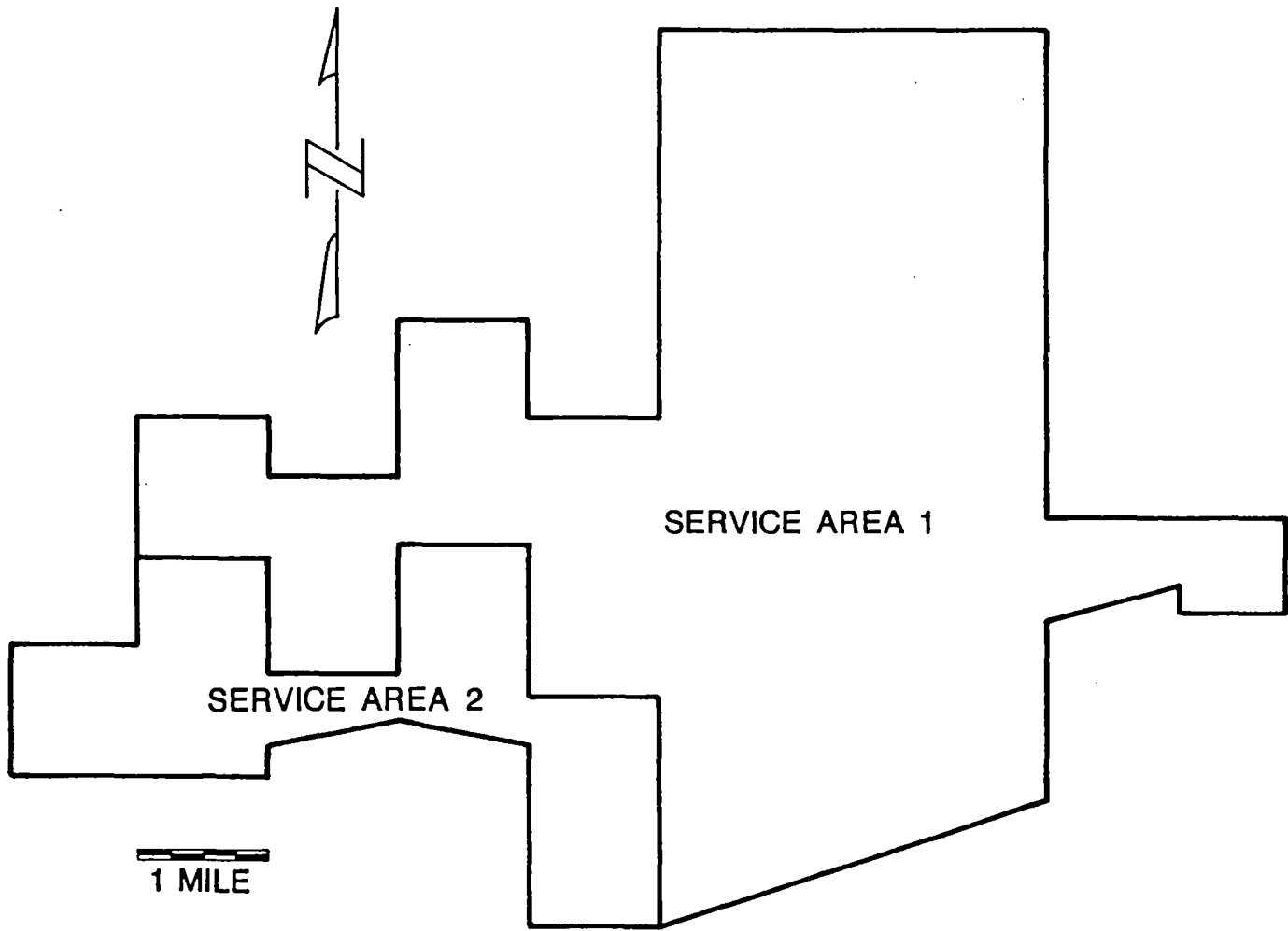
Figure 28.   PSO Substation Service Areas.

TABLE X

LOSS OF PV GENERATION DUE TO A SQUALL LINE

Substation	Time for loss of all PV generation (minutes)
1	8.0
2	4.5

TABLE XI

LOSS OF PV GENERATION DUE TO CUMULUS CLOUDS

Substation	Maximum loss of PV generation for time interval (% of total PV capacity)			
	1 min.	2 min.	3 min.	4 min.
1	6.4	9.5	10.2	10.2
2	22.2	26.9	28.0	28.0

Simulation of Southeast Tulsa

Next, the simulation service area was expanded to cover all of southeast Tulsa. This area is the first large area where residential PV generators might appear on the PSO system. Covering about 470 square kilometers, it is slightly longer east-west than north-south. The simulation results are presented in Table XII.

These results again correlate fairly well with the earlier values. The one minute value falls between the 100 and 1000 square kilometer areas as expected. The 2-4 minute values are somewhat higher, however, than the 100 square kilometer area values. This is again because of the longer east-west dimension, confirming the importance of service area shape and orientation.

Power Flow Simulation Results

The results of the PV interaction study were used to shape the final power flow studies. The worst case cumulus cloud pattern, 50% cover, 20 m/s speed, and 50% transmittance, and the squall line were simulated. Because operating penetration is much higher in the spring, both the cumulus pattern and squall line were simulated for two values of installed penetration, 15% and 30%. In the summer, only the squall line was simulated, at installed penetrations of 30% and 50%.

Power Flow Reversals

An unexpected change in direction of power flow on a transmission

TABLE XII

LOSS OF PV GENERATION IN SOUTHEAST TULSA

Squall line: Time for loss of all PV (minutes)	Cumulus clouds: Maximum loss of PV generation (% of total PV capacity)			
	1 min.	2 min.	3 min.	4 min.
17.0	5.2	7.9	8.0	9.0

or subtransmission line can cause problems with system protection devices. Reverse power relays are the most obvious example of this, but other relay and fuse coordination can also be affected. Tables XIII-XV immediately reveal that the probability of power flow reversal for either the area, tie lines, or transmission or subtransmission lines within the area increases as the operating penetration increases. There are no reversals below 30% penetration for the area or the tie lines analyzed. In the summer, when operating penetration is lower, there are no reversals at all.

Power flow into the southeast Tulsa area reverses once during the simulation period at 30% penetration for both spring cloud patterns. In the cumulus case, however, none of the tie line power flows reverse. This is possible because some tie lines initially carry power out of the area. Under the squall line, however, the direction of flow on three tie lines does reverse. It is reasonable to assume that flows could reverse in some circumstances under the cumulus pattern as well, although these results indicate it is not as likely as under the squall line.

Because of the great number of transmission and subtransmission lines in southeast Tulsa it was necessary to limit the number analyzed in this study. As indicated in the tables there were no changes in power flow direction on any of these lines. However, because of the reversals of power into the area and on some tie lines, it was felt that this might be misleading. Further detailed investigation of every line in the southeast Tulsa area revealed that power flow did indeed reverse

TABLE XIII

POWER FLOW STATISTICS FOR SPRING CUMULUS CLOUD PATTERN

Case	Power flow reversals	Overloads	Power flows above nominal	Maximum difference from nominal (% of nominal power flow)	Maximum change in power flow
Area, 15%	0		0	54%	4% / 1 min.
Ties, 15%	0	0	0		5% / 1 min.
Lines, 15%	0	0	0		22% / 1 min.
Area, 30%	1		0	110%	8% / 1 min.
Ties, 30%	0	0	0		14% / 1 min.
Lines, 30%	0	0	2		44% / 1 min.

TABLE XIV

POWER FLOW STATISTICS FOR SPRING SQUALL LINE PATTERN

Case	Power flow reversals	Overloads	Power flows above nominal	Maximum difference from nominal (% of nominal power flow)	Maximum change in power flow
Area, 15%	0		0	66%	31% / 2 min.
Ties, 15%	0	0	0		51% / 2 min.
Lines, 15%	0	0	2		140% / 2 min.
Area, 30%	1		0	134%	62% / 2 min.
Ties, 30%	3	0	0		97% / 2 min.
Lines, 30%	0	0	2		260% / 2 min.

TABLE XV

POWER FLOW STATISTICS FOR SUMMER SQUALL LINE PATTERN

Case	Power flow reversals	Overloads	Power flows above nominal	Maximum difference from nominal (% of nominal	Maximum change in power flow power flow)
Area, 30%	0		0	43%	21% / 2 min.
Ties, 30%	0	0	0		66% / 2 min.
Lines, 30%	0	0	3		792% / 2 min.
Area, 50%	0		0	73%	35% / 2 min.
Ties, 50%	0	0	0		109% / 2 min.
Lines, 50%	0	0	3		1323% / 2 min.

on at least one line in every simulation at each penetration. Power flow reversals may therefore be expected on transmission and subtransmission lines at penetrations as low as 15%.

Differences from Normal Power Flows

As PV generation decreases in any area the power flow on lines into that area must increase, leading to the possibility of line overloads. Tables XIII-XV show that there were no line overloads in any of the simulations. In the cases where lines did go over their nominal power flow values, however, they sometimes went many times over the nominal values. The PSO lines in question were normally operating significantly below their ratings, so overloads did not occur, but if the lines had been operating near rated values, the lines would have been overloaded.

Because much of the normal load is being supplied by PV generation, many of the lines are operating at less than their normal power flow values. Such significant reductions in power flow on a line may cause reactive power, voltage control, and protection problems. Tables XIII-XV indicate that severe underloading can occur when dispersed PV is operating. With 15% penetration in the spring the flow into southeast Tulsa is 66% below normal with all PV systems operating. When penetration reaches 30% power flow into southeast Tulsa reverses and reaches 34% of the normal flow magnitude, but in the opposite direction. Summer underloadings are not as severe, but are still quite significant.

Changes in Power Flows

Continuously changing power flows raise two questions for PSO. The first of these is whether the utility can maintain the necessary power flow into the southeast Tulsa area as the PV generation changes, and how much this will cost. The second question is what the tie line and distribution line swings will do to system operation and protection.

Under the cumulus cloud pattern the greatest swing in power into the area is 4% of the nominal 250 MW flow, or 10 MW, in one minute when penetration is 15%. This doubles when penetration is 30%, becoming 8%, or 20 MW, in one minute. This change can occur at any time, can be an increase or decrease in power, and is unpredictable.

When the squall line moves over, the swings are much greater, but they are also predictable. When penetration is 15%, power flow into the southeast Tulsa area can increase by as much as 78 MW in 2 minutes. When penetration increases to 30%, the maximum swing becomes 155 MW in 2 minutes in spring and 165 MW (21% of the nominal 789 MW) in 2 minutes in the summer.

As predicted by the studies of areas of various sizes in the previous chapter, the swings on transmission and subtransmission lines within southeast Tulsa are greater in percentage than those for the area or on the tie lines. What was not expected, however, is that the greatest swings occur in the summer. The flows on one line increased by more than 7 times in 2 minutes when penetration was 30%, and by more

than 13 times under 50% penetration. It is very important to note that, although they occur during the movement of a squall line, these swings, unlike the changes in flow into the area, are not at all predictable. The changes apparently are greater in the summer because the loads are greater, the lines are more heavily loaded, and the output of the PV systems is higher.

CHAPTER IX

CONCLUSIONS

Interaction of Dispersed PV Systems

The most important conclusions of the PV interaction study are the quantitative relationships between the size of the service area throughout which PV generation is dispersed and the maximum possible change in PV generation during a certain time period. The change is expressed as a percentage of the total PV generation in the area. These results are presented in Tables VIII and IX in Chapter VIII. The percentage amount of possible change drops as the area increases because of geographical diversity among the dispersed PV systems. The farther apart the systems are, the less their outputs correlate.

Other important points regarding these results are:

* For the larger areas, the maximum changes in PV output usually occur within 1-2 minutes. Longer intervals result in no greater changes in PV generation.

* While the squall line causes 100% loss of PV generation, it may not be as important as the cumulus cloud pattern because is is a one-time occurrence that can be predicted fairly accurately. The

cumulus pattern causes continuous changes as long as it is present. The loss of PV generation caused by the squall line are also mitigated in the summer by a reduction in cooling load as the line passes through. Furthermore, for large areas the squall line is not important because of the time it takes to move across the area.

* The maximum PV changes always occur during peak insolation times around solar noon, while the system peaks (for most summer-peaking utilities) occur in late afternoon or early evening. The maximum PV change therefore occurs during off-peak times, when operating PV penetration (the ratio of installed PV capacity to operating system capacity) is greater.

When two actual PSO substation service areas and then the entire southeast Tulsa area are simulated, the results agree well with the five previous service area cases. Small differences point out the importance of service area shape and orientation. The maximum PV change seems to be greater for a service area of non-uniform shape oriented in an east-west direction, when clouds are moving south to north.

All the results indicate that the effects of PV generation changes will be greatest at the substation level. This means that the power flows among substations may change significantly from those normally expected. This may have important implications for transmission, subtransmission, and distribution system protection and control. It also indicates, however, that system-wide problems such as generation ramping and changes in tie-line flows may be minimal.

The season, and the resulting load on the utility system, greatly influences the effects of PV generation changes. For a certain installed penetration (the ratio of installed PV capacity to total installed system capacity) the operating penetration varies widely as the seasons change. For the PSO system, for example, the light load case studied has a peak load of only about 30% of the summer peak load. The light season operating penetration is therefore more than three times that of the summer case. An operating penetration of 30% in July therefore becomes 100% in March. While the PV generation is lower in the spring and fall than in the summer, it is still about 75% of the summer value. The effects will therefore be much more pronounced in spring and fall.

The relatively small changes in PV generation caused by the cumulus cloud pattern will have very little effect during summer times at any foreseeable penetration of residential PV. The squall line or similar pattern is therefore the most important for the summer. This is, however, when the effects of the squall line are best mitigated by the resulting drop in cooling load. The light load seasons will therefore determine the significant penetration at which the utility begins to notice the variable PV generation.

The point at which PV penetration becomes significant will be the point where the maximum possible change in PV generation forces the utility to change its operating practices. This point can be estimated by comparing the maximum PV change with normal variations of load on the system. The swings in PV generation may cause operating problems on the

system, but more likely the utility will simply see increased operating costs.

Power Flow Studies

Power flow reversals on distribution, subtransmission, and transmission lines can cause problems for system protection equipment. On transmission lines carrying power into the southeast Tulsa area reversals occur at 30% penetration of PV systems, but not at 15%. Reversals occur at 15% penetration, however, on lines within the area.

The potential for reversals increases as PV penetration increases, and is therefore greater in the spring and fall, when operating penetrations are higher, than in the summer. The potential is also greater during a squall line than under cumulus clouds. It is, however, extremely dependent on the configuration and loading of the system, so it should be considered a possibility under any pattern and during any season.

As the cloud pattern moves, its shadows cause the PV generation in southeast Tulsa to vary. The power flows within the area therefore change to compensate for varying PV generation. Because of this transmission tie lines and transmission and subtransmission lines within southeast Tulsa may be loaded at many times under or over their normal loading for a given load configuration. This occurs at 15% and 30% penetration, but seems to become worse as penetration increases. Overloading damages equipment and underloading can cause reactive power

and voltage control problems. Although it seems worse during the squall line, it is again highly dependent on configuration and loading, so it must be assumed to be possible during any season and any pattern.

As expected, the changes in power flow over time are worst during the squall line pattern. At 15% installed penetration in the spring the power flow into southeast Tulsa increased by 78 MW in a 2-minute interval. When the penetration was 30% the increase was 155 MW in the spring and 165 MW, higher because of higher insolation, during the summer. This is predictable by the PSO operators, who monitor weather conditions constantly.

Unpredictable changes, however, occur during the cumulus cloud pattern. At 15% installed penetration in the spring swings of 10 MW per minute occurred during the simulation. At 30% these doubled to 20 MW per minute. These swings can occur continuously during the cumulus pattern.

As predicted by the previous simulations, the power swings on transmission and subtransmission lines within southeast Tulsa are worse than on external transmission tie lines. The worst swings are in the summer, probably because the system is more heavily loaded and the PV generators are producing more power. The power flow on one line changed by almost 8 times its nominal value in 2 minutes at 30% installed penetration. Although this occurred during the squall line, and the system operators could anticipate the swings, it is very unlikely the operators could predict their magnitude or on which lines such swings will occur, or do anything to mitigate the effects.

Scope for Further Work

This research has identified several issues relating to the effects of dispersed PV generation on an electric utility that should be studied further. These are outlined below.

Mathematical Modeling of Aggregated

Dispersed PV Generation

To study the effects of dispersed PV generation on one utility using the methods described in this work, a detailed two-dimensional simulation of insolation is needed. The results of this work, however, indicate that some much simpler models of the aggregate generation of dispersed PV systems might be developed. These models should be investigated.

Protection of Distribution Systems with

High Penetrations of Dispersed PV

Large power swings and power reversals on the PSO distribution system indicates there will be problems with existing protection practices. A detailed study of the distribution system should be done to determine how the PV generation will affect fuse and relay coordination, fault detection and clearing, and emergency operation.

System Stability

The effects of power swings and reversals on the transmission system should also be investigated. Detailed stability analyses will be needed to assess this.

Increasing the Limits of PV Penetration

The factors limiting the penetration of dispersed PV and the possibility of ameliorating some of these should be addressed. A list of utility actions to increase allowable penetrations, with emphasis on low cost actions, would result.

Optimal Economic Operation

Optimal economic operation of a utility system is now determined by the generation fuels and efficiency, transmission losses, and the level and location of loads on the system. Dispersed PV systems outside utility control will force changes in this. These changes should be studied.

Finally, during the work on this project some additional work was identified. During insolation model verification, for example, it was observed from the data recorded at the OSU/PSO insolation monitoring station that peak insolation actually occurs on partly cloudy days. This has been observed by others before, and one proposed explanation is that the clouds reflect additional sunlight to the earth. This should be investigated further.

A lack of research on distribution feeder modeling was also noticed during this portion of the study. The possibility of improving existing models should be investigated. Some of the research in this project is quite applicable to this.

While there are now no areas in which PV penetration has reached the levels described as significant in this work, there will be such areas in the future. Such areas will at first be isolated, such as a PV housing development. The fact that such an area may be small and isolated, however, only increases its importance, because the greatest potential changes in PV generation occur in small areas. The projects discussed here should therefore be pursued.

REFERENCES

[1] T. Hoff and G. Shushnar, "Two Years of Performance Data for the World's Largest Photovoltaic Power Plant," IEEE Paper No. 86 SM 464-2, presented at the 1986 Summer Power Meeting, Mexico City, Mexico, July 1986.

[2] T. Moore, "Pioneering the Solid-State Power Plant," EPRI Journal, Vol. 10, No. 10, pp. 6-19, December 1985.

[3] N. W. Patapoff Jr., D. R. Mattijetz, "Utility-Interconnection Experience with an Operating Central-Station MW-Sized Photovoltaic Plant," IEEE Transactions on Power Apparatus and Systems, Vol. PAS-104, No. 8, pp. 2020-2024, August 1985.

[4] D. J. Rosen, et al, "Design, Construction, and Startup of the SMUDPV1 1-MW Photovoltaic Central Station Power Plant," IEEE Paper 85 WM 098-9, to be published in IEEE Transactions on Energy Conversion.

[5] S. L. Leonard, "Photovoltaic Power Generation for Utilities: The Implications of Some Recent Projects and Design Studies," IEEE Transactions on Energy Conversion, Vol. EC-1, No. 2, pp. 61-67, June 1986.

[6] R. Ramakumar, "Photovoltaics and Electric Utilities - Promises and Prospects." Energy Information Dissemination Program, Report No. 17, pp. 62-103, Oklahoma State University, February 11, 1986.

[7] R. Taylor, et al, "Photovoltaics Generation - Recent Technology Advancements, a Panel Discussion," IEEE Transactions on Power Apparatus and Systems, Vol. PAS-104, No. 11, pp. 2962-2967, November 1985.

[8] V. K. Kapur, A. K. P. Chu, "Battery Requirements for Photovoltaic Energy Storage," Proceedings of the 16th Intersociety Energy Conversion Engineering Conference, Vol. 1, pp. 685-688, 1981.

[9] Public Utilities Regulatory Policies Act of 1978. P.L. 95-617.

[10] P.D. Maycock, E.N. Stirewalt, Photovoltaics: Sunlight to Electricity in One Step, Andover: Brick House, 1981.

[11] S. Karaki, D.S. Ward, G.O.G. Lof, "Near Future Applications of Solar Energy," IEEE Transactions on Power Apparatus and Systems, Vol. PAS-93, no. 6, November/December 1974, p. 1737.

[12] J.C. Powell, "Solar Central Electric Power Generation - A Baseline Design," Proceedings of the IEEE Power Engineering Society 1975 Summer Meeting, San Francisco, July 1975, paper A 75 580-1.

[13] R. Ramakumar, H.J. Allison, W.L. Hughes, "Solar Energy Conversion and Storage Systems for the Future," IEEE Transactions on Power Apparatus and Systems, Vol. PAS-94, no. 6, November/December 1975, pp. 1926-1934.

[14] L.O. Herwig, "Solar Energy Systems for Electricity Production," Proceedings of the IEEE Power Engineering Society 1975 Winter Meeting, paper C 75 014-6.

[15] D.B. Miller, K. W. Boer, "Solar-Electric Residential System Tests," Proceedings of the IEEE Power Engineering Society 1975 Summer Meeting, San Francisco, July 1975, paper A 75 417-6.

[16] A. Braunstein, D. Biran, "A Charging Control System for Accumulators Charged by Means of Solar Cell Arrays," IEEE Transactions on Power Apparatus and Systems, Vol. PAS-95, no. 5, September/October 1976, pp. 1567-1570.

[17] A. Braunstein, D. Biran, "Solar Electrical Systems - Theory and Applications," IEEE Power Engineering Society Papers Energy Development II, 1976, IEEE Publication No. 76 CH 1102-3-PWR.

[18] W.G. Pollard, "A General Method for the Evaluation of Possible Systems for Electric Generation with Solar Energy," IEEE Transactions on Power Apparatus and Systems, Vol. PAS-97, no. 5, September/October 1978, pp. 1656-1664.

[19] L.M. Magid, B.W. Marshall, D.G. Schueler, "Solar Photovoltaic Power Systems," Proceedings of the IEEE Power Engineering Society 1977 Summer Meeting, Mexico City, July 1977, paper A 77 695-0.

[20] C.R. Chowaniec, P.F. Pittman, B.W. Marshall, "A Reliability Assessment Technique for Generating Systems with Photovoltaic Power Plants," Proceedings of the IEEE Power Engineering Society 1977 Summer Meeting, Mexico City, July 1977, paper A 77 655-4.

[21] R. Fischl, P.R. Herczfeld, T.F. Halpin, D.B. Stewart, "Design of Integrated-Electric-Solar-Utility System for Peak Load Shaving," Proceedings of the IEEE Power Engineering Society 1979 Winter Meeting, New York, February 1979, paper A 79 102-5.

[22] A. Braunstein, D. Biran, "Some Economical Aspects of Solar Electric System Solar Power Packs," Proceedings of the IEEE Power Engineering Society 1978 Summer Meeting, Los Angeles, July 1978, paper A 78 557-1.

[23] A. Braunstein, D. Biran, "On the Strategy of Development and Production of Solar Electric Systems," IEEE Transactions on Power Apparatus and Systems, Vol. PAS-98, no. 4, July/August 1976, pp. 1208-1212.

[24] P.H. Stiller, C.H. Eichler, L.A. Kilar, "Interconnection of On-Site Photovoltaic Generation with the Electric Utility - Site Owner Concerns," Proceedings of the 14th IEEE Photovoltaics Specialists Conference, San Diego, California, 1980, pp. 240-245.

[25] R.D. Tabors, S. Finger, A.J. Cox, "Economic Operation of Distributed Power Systems within an Electric Utility," IEEE Transactions on Power Apparatus and Systems, Vol. PAS-100, no. 9, September 1981, pp. 4186-4195.

[26] J. Fitzer, W.E. Dillon, "Impact of Residential Photovoltaic Power System on an Electric Utility," Proceedings of the 15th IEEE Photovoltaics Specialists Conference, Kissimmee, Florida, 1981, pp. 278-279.

[27] P.F. DeBuck, R.W. Neal, "Assessment of the Effects of Distributed Photovoltaic Systems on Utility Subtransmission and Distribution Networks," Proceedings of the 15th IEEE Photovoltaics Specialists Conference, Kissimmee, Florida, 1981, pp. 299-304.

[28] S.T. Lee, Z.A. Yamayee, "Load-Following and Spinning-Reserve Penalties for Intermittent Generation," IEEE Transactions on Power Apparatus and Systems, Vol. PAS-100, no. 3, March 1981, pp. 1203-1211.

[29] Z.A. Yamayee, "Financial Transactions Between the Electric Utility and the Solar Photovoltaic System Owner," IEEE Transactions on Power Apparatus and Systems, Vol. PAS-100, no. 8, August 1981, pp. 3950-3958.

[30] Z.A. Yamayee, "Utility Integration Issues of Residential Photovoltaic Systems," IEEE Transactions on Power Apparatus and Systems, Vol. PAS-100, no. 5, May 1981, pp. 2365-2373.

[31] M.C. Caramanis, R.D. Tabors, K.S. Nochur, "The Introduction of Non-Dispatchable Technologies as Decision Variables in Long-Term Generation Expansion Models," IEEE Transactions on Power Apparatus and Systems, Vol. PAS-101, no. 8, August 1982, pp. 2658-2662.

[32] J.T. Day, M.J. Malone, "Electric Utility Modeling Extensions to Evaluate Solar Plants," IEEE Transactions on Power Apparatus and Systems, Vol. PAS-101, no. 1, January 1982, pp. 120-126.

[33] F.S. Ma, D.H. Curtice, "Distribution Planning and Operations with Intermittent Power Production," IEEE Transactions on Power Apparatus and Systems, Vol. PAS-101, no. 8, August 1982, pp. 2931-2940.

[34] H. Chestnut, et al, "Monitoring and Control Requirements for Dispersed Storage and Generation," IEEE Transactions on Power Apparatus and Systems, Vol. PAS-101, no. 7, July 1982, pp. 2355-2363.

[35] G.L. Campen, "Residential Photovoltaic System Tied to Utility System: Harmonics and Power Factor Considerations," IEEE Transactions on Power Apparatus and Systems, Vol. PAS-101, no. 12, December 1982, pp. 4632-4639.

[36] T.S. Key, J.W. Klein, "Residential Photovoltaic Power Conditioning Technology for Grid Connected Applications," Proceedings of the 16th IEEE Photovoltaics Specialists Conference, San Diego, California, 1982, pp. 1456-1458.

[37] B.W. McNeill, M.A. Mirza, "Line-commutated Photovoltaic Residential System: Estimated Power Quality," IEEE Transactions on Power Apparatus and Systems, Vol. PAS-102, no. 10, October 1983, pp. 3288-3295.

[38] R.C. Dugan, W.T. Jewell, D.J. Roesler, "Harmonics and Reactive Power from Line Commutated Inverters in Proposed Photovoltaic Subdivision," IEEE Transactions on Power Apparatus and Systems, Vol. PAS-102, no. 9, September 1983, pp. 3205-3211.

[39] A.J. Stranix, A.H. Firester, "Conceptual Design of a 50 MW Central Station Photovoltaic Power Plant," IEEE Transactions on Power Apparatus and Systems, Vol. PAS-102, no. 9, September 1983, pp. 3218-3225.

[40] E.J. Simburger, R.B. Fling, "Engineering Design for a Central Station Photovoltaic Power Plant," IEEE Transactions on Power Apparatus and Systems, Vol. PAS-102, no. 6, June 1983, pp. 1668-1677.

[41] W.S. Ku, et al, "Economic Evaluation of Photovoltaic Generation Applications in a Large Electric Utility System," IEEE Transactions on Power Apparatus and Systems, Vol. PAS-102, no. 8, August 1983, pp. 2811-2816.

[42] A. Traca de Almeida, "Source Reliability in a Combined Wind-Solar-Hydro System," IEEE Transactions on Power Apparatus and Systems, Vol. PAS-102, no. 6, June 1983, pp. 1515-1520.

[43] J. Klein, et al, "Requirements for a Transformerless Power Conditioning Subsystem," IEEE Transactions on Power Apparatus and Systems, Vol. PAS-103, no. 8, August 1984, pp. 2269-2276.

[44] C.M. Ong, "Line Commutated Photovoltaic Systems on a Distribution Feeder; Operational Behavior," IEEE Transactions on Power Apparatus and Systems, Vol. PAS-103, no. 8, August 1984, pp. 2262-2268.

[45] G. Cokleinides, et al, "Investigation of Utility Interface Problems of Photovoltaic Systems," Proceedings of the 16th IEEE Photovoltaics Specialists Conference, Kissimmee, Florida, 1984, pp. 1234-1241.

[46] Y. Takeda, et al, "Utility Interface Problems of Distributed Photovoltaic System," Proceedings of the 16th IEEE Photovoltaics Specialists Conference, Kissimmee, Florida, 1984, pp. 541-546.

[47] J.W. Stevens, T.S. Key, "The Utility Interface - Can State-of-the-Art Power Conditioners Alleviate Our Concerns?" Proceedings of the 16th IEEE Photovoltaics Specialists Conference, Kissimmee, Florida, 1984, pp. 1168-1174.

[48] G.T. Chinery, J.M. Wood, "TVA'S Photovoltaic Activities," IEEE Transactions on Power Apparatus and Systems, Vol. PAS-104, no. 8, August 1985.

[49] S.M. Chalmers, et al, "The Effect of Photovoltaic Power Generation on Utility Operation," IEEE Transactions on Power Apparatus and Systems, Vol. PAS-104, no. 3, March 1985, pp. 524-530.

[50] W. T. Jewell, D. T. Rizy, "Interconnection Problems Associated with Small Dispersed Generators and Inverter Devices," ISA Transactions, Vol. 23, No. 2, pp. 21-26.

[51] Draft Interim Working Guidelines and Discussion Concerning the Interface of Small Dispersed Photovoltaic Power Producers with Electric Utility Systems. IEEE Standards Coordinating Committee on Photovoltaics, October, 1981. Published in Interconnecting DC Energy Systems: Responses to Technical Issues. (EPRI AP/EM-3124). Electric Power Research Institute, Palo Alto, California, June 1983.

[52] R. Ramakumar, Ward Jewell, Proposed Guide to Utility-Interactive Photovoltaic Systems, Public Service Company of Oklahoma Research and Development, November 1984.

[53] R. P. Schulz, "Impacts of New Energy Technology Generation and Storage Processes on Power System Stability and Operability," Proceedings: Research Needs for the Effective Integration of New Technologies into the Electric Utility. (CONF-820772) Oak Ridge National Laboratory, May 1983, pp. 193-220.

[54] R. D. Dunlop, D. N. Ewart, "System Requirements for Dynamic Performance and Response of Generating Units," IEEE Transactions on Power Apparatus and Systems, Vol. PAS-94, No. 3, May/June 1975, pp. 838-849.

[55] D. N. Ewart, et al, "Power Response Requirements for Electric Utility Generating Units." Proceedings of the American Power Conference, Volume 40, 1978, pp. 1139-1150.

[56] D. T. Rizy, W. T. Jewell, J. P. Stovall, "Operational and Design Considerations for Electric Distribution Systems with Dispersed Storage and Generation," IEEE Transactions on Power Apparatus and Systems, Vol. PAS-104, No. 10, pp. 2684-2871, October 1985.

[57] L. H. Fink, W. E. Feero, "Effective Integration of New Technologies in Electric Energy Systems," IEEE Transactions on Power Apparatus and Systems, Vol. PAS-101, No. 7, July 1982, pp. 1833-1842.

[58] International Cloud Atlas, Volume I: Manual on the Observation of Clouds and Other Meteors. World Meteorological Organization, 1975.

[59] The Effect of Photovoltaic Power Generation on Utility Operation. (SAND 84-7000). Arizona State University, February 1984.

[60] R. T. Hall, Cloud Shadow Modeling. (ATM76(7506-01)-1). Aerospace Corporation, September 1975.

[61] R. H. Blackmer, Jr., S. M. Serebreny, "Dimensions and Distributions of Cumulus Clouds as Shown by U-2 Photographs." Stanford Research Institute Scientific Report 4, (AFCRL-62-609), July 1962.

[62] R. H. Blackmer, Jr., S. M. Serebreny, "Statistical Distribution of Cumulus Clouds from U-2 Photographs." Stanford Research Institute Technical Report 1, November 1962.

[63] R.H. Blackmer, Jr., J. E. Alder, "Statistics of Cumuliform Clouds from U-2 Photographs." Stanford Research Institute Final Report, May 1963.

[64] T. Yagi, T. Harimaya, C. Magono, "On the Shape and Movement of Cirrus Uncinus Clouds by the Trigonometric Method Utilizing Stereophotographs - Studies of Cirrus Clouds: Part II." Journal of the Meteorological Society of Japan, Vol. 46, No. 4, August 1968, pp. 266-278.

[65] B. Haurwitz, "Insolation in Relation to Cloud Type." Journal of Meteorology, Vol. 5, June 1948, pp. 110-113.

[66] F. Kasten, G. Czeplak, "Solar and Terrestrial Radiation Dependent on the Amount and Type of Cloud." Solar Energy, Vol. 24, 1980, pp. 177-189.

[67] M. A. Atwater, J. T. Ball, "A Numerical Solar Radiation Model Based on Standard Meteorological Observations." Solar Energy, Vol. 21, 1978, pp. 163-170.

[68] M. A. Atwater, J. T. Ball, "A Surface Solar Radiation Model for Cloudy Atmospheres." Monthly Weather Review, Vol. 109, April 1981, pp. 878-888.

[69] T. P. Meyers, R. F. Dale, "Predicting Daily Solar Insolation with Hourly Cloud Height and Coverage." Journal of Climate and Applied Meteorology, Vol. 22, April 1983, pp. 537-545.

[70] T. Chiyu, H. Kon, C. Magono, "The Moving Velocity of Cumulus Humilis Clouds." Journal of the Meteorological Society of Japan, Vol. 51, No. 1, February 1973, pp. 43-53.

[71] W. E Shenk, E. R. Kreins, "A Comparison Between Observed Winds and Cloud Motions Derived from Satellite Infrared Measurements." Journal of Applied Meteorology, Vol. 9, August 1970, pp. 702-710.

[72] W.T. Jewell, R. Ramakumar, "Insolation Model for Simulation of an Electric Utility with High Penetration of Dipsersed Photovoltaic Generation," Proceedings of the 1985 International Solar Energy Society Biennial Congress, Montreal, June 1985.

[73] Statement by Otto Bryant, Energy Control Center, Public Service Company of Oklahoma, Tulsa, Oklahoma, August 4, 1986.

APPENDIX A

LISTING OF INSOLATION SIMULATION PROGRAMS

```
C        Two-dimensional time-domain insolation model.
C        Ward Jewell.     May 1985.

C        This program simulates time-domain insolation over a
C            large geographical area.  The model includes the effects
C            of time of year, time of day, and of moving clouds
C            passing over the area.

C        Output is the insolation at each defined location within
C            the area at each time increment for the period of the
C            simulation.

C        REVISION: FEBRUARY 1986.

C        Input to the model now includes a group (substation) number
C            for each PV system, and one value of efficiency for
.C           all PV systems simulated.  The arrays are dimensioned for
C            up to 1000 PV systems and 300 substations.

C        Output is now the sum of the power generated by all PV
C            systems on each substation for up to 10 output time
C            increments specified in the input data.

C        The variable PV_KW_SIZE is used in this revision.  It is
C            assumed that this is the output of the PV system at
C            insolation of 1000 watts per square meter.  This is
C.           a common way of rating PV systems.

         REAL*8 N_LAT, S_LAT, E_LONG, W_LONG, PV_LAT, PV_LONG,
        1       N_S_INCREMENT_LENGTH,
        2       LENGTH_DEGREE_LAT, LENGTH_DEGREE_LONG,
        3       PV_LATITUDE (1000), PV_LONGITUDE (1000),
        4       PV_KW, PV_KW_SIZE (1000), BEGIN_TIME, END_TIME,
        5       PERCENT_COVER, SPEED, TRANSMISSIVITY,
        6       TIME, TIME_INCREMENT, CENTER_LAT, INSOLATION,
        7       ALTITUDE, DATE, FILL_LEVEL, e_w_increment_count,
        8       INCREMENT_NUMBER, SHADOW_EW

         INTEGER*4 PV_SYSTEM_NUMBER,
        1         PV_LOC_WEST (1000), PV_LOC_NORTH (1000),
        2         MAX_PV, PV_LINK (0:1000), PRESENT,
```

```
   3            START_CLOUD (100), SEED, shadow_ns

    COMMON N_LAT, S_LAT, E_LONG, W_LONG, PV_LAT, PV_LONG,
   1       e_w_increment_count, N_S_INCREMENT_LENGTH,
   2       LENGTH_DEGREE_LAT, LENGTH_DEGREE_LONG, PV_LINK,
   3       PV_LOC_WEST, PV_LOC_NORTH, PV_SYSTEM_NUMBER,
   4       DATE, PERCENT_COVER, SPEED,
   5       TRANSMISSIVITY, TIME, TIME_INCREMENT, CENTER_LAT,
   6       INSOLATION, ALTITUDE, INCREMENT_NUMBER, START_CLOUD,
   7       FILL_LEVEL, SEED, shadow_ns, SHADOW_EW

C        Set up the arrays for storing insolation data for the PV systems.

    REAL*8 PV_INSOL (1000, 100), SUB_POWER (300),
   1       start_output_time
    REAL*8 PSO_LOAD_DATA (300),
   1       BUS_LOAD (10,300), OUTPUT_TIME_INCREMENT,
   2       LOAD_DATA, OUTPUT_TIME (10),
   3       peak_sub_power (300), load_factor (24)
    INTEGER*4 PSO_BUS_NUMBER (300),
   1       SUBSTATION (1000), SUB, NUMBER_OF_SUBS,
   2       OUTPUT_INCREMENT, BUS_NUMBER

    INTEGER I, II, INDEX, J

C        Initialize the linked list.
    PV_LINK (0) = 0

C        Open the output file.

    OPEN (UNIT = 1, FILE = 'MAIN.DAT', STATUS = 'NEW')

C        Call the service area subroutine.

C        Read the service area data.

    OPEN (UNIT = 2, FILE = 'SERVAREA.DAT', STATUS = 'OLD')
    READ (2, 50) N_LAT, S_LAT, E_LONG, W_LONG
    CALL SERVICE_AREA
    CLOSE (UNIT = 2)

C        Call the PV location subroutine.

    WRITE (1,100)

    PV_SYSTEM_NUMBER = 0

    OPEN (UNIT = 3, FILE = 'PVLOC.DAT', STATUS = 'OLD')

    DO MAX_PV = 1, 1000
        READ (3, 150, END = 8000) PV_LAT, PV_LONG, PV_KW, SUB
```

```
              PV_SYSTEM_NUMBER = PV_SYSTEM_NUMBER + 1
              PV_LATITUDE (PV_SYSTEM_NUMBER) = PV_LAT
              PV_LONGITUDE (PV_SYSTEM_NUMBER) = PV_LONG
              SUBSTATION (PV_SYSTEM_NUMBER) = SUB
              PV_KW_SIZE (PV_SYSTEM_NUMBER) = PV_KW
              CALL PV_LOCATION
              END DO

   8000 CLOSE (UNIT = 3)

C           print pv location information.

C           DISABLED.
C        WRITE (1, 200)

C        DO I = 1, PV_SYSTEM_NUMBER
C           WRITE (1, 300) I, PV_LATITUDE (I), PV_LONGITUDE (I),
C        1                 PV_LOC_WEST (I), PV_LOC_NORTH (I),
C        2                 PV_KW_SIZE (I), SUBSTATION (I)
C        END DO

C           Read from the input file SIMULATE.DAT the date, time, and
C           cloud pattern information:

C              DATE is a real number, 1 to 365, representing day of the year.
C              BEGIN_TIME and END_TIME are entered in decimal hours.
C              OUTPUT_TIME_INCREMENT, the time increment at which output data
C                 is printed, is entered in decimal hours.
C              PERCENT_COVER is entered as a real number in percent (0-100).
C              SPEED is entered as a real number in meters per second.
C              TRANSMISSIVITY is entered as a real number in percent, the
C                 percent of total sun that passes through the cloud.

         OPEN (UNIT = 4, FILE = 'SIMULATE.DAT', STATUS = 'OLD')
         READ (4, 350) DATE, BEGIN_TIME, END_TIME, OUTPUT_TIME_INCREMENT,
        1              start_output_time
         READ (4, 450) PERCENT_COVER, SPEED, TRANSMISSIVITY
         CLOSE (UNIT = 4)

C           Calculate the time increment.  This will be the amount of
C           time it will take the clouds to move across one east-west
C           distance increment.

         TIME_INCREMENT = (n_s_increment_length / SPEED) / 3600.

C           Print the data.

         WRITE (1, 500) DATE, BEGIN_TIME, END_TIME, TIME_INCREMENT
         write (1, 550) start_output_time, output_time_increment
         WRITE (1, 600) PERCENT_COVER
         WRITE (1, 700) SPEED
```

```
            WRITE (1, 800) TRANSMISSIVITY

C           Read the PSO load data for each substation.

            OPEN (UNIT = 5, FILE = 'LOAD.DAT', STATUS = 'OLD')

            NUMBER_OF_SUBS = 0
            DO I = 1, 300
               READ (5, 850, END = 9000) BUS_NUMBER, LOAD_DATA
               NUMBER_OF_SUBS = NUMBER_OF_SUBS + 1
               PSO_BUS_NUMBER (NUMBER_OF_SUBS) = BUS_NUMBER
               PSO_LOAD_DATA (NUMBER_OF_SUBS) = LOAD_DATA
               END DO

 9000 CLOSE (UNIT = 5)


C           Sum the peak PV generation on each substation.

            DO I = 1, NUMBER_OF_SUBS
               PEAK_SUB_POWER (I) = 0.D0
               END DO

            DO I = 1, PV_SYSTEM_NUMBER
               PEAK_SUB_POWER (SUBSTATION (I)) =
     1            PEAK_SUB_POWER (SUBSTATION (I)) + PV_KW_SIZE (I)
               END DO

C           Print the bus and load data.

            WRITE (1, 860)
            DO I = 1, NUMBER_OF_SUBS
               WRITE (1, 870) PSO_BUS_NUMBER (I), PSO_LOAD_DATA (I),
     1            PEAK_SUB_POWER (I),
     2            PEAK_SUB_POWER (I) / PSO_LOAD_DATA (I)
               END DO


C           Read in the load curve data.

            OPEN (UNIT = 6, FILE = 'CURVE.DAT', STATUS = 'OLD')
            DO I = 1, 24
               READ (6, 880) LOAD_FACTOR (I)
               END DO

            CLOSE (UNIT = 6)
            WRITE (1, 890)
            DO I = 1, 24
               WRITE (1, 895) I, LOAD_FACTOR (I)
               END DO
```

```
C          Begin the simulation.

           OUTPUT_INCREMENT = 0
           INCREMENT_NUMBER = 0.
           SEED = 457435643
           FILL_LEVEL = 0.

           DO TIME = BEGIN_TIME, END_TIME, TIME_INCREMENT

C          Calculate the insolation on a PV array in the center of the
C          service area.  The array is fixed, facing due south, tilted
C          at an angle equal to its latitude.  The subroutine INSOLATION
C          returns values of insolation and altitude angle.

           CALL INSOLATION_SUB

C          Generate one increment of clouds.  This is stored in the array
C          START_CLOUD.

           CALL FILL

C          Go through all the PV systems and store the insolation caused
C          by this cloud pattern.  The value stored in the array PV_INSOL
C          will be 0, for full sun, or positive, for shadow.

C          The cloud pattern moves one increment in each time increment.
C          Consider a PV system located in the north-south grid at PV_LOC_NORTH.
C          A cloud pattern generated at time increment INCREMENT_NUMBER will
C          affect the PV system at time increment
C          INCREMENT_NUMBER + PV_LOC_NORTH.

           DO I = 1, PV_SYSTEM_NUMBER
              II = INCREMENT_NUMBER + PV_LOC_NORTH (I) - 1
              II = II - ((II / 100) * 100)
              IF (II .EQ. 0) II = 100
              PV_INSOL (I, II) = START_CLOUD (PV_LOC_WEST (I))
           END DO

C          At each specified output time increment
C          calculate the insolation data for the present time increment.

           IF (TIME .GE. start_output_TIME + OUTPUT_TIME_INCREMENT *
       1       OUTPUT_INCREMENT) THEN

              II = INCREMENT_NUMBER
              II = II - ((II / 100) * 100)
              IF (II .EQ. 0) II = 100
              DO I = 1, PV_SYSTEM_NUMBER
                 IF (PV_INSOL (I, II) .GT. 0) PV_INSOL (I, II) =
       1           TRANSMISSIVITY / 100. * INSOLATION
                 IF (PV_INSOL (I, II) .EQ. 0) PV_INSOL (I, II) =
```

```
      1              INSOLATION
                     END DO


C             The array PV_INSOL now contains the insolation for PV
C                  system I at time increment INCREMENT_NUMBER.


C             Sum the power generated on each substation.

                 DO I = 1, NUMBER_OF_SUBS
                    SUB_POWER (I) = 0.D0
                    END DO

                 DO I = 1, PV_SYSTEM_NUMBER
                    SUB_POWER (SUBSTATION (I)) = SUB_POWER (SUBSTATION (I))
      1                + ((PV_INSOL (I, II) / 1000.) * PV_KW_SIZE (I))

C             The array SUB_POWER now contains the total PV generation
C                  for each substation at TIME.

C             If power factor is not 1, reactive power can be computed
C                  here.  Set up an array SUB_REACTIVE (300) to hold the
C                  reactive power values.  Read in the power factor as part
C                  of simulation data (SIMULATE.DAT).  Then compute reactive
C                  power consumed by each PV system:
C
C                    S = P / PF
C                    Q = S * DSIN (DASIN (PF))
C             Sum these for each substation and alter the write and
C                  format statements accordingly.

                 END DO


C*******************************************************************
C
C             This print loop is now set up for only 20 substations.
C             Change this when more than 20 are included.
C
C*******************************************************************

C             At each specified output increment, store the TIME in
C                  the array OUTPUT_TIME and the corresponding substation
C                  load (nominal load - PV generation) in the array
C                  BUS_LOAD.

                 OUTPUT_INCREMENT = OUTPUT_INCREMENT + 1
                 OUTPUT_TIME (OUTPUT_INCREMENT) = TIME
                 DO I = 1, NUMBER_OF_SUBS
                    BUS_LOAD (OUTPUT_INCREMENT, I) = 0.001 *
      1                ((pso_LOAD_DATA (I) * load_factor (nint (time)))
      2                - sub_power (i))
                    END DO
```

```
          END IF

          END DO

C         The simulation is completed.  Print out the substation
C            load summary.

      WRITE (1, 1300)
      WRITE (1, 1400)
      WRITE (1, 1500) (OUTPUT_TIME (I), I = 1, 10)
      WRITE (1, 1600)
      DO I = 1, NUMBER_OF_SUBS
C         Divide bus load by load factor so that when the PSO power
C            flow program multiplies by load factor the correct value
C            will be obtained.

      WRITE (1, 1700) PSO_BUS_NUMBER (I),
     1      (bus_load (j, i) / load_factor (nint (output_time (j))),
     2      j = 1, 10)
          END DO

      CLOSE (UNIT = 1)
      STOP

C         Here are the format statements for the main program.

   50 FORMAT (4 F15.11)
  100 FORMAT ('1')
  150 FORMAT (3 F15.11, I15)
  200 FORMAT ('1PV System   Latitude   Longitude
     1 East-West   North-South  Size (kw)  Substation')
  300 FORMAT (' ', I5, 7X, F6.2, 6X, F6.2, 3X, I7, 5X, I7, 8X, F6.2,
     1         6X, I5)
  350 FORMAT (4 F15.4, f15.8)
  450 FORMAT (3 F15.2)
  500 FORMAT ('1Simulation on day ', F4.0, ' from ', F7.4, ' to ', F7.4,
     1         ' hours; increment ', F6.4, ' hours.')
  550 format (' Output begins at time ', F7.4,
     1    ' with increment ', F12.8)
  600 FORMAT (' Percentage of sky covered by clouds: ', F4.0)
  700 FORMAT (' Speed of cloud movement: ', F4.0)
  800 FORMAT (' Percentage of light transmitted by clouds: ', F4.0)
  850 FORMAT (I10, F15.5)
  860 FORMAT ('1    PSO Bus Number          Nominal Load
     1          PV Generation          Penetration')
  870 FORMAT (' ',I12, 10X, F10.0, 10X, F10.0, 10X, F10.5)
  880 FORMAT (F10.5)
  890 FORMAT ('1   HOUR ENDING     LOAD FACTOR')
  895 FORMAT (I10, F18.3)
  900 FORMAT ('1            Date            Time
     1            Altitude Angle      Isolation')
```

```
1000 FORMAT (4F15.4)
1200 FORMAT (40I3)
1300 FORMAT ('1                              Time')
1400 FORMAT ('0Bus No.')
1500 FORMAT ('0              ', 10 F12.4)
1600 FORMAT (' ')
1700 FORMAT (' ', I6, 4X, 10 F12.1)
     END
```

```
      SUBROUTINE SERVICE_AREA


      REAL*8 N_LAT, S_LAT, E_LONG, W_LONG, PV_LAT, PV_LONG,
     1       n_s_increment_length,
     2       LENGTH_DEGREE_LAT, LENGTH_DEGREE_LONG,
     3       PV_LATITUDE (1000), PV_LONGITUDE (1000),
     4       PV_KW, PV_KW_SIZE (1000), BEGIN_TIME, END_TIME,
     5       PERCENT_COVER, SPEED, TRANSMISSIVITY,
     6       TIME, TIME_INCREMENT, CENTER_LAT, INSOLATION,
     7       ALTITUDE, DATE, FILL_LEVEL, e_w_increment_count,
     8       INCREMENT_NUMBER, SHADOW_EW


      INTEGER*4 PV_SYSTEM_NUMBER,
     1          PV_LOC_WEST (1000), PV_LOC_NORTH (1000),
     2          MAX_PV, PV_LINK (0:1000), PRESENT,
     3          START_CLOUD (100), SEED, SHADOW_NS


      COMMON N_LAT, S_LAT, E_LONG, W_LONG, PV_LAT, PV_LONG,
     1       e_w_increment_count, n_s_increment_length,
     2       LENGTH_DEGREE_LAT, LENGTH_DEGREE_LONG, PV_LINK,
     3       PV_LOC_WEST, PV_LOC_NORTH, PV_SYSTEM_NUMBER,
     4       DATE, PERCENT_COVER, SPEED,
     5       TRANSMISSIVITY, TIME, TIME_INCREMENT, CENTER_LAT,
     6       INSOLATION, ALTITUDE, INCREMENT_NUMBER, START_CLOUD,
     7       FILL_LEVEL, SEED, SHADOW_NS, SHADOW_EW



      REAL*8 E_W_DISTANCE, N_S_DISTANCE

C         Find the latitude of the center of the service area.
      CENTER_LAT = (N_LAT + S_LAT) / 2

C         Calculate teh length of one degree of latitude at the center.
      LENGTH_DEGREE_LAT = 111132.09
     1 - (566.05 * DCOSD (2 * CENTER_LAT))
     2 + (1.20 * DCOSD (4 * CENTER_LAT))
     3 - (0.002 * DCOSD (6 * CENTER_LAT))

C         Calculate the length of one degree of longitude at the center.
      LENGTH_DEGREE_LONG = (111415.13 * DCOSD (CENTER_LAT))
     1 - (94.55 * DCOSD (3 * CENTER_LAT))
     2 + (0.12 * DCOSD (5 * CENTER_LAT))

C         Calculate the distance between the north and south borders
C         of the service area.
      N_S_DISTANCE = (N_LAT - S_LAT) * LENGTH_DEGREE_LAT

C         Calculate the distance between the east and west borders.
      E_W_DISTANCE = (W_LONG - E_LONG) * LENGTH_DEGREE_LONG

C         Calculate the number of east-west increments of 414 meters.
```

```
         e_w_increment_count = E_W_DISTANCE / 414. + 1.

C          Calculate the length of the north-south increments.
         n_s_increment_length = N_S_DISTANCE / 100

C          Print all variables.
         WRITE (1, 100)
         WRITE (1, 200) N_LAT
         WRITE (1, 300) S_LAT
         WRITE (1, 400) E_LONG
         WRITE (1, 500) W_LONG
         WRITE (1, 600) E_W_DISTANCE
         WRITE (1, 700) N_S_DISTANCE
         WRITE (1, 800) LENGTH_DEGREE_LONG
         WRITE (1, 900) LENGTH_DEGREE_LAT
         WRITE (1, 1000) n_s_increment_length
         WRITE (1, 1100) e_w_increment_count
         WRITE (1, 1200)

C          Return to the main program.
         RETURN

C          Here are the format statements for the subroutine.
   100 FORMAT ('1Description of service area:')
   200 FORMAT (' Latitude of northern border is ', F6.2,
      1 ' degrees north.')
   300 FORMAT (' Latitude of southern border is ', F6.2,
      1 ' degrees north.')
   400 FORMAT (' Longitude of eastern border is ', F6.2,
      1 ' degrees west.')
   500 FORMAT (' Longitude of western border is ', F6.2,
      1 ' degrees west.')
   600 FORMAT (' The length of the northern and southern borders is ',
      1 F9.2, ' meters.')
   700 FORMAT (' The length of the eastern and western borders is ',
      1 F9.2, ' meters.')
   800 FORMAT (' The length of one degree of longitude is ', F9.2,
      1 ' meters.')
   900 FORMAT (' The length of one degree of latitude is ', F9.2,
      1 ' meters.')
  1000 FORMAT (' There are 100 north-south increments, each of length ',
      1 F7.2, ' meters.')
  1100 FORMAT (' There are ', F6.0, ' east-west increments, each of
      1 length 414 meters.')
  1200 FORMAT ('1')

         END
```

```
      SUBROUTINE PV_LOCATION

      REAL*8 N_LAT, S_LAT, E_LONG, W_LONG, PV_LAT, PV_LONG,
     1       n_s_increment_length,
     2       LENGTH_DEGREE_LAT, LENGTH_DEGREE_LONG,
     3       PV_LATITUDE (1000), PV_LONGITUDE (1000),
     4       PV_KW, PV_KW_SIZE (1000), BEGIN_TIME, END_TIME,
     5       PERCENT_COVER, SPEED, TRANSMISSIVITY,
     6       TIME, TIME_INCREMENT, CENTER_LAT, INSOLATION,
     7       ALTITUDE, DATE, FILL_LEVEL, e_w_increment_count,
     8       INCREMENT_NUMBER, SHADOW_EW

      INTEGER*4 PV_SYSTEM_NUMBER,
     1       PV_LOC_WEST (1000), PV_LOC_NORTH (1000),
     2       MAX_PV, PV_LINK (0:1000), PRESENT,
     3       START_CLOUD (100), SEED, SHADOW_NS

      COMMON N_LAT, S_LAT, E_LONG, W_LONG, PV_LAT, PV_LONG,
     1       e_w_increment_count, n_s_increment_length,
     2       LENGTH_DEGREE_LAT, LENGTH_DEGREE_LONG, PV_LINK,
     3       PV_LOC_WEST, PV_LOC_NORTH, PV_SYSTEM_NUMBER,
     4       DATE, PERCENT_COVER, SPEED,
     5       TRANSMISSIVITY, TIME, TIME_INCREMENT, CENTER_LAT,
     6       INSOLATION, ALTITUDE, INCREMENT_NUMBER, START_CLOUD,
     7       FILL_LEVEL, SEED, SHADOW_NS, SHADOW_EW


      REAL*8 LONG_DIFFERENCE, LAT_DIFFERENCE,
     1       PV_METERS_FROM_WEST, PV_METERS_FROM_NORTH
C         This subroutine accepts as input one value of latitude and one of
C         of longitude that identify the location within the service area.
C         It then calculates the PV system's position within the grid
C         set up by the subroutine SERVICE_AREA (SERVAREA.FOR).

C         The PV system grid locations are stored in the arrays PV_LOC_WEST
C         and PV_LOC_NORTH.

C         The PV location is received from the main program in the variables
C         PV_LAT and PV_LONG.  These are in decimal form.

C         Check to see if the location is within the service area.

      IF (PV_LAT .GT. N_LAT) THEN
         WRITE (1, 200) PV_LAT, N_LAT
         PV_SYSTEM_NUMBER = PV_SYSTEM_NUMBER - 1
         RETURN
         END IF

      IF (PV_LAT .LT. S_LAT) THEN
         WRITE (1, 300) PV_LAT, S_LAT
```

```
                PV_SYSTEM_NUMBER = PV_SYSTEM_NUMBER - 1
                RETURN
                END IF

           IF (PV_LONG .GT. W_LONG) THEN
                WRITE (1, 400) PV_LONG, W_LONG
                PV_SYSTEM_NUMBER = PV_SYSTEM_NUMBER - 1
                RETURN
                END IF

           IF (PV_LONG .LT. E_LONG) THEN
                WRITE (1, 500) PV_LONG, E_LONG
                PV_SYSTEM_NUMBER = PV_SYSTEM_NUMBER - 1
                RETURN
                END IF

C          Determine where the PV system is located in the north-south
C          increments.

           LONG_DIFFERENCE = W_LONG - PV_LONG
           PV_METERS_FROM_WEST = LONG_DIFFERENCE * LENGTH_DEGREE_LONG
           PV_LOC_WEST (PV_SYSTEM_NUMBER) = (PV_METERS_FROM_WEST / 414) + 1

C          Check again to be sure the PV system is within the area.

           IF (PV_LOC_WEST (PV_SYSTEM_NUMBER) .GT. E_W_INCREMENT_COUNT) THEN
                WRITE (1, 600) PV_LAT, PV_LONG,
         1      PV_LOC_WEST (PV_SYSTEM_NUMBER), E_W_INCREMENT_COUNT
                PV_SYSTEM_NUMBER = PV_SYSTEM_NUMBER - 1
                RETURN
                END IF

C          Determine where the PV system is located in the east-west
C          increments.

           LAT_DIFFERENCE = N_LAT - PV_LAT
           PV_METERS_FROM_NORTH = LAT_DIFFERENCE * LENGTH_DEGREE_LAT
           PV_LOC_NORTH (PV_SYSTEM_NUMBER) =
         1 (PV_METERS_FROM_NORTH / N_S_INCREMENT_LENGTH) + 1

C          Check again to be sure the PV system is within the area.

           IF (PV_LOC_NORTH (PV_SYSTEM_NUMBER) .GT. 100) THEN
                WRITE (1, 700) PV_LAT, PV_LONG,
         1      PV_LOC_NORTH (PV_SYSTEM_NUMBER)
                PV_SYSTEM_NUMBER = PV_SYSTEM_NUMBER - 1
                RETURN
                END IF

C          Sort the PV location arrays using a linked list.
C          The array is first sorted from east to west, then from north
```

```
C          to south.

      PRESENT = PV_LINK (0)
      PREVIOUS = 0

C          Find the place in the east-west order.

      DO WHILE (PRESENT .NE. 0 .AND.
     1          PV_LOC_WEST (PV_SYSTEM_NUMBER) .GT.
     2          PV_LOC_WEST (PRESENT))
         PREVIOUS = PRESENT
         PRESENT = PV_LINK (PRESENT)
         END DO

C          Find the place in the north-south order.

      DO WHILE (PRESENT. NE. 0 .AND.
     1          PV_LOC_WEST (PV_SYSTEM_NUMBER) .EQ.
     2          PV_LOC_WEST (PRESENT) .AND.
     3          PV_LOC_NORTH (PV_SYSTEM_NUMBER) .GT.
     4          PV_LOC_NORTH (PRESENT))
         PREVIOUS = PRESENT
         PRESENT = PV_LINK (PRESENT)
         END DO

C          Adjust the links.
      PV_LINK (PV_SYSTEM_NUMBER) = PV_LINK (PREVIOUS)
      PV_LINK (PREVIOUS) = PV_SYSTEM_NUMBER

C          Here are the format statements for the subroutine.

  200 FORMAT (' The PV latitude ', F6.2, ' is north of the northern
     1 border, latitude ', F6.2, '.')
  300 FORMAT (' The PV latitude ', F6.2, ' is south of the southern
     1 border, latitude ', F6.2, '.')
  400 FORMAT (' The PV longitude ', F6.2, ' is west of the western
     1 border, longitude ', F6.2, '.')
  500 FORMAT (' The PV longitude ', F6.2, ' is east of the eastern
     1 border, longitude ', F6.2, '.')
C  600 FORMAT (' The PV system located at latitude ', F6.2, ' and
C     1 longitude ', F6.2, ' has an east-west increment number of ',
C     2 I5, ' which is greater than the allowable value of ', I5)
C  700 FORMAT (' The PV system located at latitude ', F6.2, ' and
C     1 longitude ', F6.2, ' has a north-south increment number of ',
C     2 I5, ' which is greater than the allowable value of 100.')

  600 FORMAT (2F6.2, 2I5)
  700 FORMAT (2F6.2, I5)

      RETURN
      END
```

```
        SUBROUTINE INSOLATION_SUB

        REAL*8 N_LAT, S_LAT, E_LONG, W_LONG, PV_LAT, PV_LONG,
       1        n_s_increment_length,
       2        LENGTH_DEGREE_LAT, LENGTH_DEGREE_LONG,
       3        PV_LATITUDE (1000), PV_LONGITUDE (1000),
       4        PV_KW, PV_KW_SIZE (1000), BEGIN_TIME, END_TIME,
       5        PERCENT_COVER, SPEED, TRANSMISSIVITY,
       6        TIME, TIME_INCREMENT, CENTER_LAT, INSOLATION,
       7        ALTITUDE, DATE, FILL_LEVEL, e_w_increment_count,
       8        INCREMENT_NUMBER, SHADOW_EW

        INTEGER*4 PV_SYSTEM_NUMBER,
       1        PV_LOC_WEST (1000), PV_LOC_NORTH (1000),
       2        MAX_PV, PV_LINK (0:1000), PRESENT,
       3        START_CLOUD (100), SEED, SHADOW_NS

        COMMON N_LAT, S_LAT, E_LONG, W_LONG, PV_LAT, PV_LONG,
       1        e_w_increment_count, n_s_increment_length,
       2        LENGTH_DEGREE_LAT, LENGTH_DEGREE_LONG, PV_LINK,
       3        PV_LOC_WEST, PV_LOC_NORTH, PV_SYSTEM_NUMBER,
       4        DATE, PERCENT_COVER, SPEED,
       5        TRANSMISSIVITY, TIME, TIME_INCREMENT, CENTER_LAT,
       6        INSOLATION, ALTITUDE, INCREMENT_NUMBER, START_CLOUD,
       7        FILL_LEVEL, SEED, SHADOW_NS, SHADOW_EW


        REAL*8 HOUR_ANGLE, DECLINATION, AIR_MASS, TRANSMITTANCE,
       1        BEAM, COS_I


C        This subroutine calculates the clear sky insolation for a
C        PV array tilted at an angle equal to its latitude located
C        at the center of the service area, denoted by CENTER_LAT.
C        The calculation is done for each time increment during
C        the simulation.

C        The main program provides the following variables.

C            CENTER_LAT: The center latitude of the service area.
C            E_LONG, W_LONG: The eastern and western service area borders.
C            DATE, TIME: The date and time at which the insolation is to be
C                        calculated.

C        The subroutine returns the following values.

C            INSOLATION: the clear sky insolation.
C            ALTITUDE: The altitude angle of the sun.
C            AZIMUTH: The azimuth angle of the sun.
C            DECLINATION: The declination of the sun.
```

```
C          Calculate the declination of the sun.

      DECLINATION = 23.5 * DSIND ((DATE - 80.) * (360. / 365.))

C          Calculate the hour angle of the sun. (Assume time is solar time.)

      HOUR_ANGLE = (12.0 - TIME) * 15.

C          Calculate the altitude angle of the sun.

      ALTITUDE = DASIND ((DSIND (CENTER_LAT) * DSIND (DECLINATION)) +
     1           (DCOSD (CENTER_LAT) * DCOSD (DECLINATION) *
     2           DCOSD (HOUR_ANGLE)))

C          Calculate the air mass at sea level.  Assume this value for
C          the air mass at the service area.

      AIR_MASS = (DSQRT (1229. + ((614. * DSIND (ALTITUDE)) ** 2 ))) -
     1           (614. * DSIND (ALTITUDE))

C          Calculate the atmospheric transmittance.

      TRANSMITTANCE = 0.5 * (DEXP (-0.65 * AIR_MASS) +
     1               DEXP (-0.095 * AIR_MASS))

C          Calculate the beam radiation on the earth's surface.

      BEAM = 1353. * TRANSMITTANCE

C          Calculate the cosine of the incidence angle for the PV array:
C          south facing, tilted at angle equal to latitude.

      COS_I = DCOSD (DECLINATION) * DCOSD (HOUR_ANGLE)
      IF (COS_I .LT. 0.0) THEN
         COS_I = 0.0
         END IF

C          Calculate the clear-sky insolation incident on the array.

      INSOLATION = BEAM * COS_I

C          Return to the main program.

      RETURN
      END
```

```
      SUBROUTINE FILL
      REAL*8 N_LAT, S_LAT, E_LONG, W_LONG, PV_LAT, PV_LONG,
     1       N_S_INCREMENT_LENGTH,
     2       LENGTH_DEGREE_LAT, LENGTH_DEGREE_LONG,
     3       PV_LATITUDE (1000), PV_LONGITUDE (1000),
     4       PV_KW, PV_KW_SIZE (1000), BEGIN_TIME, END_TIME,
     5       PERCENT_COVER, SPEED, TRANSMISSIVITY,
     6       TIME, TIME_INCREMENT, CENTER_LAT, INSOLATION,
     7       ALTITUDE, DATE, FILL_LEVEL, e_w_increment_count,
     8       INCREMENT_NUMBER, SHADOW_EW

      INTEGER*4 PV_SYSTEM_NUMBER,
     1          PV_LOC_WEST (1000), PV_LOC_NORTH (1000),
     2          MAX_PV, PV_LINK (0:1000), PRESENT,
     3          START_CLOUD (100), SEED, shadow_ns

      COMMON N_LAT, S_LAT, E_LONG, W_LONG, PV_LAT, PV_LONG,
     1       e_w_increment_count, N_S_INCREMENT_LENGTH,
     2       LENGTH_DEGREE_LAT, LENGTH_DEGREE_LONG, PV_LINK,
     3       PV_LOC_WEST, PV_LOC_NORTH, PV_SYSTEM_NUMBER,
     4       DATE, PERCENT_COVER, SPEED,
     5       TRANSMISSIVITY, TIME, TIME_INCREMENT, CENTER_LAT,
     6       INSOLATION, ALTITUDE, INCREMENT_NUMBER, START_CLOUD,
     7       FILL_LEVEL, SEED, shadow_ns, SHADOW_EW

C         This subroutine fills the starting cloud increment array with
C         a cloud pattern generated according to the input variables
C         PERCENT COVER and TRANSMISSIVITY.

C         The output is the array START_CLOUD, which represents clouds
C         in an east-west increment on the south end of the service area.

C         The array has size e_w_increment_count.

C         The values in the array represent the number of increments following
C         the present increment that will have portions of the same cloud.
C         A value of 0, to which the array is initialized, represents no cloud
C         (full sun).

      REAL*8 CDF_AREA, AREA, NEW_AREA, CLOUD_LENGTH, CLOUD_WIDTH,
     1       shadow_length, shadow_width, FILL_LEVEL_COUNT

      INTEGER*4 COUNT

C         The variable FILL_LEVEL is the sum of the percentages to which each
C         previous increment was filled with clouds.  This value is divided
C         by INCREMENT_NUMBER and the result is compared with PERCENT_COVER
C         to see if more clouds should be added to the starting increment.

      FILL_LEVEL_COUNT = 0.
```

```
C           Update the previous starting increment.  This continues the clouds
C           from the previous increment that have not yet reached their full
C           size.

        INCREMENT_NUMBER = INCREMENT_NUMBER + 1.

        DO COUNT = 1, e_w_increment_count
            IF (START_CLOUD (COUNT) .GT. 0) THEN
                START_CLOUD (COUNT) = START_CLOUD (COUNT) - 1
                FILL_LEVEL_COUNT = FILL_LEVEL_COUNT + 1.
            END IF
        END DO

C           Calculate the new FILL_LEVEL.

        FILL_LEVEL = FILL_LEVEL + (FILL_LEVEL_COUNT / e_w_increment_count)

C           Add clouds if the fill level is less than the required range.

        DO WHILE ((FILL_LEVEL / INCREMENT_NUMBER) .LT.
      1           (0.009 * PERCENT_COVER))

C           Generate a cloud size.

C           First get a random number.

        CDF_AREA = RAN (SEED)

C           Now solve the cumulative distribution function of the cloud area
C           for the area that corresponds to this random number.

        AREA = 0.0
        NEW_AREA = 1.0

        DO WHILE (DABS (AREA - NEW_AREA) .GT. 0.001)
            AREA = NEW_AREA
            NEW_AREA = (CDF_AREA + 0.180) /
      1           (0.880 - (0.442 * DLOG (AREA)))
            END DO

C           This formula calculates the area in square nautical miles.
C           Convert to square meters.

        AREA = 3433609. * NEW_AREA

C           Calculate the width and length of the cloud.  The cloud width is
C           0.582 * cloud length.  Length runs north-south, width runs east-west.

        CLOUD_LENGTH = DSQRT (AREA / 0.582)
        CLOUD_WIDTH = 0.582 * CLOUD_LENGTH
```

```fortran
C          Calculate the elongation of the shadow caused by the position of
C          the sun.

           shadow_width = CLOUD_width *
1              (1 + (0.963 * (1 / DTAND (ALTITUDE))))

C          The shadow width then equals the cloud width.

           shadow_length = CLOUD_length

C          Determine how many east-west and north-south increments the shadow
C          will fill.

           shadow_ns = shadow_length / N_S_INCREMENT_LENGTH + 1
           SHADOW_EW = shadow_width / 414. + 1.

C          Place the cloud in the starting increment if it will fit.

           CALL PLACE_CLOUD

           END DO

       RETURN
       END



       SUBROUTINE PLACE_CLOUD
       REAL*8 N_LAT, S_LAT, E_LONG, W_LONG, PV_LAT, PV_LONG,
1          N_S_INCREMENT_LENGTH,
2          LENGTH_DEGREE_LAT, LENGTH_DEGREE_LONG,
3          PV_LATITUDE (1000), PV_LONGITUDE (1000),
4          PV_KW, PV_KW_SIZE (1000), BEGIN_TIME, END_TIME,
5          PERCENT_COVER, SPEED, TRANSMISSIVITY,
6          TIME, TIME_INCREMENT, CENTER_LAT, INSOLATION,
7          ALTITUDE, DATE, FILL_LEVEL, e_w_increment_count,
8          INCREMENT_NUMBER, SHADOW_EW

       INTEGER*4 PV_SYSTEM_NUMBER,
1          PV_LOC_WEST (1000), PV_LOC_NORTH (1000),
2          MAX_PV, PV_LINK (0:1000), PRESENT,
3          START_CLOUD (100), SEED, shadow_ns

       COMMON N_LAT, S_LAT, E_LONG, W_LONG, PV_LAT, PV_LONG,
1          e_w_increment_count, N_S_INCREMENT_LENGTH,
2          LENGTH_DEGREE_LAT, LENGTH_DEGREE_LONG, PV_LINK,
3          PV_LOC_WEST, PV_LOC_NORTH, PV_SYSTEM_NUMBER,
4          DATE, PERCENT_COVER, SPEED,
5          TRANSMISSIVITY, TIME, TIME_INCREMENT, CENTER_LAT,
6          INSOLATION, ALTITUDE, INCREMENT_NUMBER, START_CLOUD,
7          FILL_LEVEL, SEED, shadow_ns, SHADOW_EW
```

```
        INTEGER*4 ORIG_LOC, START_LOC, PRES_LOC, COUNT, I, II

C            This subroutine checks the starting increment to see if there
C            is enough room to put the cloud generated in the subroutine FILL.
C            If there is it inserts the cloud.  If not, it returns to the
C            subroutine FILL.

C            A random location in the starting array is first chosen.  The cloud
C            is placed in the first location to the south that is large enough to
C            hold the cloud.  If the southern edge is reached, the subroutine
C            proceeds to the northern edge and begins looking there until the
C            cloud is inserted or the original location is reached.

C            Pick a random location in the starting array.

        ORIG_LOC = RAN (SEED) * e_w_increment_count + 1
        IF (ORIG_LOC .GT. e_w_increment_count) THEN
            ORIG_LOC = e_w_increment_count
            END IF

C            Begin looking for an opening large enough for the cloud at one
C            increment east of the original location.  This simplifies the
C            programming.

        START_LOC = ORIG_LOC + 1

C            First check the starting location.

        PRES_LOC = START_LOC

C            COUNT counts the number of empty increments found east from
C            START_LOC.

        COUNT = 0

C            Keep trying to put the cloud in the array until you reach the
C            original location.

        DO WHILE (PRES_LOC .NE. ORIG_LOC)

C            Check for an empty increment in the starting array.

            IF (START_CLOUD (PRES_LOC) .EQ. 0) THEN

C            If the increment is empty, add 1 to COUNT.
                COUNT = COUNT + 1
C            Check to see if there is room to insert the cloud.

                IF (COUNT .GE. SHADOW_EW) THEN
```

```
C          If there is room, insert the cloud and return.

           DO I = START_LOC, START_LOC + SHADOW_EW
              II = I
              IF (I .GT. e_w_increment_count) II =
     1            I - e_w_increment_count
              START_CLOUD (II) = shadow_ns
           END DO
           FILL_LEVEL = FILL_LEVEL + SHADOW_EW / e_w_increment_count
           RETURN

C          If there is not room, then increment PRES_LOC.
        ELSE

           PRES_LOC = PRES_LOC + 1
           IF (PRES_LOC .GT. e_w_increment_count) PRES_LOC = 1.
        END IF

C          If the increment is not empty, then reset START_LOC and COUNT.
     ELSE

        START_LOC = PRES_LOC + 1
        IF (START_LOC .GT. e_w_increment_count) START_LOC = 1.
        PRES_LOC = START_LOC
        COUNT = 0
     END IF

C     Check the next increment.

  END DO

C     If you drop out of this loop, it means there is no room for the
C     cloud.  Return to the subroutine FILL for another cloud.

  RETURN
  END
```

APPENDIX B

ONE-LINE DIAGRAM OF PUBLIC SERVICE COMPANY OF OKLAHOMA

ELECTRIC UTILITY SYSTEM IN SOUTHEAST TULSA
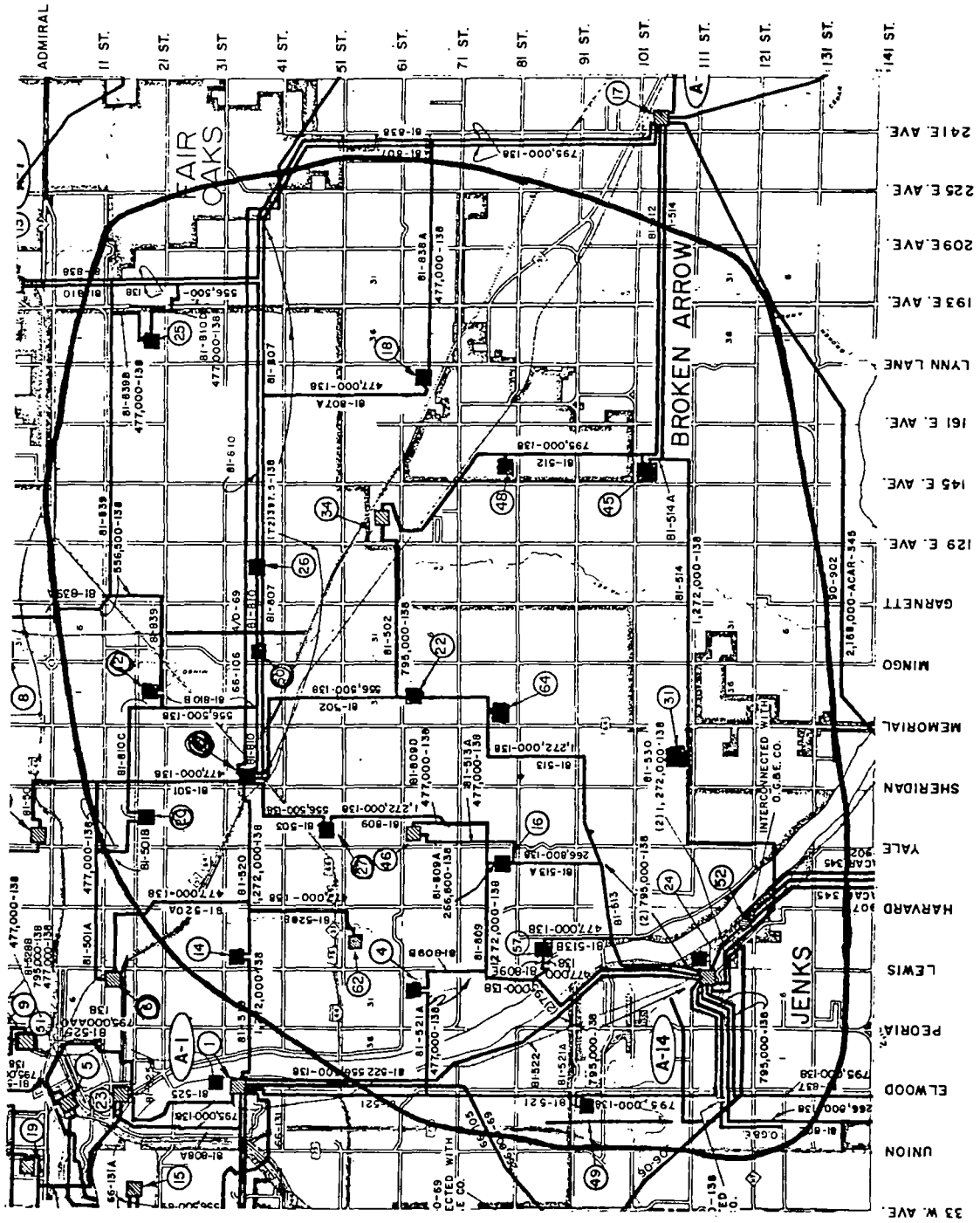
APPENDIX C

SAMPLE PUBLIC SERVICE COMPANY OF OKLAHOMA

POWER FLOW SIMULATION OUTPUT

FROM		AREA	VOLT		GEN	LOAD	SHUNT	TO						TRANSFORMER		RATING	
BUS	NAME	ZONE	PU/KV	ANGLE	MW/MVAR	MW/MVAR	MW/MVAR	BUS	NAME	CKT	AREA	MW	MVAR	RATIO	ANGLE	%I	MVA
4163 ONETA4PT		23	1.049	-8.5	0.0	16.6	0.0										
		1			0.0	3.4	0.0	4125 B101S4PT		1	30	40.4	19.1			15	287
								4126 B101N4PT		1	30	42.1	24.1			22	215
								4142 BARR 4PT		1	30	33.5	21.3			18	215
								4143 BARRS4PT		1	30	9.5	45.8			21	215
								4164 ONETA7PT		1	23	-142.1	-113.6	1.079LK		35	500
4140 RIVSD4PT		23	1.035	-9.7	100.0	0.0	0.0										
		1			55.0R	0.0	0.0	3134 WELEETK4		1	15	64.9	-10.4			58	110
								3948 BEE 4		1	22	148.8	39.2			63	237
								4114 WEKWA4PT		1	23	-1.5	-0.7			1	215
								4116 JENKS4PT		1	30	14.4	6.6			7	215
								4124 B111-4PT		1	30	-39.0	-16.9			14	287
								4139 RIVSD7PT		1	23	-168.4	7.8	1.025LK		33	500
								4145 TPS 4PT		1	23	17.5	6.0			8	215
								4208 ORU W4PT		1	30	-14.5	10.5			5	344
								4212 ORU E4PT		1	23	-6.9	13.1			4	344
								4269 OKMUL4PE		1	23	84.6	0.1			38	215
4114 WEKWA4PT		23	1.035	-9.7	0.0	1.0	0.0										
		1			0.0	0.2	0.0	3128 KEYSTON4		1	15	42.9	-10.0			27	160
								4112 WEKWA7PT		1	23	-127.1	-13.0	1.025LK		25	500
								4140 RIVSD4PT		1	23	1.5	-1.9			1	215
								4172 SSPRS4PT		1	23	63.0	14.3			27	229
								4180 WEDTP4PT		1	23	39.2	7.7			17	229
								4210 TNTAP4PT		1	23	-20.5	2.6			9	229
4174 TULSN4PT		23	1.035	-8.7	0.0	7.0	0.0										
		1			0.0	1.3	0.0	4196 HARVE4PT		1	23	36.9	8.2			23	160
								4197 N46W 4PT		1	23	15.2	1.9			9	160
								4198 CHER 4PT 138		1	23	-3.4	14.9			8	174
								4203 OWSAN4PT		1	23	-5.8	2.1			3	186
								4210 TNTAP4PT		1	23	27.7	-4.3			15	186
								4211 TULSN7PT		1	23	-123.7	-24.1	1.025LK		24	500
								4216 BARNS4PB		1	23	55.0	-0.8			25	215
								4224 NEASN4PB		1	23	-8.8	0.8			4	215
4147 CATSA4PT		23	1.028	-8.4	0.0	8.6	0.0										
		1			0.0	1.7	0.0	3313 CATSA5GR		1	21	-49.6	37.1	1.000LK		40	150
								3313 CATSA5GR		2	21	-50.1	37.5			41	150
								4128 LYNNE4PT		1	23	43.1	-15.2			26	174
								4151 TCEMT2PT		1	23	15.6	-4.9	1.000UN		32	50
								4161 E211P4PT		1	23	26.0	-24.7			20	174
								4194 AGR W4PT		1	23	1.8	-6.6			5	141
								4198 CHER 4PT 138		1	23	5.8	-16.7			10	174
								4202 OWASS4PT		1	23	-1.2	-8.1			6	145

PTI INTERACTIVE POWER SYSTEM SIMULATOR--PSS/E   WED, JUL 30 1986 09:31
12-85 1988 APR 100 BASE   GROUP B
GB88APR, SPRING, NO.2, CASE 2

FROM BUS	NAME	AREA ZONE	VOLT PU/KV	ANGLE	GEN MW/MVAR	LOAD MW/MVAR	SHUNT MW/MVAR	TO BUS	NAME	CKT	AREA	MW	MVAR	TRANSFORMER RATIO	ANGLE	RATING %I	MVA
4163	ONETA4PT	23	1.049	-8.3	0.0	16.6	0.0										
		1			0.0	3.4	0.0	4125	B101S4PT	1	30	40.4	19.2			15	287
								4126	B101N4PT	1	30	41.7	24.1			21	215
								4142	BARR 4PT	1	30	32.6	21.3			17	215
								4143	BARRS4PT	1	30	9.4	45.8			21	215
								4164	ONETA7PT	1	23	-140.7	-113.7	1.079LK		34	500
4140	RIVSD4PT	23	1.035	-9.6	100.0	0.0	0.0										
		1			54.4R	0.0	0.0	3134	WELEETK4	1	15	65.2	-10.5			58	110
								3948	BEE 4	1	22	149.0	39.2			63	237
								4114	WEKWA4PT	1	23	-1.3	-0.8			1	215
								4116	JENKS4PT	1	30	13.6	6.5			7	215
								4124	B111-4PT	1	30	-38.9	-17.0			14	287
								4139	RIVSD7PT	1	23	-166.4	7.5	1.025LK		32	500
								4145	TPS 4PT	1	23	16.8	5.9			8	215
								4208	ORU W4PT	1	30	-15.1	10.4			5	344
								4212	ORU E4PT	1	23	-8.0	13.0			4	344
								4269	OKMUL4PE	1	23	84.9	0.1			38	215
4114	WEKWA4PT	23	1.035	-9.5.	0.0	1.0	0.0										
		1			0.0	0.2	0.0	3128	KEYSTON4	1	15	43.2	-10.0			27	160
								4112	WEKWA7PT	1	23	-126.4	-13.1	1.025LK		25	500
								4140	RIVSD4PT	1	23	1.3	-1.9			1	215
								4172	SSPRS4PT	1	23	62.4	14.4			27	229
								4180	WEDTP4PT	1	23	38.8	7.7			17	229
								4210	TNTAP4PT	1	23	-20.3	2.6			9	229
4174	TULSN4PT	23	1.035	-8.5	0.0	7.0	0.0										
		1			0.0	1.3	0.0	4196	HARVE4PT	1	23	36.8	8.2			23	160
								4197	N46W 4PT	1	23	15.1	1.9			9	160
								4198	CHER 4PT 138	1	23	-3.6	14.9			9	174
								4203	OWSAN4PT	1	23	-5.7	2.1			3	186
								4210	TNTAP4PT	1	23	27.5	-4.3			14	186
								4211	TULSN7PT	1	23	-123.4	-24.1	1.025LK		24	500
								4216	BARNS4PB	1	23	55.1	-0.8			25	215
								4224	NEASN4PB	1	23	-8.8	0.8			4	215
4147	CATSA4PT	23	1.028	-8.2	0.0	8.6	0.0										
		1			0.0	1.7	0.0	3313	CATSA5GR	1	21	-49.0	37.0	1.000LK		40	150
								3313	CATSA5GR	2	21	-49.5	37.4			40	150
								4128	LYNNE4PT	1	23	41.9	-15.1			25	174
								4151	TCEMT2PT	1	23	15.7	-4.9	1.000UN		32	50
								4161	E21TP4PT	1	23	25.4	-24.6			20	174
								4194	AGR W4PT	1	23	2.0	-6.6			5	141
								4198	CHER 4PT 138	1	23	6.1	-16.7			10	174
								4202	OWASS4PT	1	23	-1.0	-8.1			5	145

FROM BUS	NAME	AREA ZONE	VOLT PU/KV	ANGLE	GEN MW/MVAR	LOAD MW/MVAR	SHUNT MW/MVAR	TO BUS	NAME	CKT	AREA	MW	MVAR	TRANSFORMER RATIO	ANGLE	RATING %I	MVA
4163	ONETA4PT	23	1.049	-8.4	0.0	16.6	0.0										
		1			0.0	3.4	0.0	4125	B101S4PT	1	30	40.5	19.2			15	287
								4126	B101N4PT	1	30	41.8	24.1			21	215
								4142	BARR 4PT	1	30	32.2	21.3			17	215
								4143	BARRS4PT	1	30	9.8	45.8			21	215
								4164	ONETA7PT	1	23	-141.0	-113.7	1.079LK		35	500
4140	RIVSD4PT	23	1.035	-9.6	100.0	0.0	0.0										
		1			54.5R	0.0	0.0	3134	WELEETK4	1	15	65.2	-10.5			58	110
								3948	BEE 4	1	22	149.0	39.2			63	237
								4114	WEKWA4PT	1	23	-1.3	-0.8			1	215
								4116	JENKS4PT	1	30	13.9	6.5			7	215
								4124	B111-4PT	1	30	-38.9	-17.0			14	287
								4139	RIVSD7PT	1	23	-166.6	7.6	1.025LK		32	500
								4145	TPS 4PT	1	23	16.8	5.9			8	215
								4208	ORU W4PT	1	30	-15.3	10.4			5	344
								4212	ORU E4PT	1	23	-7.7	13.0			4	344
								4269	OKMUL4PE	1	23	84.9	0.1			38	215
4114	WEKWA4PT	23	1.035	-9.5	0.0	1.0	0.0										
		1			0.0	0.2	0.0	3128	KEYSTON4	1	15	43.2	-10.0			27	160
								4112	WEKWA7PT	1	23	-126.4	-13.0	1.025LK		25	500
								4140	RIVSD4PT	1	23	1.3	-1.9			1	215
								4172	SSPRS4PT	1	23	62.4	14.4			27	229
								4180	WEDTP4PT	1	23	38.8	7.7			17	229
								4210	TNTAP4PT	1	23	-20.2	2.6			9	229
4174	TULSN4PT	23	1.035	-8.6	0.0	7.0	0.0										
		1			0.0	1.3	0.0	4196	HARVE4PT	1	23	36.9	8.2			23	160
								4197	N46W 4PT	1	23	15.1	1.9			9	160
								4198	CHER 4PT 138	1	23	-3.5	14.9			8	174
								4203	OWSAN4PT	1	23	-5.7	2.1			3	186
								4210	TNTAP4PT	1	23	27.5	-4.3			14	186
								4211	TULSN7PT	1	23	-123.6	-24.1	1.025LK		24	500
								4216	BARNS4PB	1	23	55.1	-0.8			25	215
								4224	NEASN4PB	1	23	-8.8	0.8			4	215
4147	CATSA4PT	23	1.028	-8.3	0.0	8.6	0.0										
		1			0.0	1.7	0.0	3313	CATSA5GR	1	21	-49.2	37.1	1.000LK		40	150
								3313	CATSA5GR	2	21	-49.7	37.5			40	150
								4128	LYNNE4PT	1	23	41.4	-15.2			25	174
								4151	TCEMT2PT	1	23	15.7	-4.8	1.000UN		32	50
								4161	E21TP4PT	1	23	26.5	-24.7			20	174
								4194	AGR W4PT	1	23	1.9	-6.6			5	141
								4198	CHER 4PT 138	1	23	5.9	-16.7			10	174
								4202	OWASS4PT	1	23	-1.1	-8.1			6	145

FROM BUS	NAME	AREA ZONE	VOLT PU/KV	ANGLE	GEN MW/MVAR	LOAD MW/MVAR	SHUNT MW/MVAR	TO BUS	NAME	CKT	AREA	MW	MVAR	TRANSFORMER RATIO	ANGLE	RATING %I	MVA
4163	ONETA4PT	23 1	1.049	-8.7	0.0 0.0	16.6 3.4	0.0 0.0										
								4125	B101S4PT	1	30	40.2	19.0			15	287
								4126	B101N4PT	1	30	42.5	24.0			22	215
								4142	BARR 4PT	1	30	33.7	21.3			18	215
								4143	BARRS4PT	1	30	10.6	45.9			21	215
								4164	ONETA7PT	1	23	-143.6	-113.6	1.079LK		35	500
4140	RIVSD4PT	23 1	1.035	-9.9	100.0 55.6R	0.0 0.0	0.0 0.0										
								3134	WELEETK4	1	15	64.7	-10.4			58	110
								3948	BEE 4	1	22	148.7	39.2			63	237
								4114	WEKWA4PT	1	23	-1.4	-0.7			1	215
								4116	JENKS4PT	1	30	15.2	6.6			7	215
								4124	B111-4PT	1	30	-38.6	-16.9			14	287
								4139	RIVSD7PT	1	23	-169.7	8.0	1.025LK		33	500
								4145	TPS 4PT	1	23	18.1	6.0			9	215
								4208	ORU W4PT	1	30	-15.4	10.5			5	344
								4212	ORU E4PT	1	23	-5.7	13.2			4	344
								4269	OKMUL4PE	1	23	84.3	0.1			38	215
4114	WEKWA4PT	23 1	1.035	-9.8	0.0 0.0	1.0 0.2	0.0 0.0										
								3128	KEYSTON4	1	15	42.8	-10.0			27	160
								4112	WEKWA7PT	1	23	-127.4	-12.9	1.025LK		25	500
								4140	RIVSD4PT	1	23	1.4	-2.0			1	215
								4172	SSPRS4PT	1	23	63.3	14.3			27	229
								4180	WEDTP4PT	1	23	39.4	7.7			17	229
								4210	TNTAP4PT	1	23	-20.4	2.6			9	229
4174	TULSN4PT	23 1	1.035	-8.8	0.0 0.0	7.0 1.3	0.0 0.0										
								4196	HARVE4PT	1	23	37.0	8.2			23	160
								4197	N46W 4PT	1	23	15.2	1.9			9	160
								4198	CHER 4PT 138	1	23	-2.7	14.9			8	174
								4203	OWSAN4PT	1	23	-5.7	2.0			3	186
								4210	TNTAP4PT	1	23	27.7	-4.3			15	186
								4211	TULSN7PT	1	23	-124.6	-24.0	1.025LK		25	500
								4216	BARNS4PB	1	23	54.9	-0.8			25	215
								4224	NEASN4PB	1	23	-8.7	0.8			4	215
4147	CATSA4PT	23 1	1.027	-8.6	0.0 0.0	8.6 1.7	0.0 0.0										
								3313	CATSA5GR	1	21	-50.4	37.2	1.000LK		41	150
								3313	CATSA5GR	2	21	-50.9	37.6			41	150
								4128	LYNNE4PT	1	23	43.4	-15.3			26	174
								4151	TCEMT2PT	1	23	15.7	-4.8	1.000UN		32	50
								4161	E21TP4PT	1	23	28.5	-24.8			21	174
								4194	AGR W4PT	1	23	1.5	-6.6			5	141
								4198	CHER 4PT 138	1	23	5.2	-16.7			10	174
								4202	OWASS4PT	1	23	-1.5	-8.2			6	145

PTI INTERACTIVE POWER SYSTEM SIMULATOR--PSS/E   WED, JUL 30 1986 12:59
12-85 1988 APR 100 BASE   GROUP B
GB89APR, SPRING, NO.2, CASE5

FROM BUS	NAME	AREA ZONE	VOLT PU/KV	ANGLE	GEN MW/MVAR	LOAD MW/MVAR	SHUNT MW/MVAR	TO BUS	NAME	CKT	AREA	MW	MVAR	TRANSFORMER RATIO	ANGLE	RATING %I	MVA
4163	ONETA4PT	23 1	1.049	-8.5	0.0 0.0	16.6 3.4	0.0 0.0										
								4125	B101S4PT	1	30	39.8	19.1			15	287
								4126	B101N4PT	1	30	41.8	24.1			21	215
								4142	BARR 4PT	1	30	33.2	21.3			17	215
								4143	BARRS4PT	1	30	10.9	45.8			21	215
								4164	ONETA7PT	1	23	-142.3	-113.7	1.079LK		35	500
4140	RIVSD4PT	23 1	1.035	-9.7	100.0 54.7R	0.0 0.0	0.0 0.0										
								3134	WELEETK4	1	15	65.0	-10.5			58	110
								3948	BEE 4	1	22	149.0	39.2			63	237
								4114	WEKWA4PT	1	23	-1.1	-0.8			1	215
								4116	JENKS4PT	1	30	14.9	6.6			7	215
								4124	B111-4PT	1	30	-38.7	-17.0			14	287
								4139	RIVSD7PT	1	23	-167.4	7.7	1.025LK		32	500
								4145	TPS 4PT	1	23	17.9	5.9			8	215
								4208	ORU W4PT	1	30	-17.3	10.4			6	344
								4212	ORU E4PT	1	23	-7.2	13.0			4	344
								4269	OKMUL4PE	1	23	84.7	0.1			38	215
4114	WEKWA4PT	23 1	1.035	-9.7	0.0 0.0	1.0 0.2	0.0 0.0										
								3128	KEYSTON4	1	15	43.0	-10.0			27	160
								4112	WEKWA7PT	1	23	-126.7	-13.0	1.025LK		25	500
								4140	RIVSD4PT	1	23	1.1	-1.9			1	215
								4172	SSPRS4PT	1	23	62.8	14.4			27	229
								4180	WEDTP4PT	1	23	39.0	7.7			17	229
								4210	TNTAP4PT	1	23	-20.2	2.6			9	229
4174	TULSN4PT	23 1	1.035	-8.7	0.0 0.0	7.0 1.3	0.0 0.0										
								4196	HARVE4PT	1	23	37.0	8.2			23	160
								4197	N46W 4PT	1	23	15.1	1.9			9	160
								4198	CHER 4PT 138	1	23	-3.0	14.9			8	174
								4203	OWSAN4PT	1	23	-5.6	2.0			3	186
								4210	TNTAP4PT	1	23	27.5	-4.2			14	186
								4211	TULSN7PT	1	23	-124.2	-24.0	1.025LK		24	500
								4216	BARNS4PB	1	23	55.0	-0.8			25	215
								4224	NEASN4PB	1	23	-8.7	0.8			4	215
4147	CATSA4PT	23 1	1.027	-8.4	0.0 0.0	8.6 1.7	0.0 0.0										
								3313	CATSA5GR	1	21	-49.8	37.1	1.000LK		40	150
								3313	CATSA5GR	2	21	-50.3	37.5			41	150
								4128	LYNNE4PT	1	23	42.1	-15.2			25	174
								4151	TCEMT2PT	1	23	15.7	-4.8	1.000UN		32	50
								4161	E21TP4PT	1	23	27.9	-24.7			21	174
								4194	AGR W4PT	1	23	1.7	-6.6			5	141
								4198	CHER 4PT 138	1	23	5.4	-16.7			10	174
								4202	OWASS4PT	1	23	-1.3	-8.2			6	145

PTI INTERACTIVE POWER SYSTEM SIMULATOR--PSS/E   THU. JUL 31 1986   10:04
12-85 1988 APR 100 BASE   GROUP B
GB88APR. SPRING, NO.2, CASE6

FROM BUS	NAME	AREA ZONE	VOLT PU/KV	ANGLE	GEN MW/MVAR	LOAD MW/MVAR	SHUNT MW/MVAR	TO BUS	NAME	CKT	AREA	MW	MVAR	TRANSFORMER RATIO	ANGLE	RATING %I	MVA
4163	ONETA4PT	23 1	1.049	-8.2	0.0 0.0	16.6 3.4	0.0 0.0	4125	B101S4PT	1	30	39.7	19.2			15	287
								4126	B101N4PT	1	30	40.8	24.2			21	215
								4142	BARR 4PT	1	30	32.2	21.4			17	215
								4143	BARRS4PT	1	30	10.3	45.7			21	215
								4164	ONETA7PT	1	23	-139.6	-113.9	1.079LK		34	500
4140	RIVSD4PT	23 1	1.035	-9.4	100.0 53.4R	0.0 0.0	0.0 0.0	3134	WELEETK4	1	15	-65.6	-10.6			58	110
								3948	BEE 4	1	22	149.4	39.2			63	237
								4114	WEKWA4PT	1	23	-0.9	-0.8			1	215
								4116	JENKS4PT	1	30	13.8	6.5			7	215
								4124	B111-4PT	1	30	-39.1	-17.1			14	287
								4139	RIVSD7PT	1	23	-163.8	7.2	1.025LK		32	500
								4145	TPS 4PT	1	23	17.0	5.8			8	215
								4208	ORU W4PT	1	30	-18.4	10.3			6	344
								4212	ORU E4PT	1	23	-9.1	12.9			4	344
								4269	OKMUL4PE	1	23	85.3	0.1			38	215
4114	WEKWA4PT	23 1	1.035	-9.4	0.0 0.0	1.0 0.2	0.0 0.0	3128	KEYSTON4	1	15	43.5	-10.0			27	160
								4112	WEKWA7PT	1	23	-125.6	-13.1	1.025LK		24	500
								4140	RIVSD4PT	1	23	0.9	-1.8			1	215
								4172	SSPRS4PT	1	23	61.8	14.5			27	229
								4180	WEDTP4PT	1	23	38.5	7.8			17	229
								4210	TNTAP4PT	1	23	-20.0	2.5			8	229
4174	TULSN4PT	23 1	1.035	-8.4	0.0 0.0	7.0 1.3	0.0 0.0	4196	HARVE4PT	1	23	36.8	8.2			23	160
								4197	N46W 4PT	1	23	15.1	1.9			9	160
								4198	CHER 4PT 138	1	23	-3.7	14.9			9	174
								4203	OWSAN4PT	1	23	-5.6	2.1			3	186
								4210	TNTAP4PT	1	23	27.3	-4.2			14	186
								4211	TULSN7PT	1	23	-123.3	-24.1	1.025LK		24	500
								4216	BARNS4PB	1	23	55.2	-0.8			25	215
								4224	NEASN4PB	1	23	-8.7	0.8			4	215
4147	CATSA4PT	23 1	1.028	-8.1	0.0 0.0	8.6 1.7	0.0 0.0	3313	CATSA5GR	1	21	-48.6	36.9	1.000LK		40	150
								3313	CATSA5GR	2	21	-49.1	37.3			40	150
								4128	LYNNE4PT	1	23	40.7	-15.0			24	174
								4151	TCEMT2PT	1	23	15.7	-4.9	1.000UN		32	50
								4161	E21TP4PT	1	23	25.4	-24.6			20	174
								4194	AGR W4PT	1	23	2.1	-6.6			5	141
								4198	CHER 4PT 138	1	23	6.1	-16.7			10	174
								4202	OWASS4PT	1	23	-0.9	-8.1			5	145

FROM BUS	NAME	AREA ZONE	VOLT PU/KV	ANGLE	GEN MW/MVAR	LOAD MW/MVAR	SHUNT MW/MVAR	TO BUS	NAME	CKT	AREA	MW	MVAR	TRANSFORMER RATIO	ANGLE	RATING %I	MVA
4163	ONETA4PT	23	1.049	-8.6	0.0	16.6	0.0										
		1			0.0	3.4	0.0	4125	B101S4PT	1	30	40.0	19.0			15	287
								4126	B101N4PT	1	30	42.6	24.0			22	215
								4142	BARR 4PT	1	30	33.9	21.3			18	215
								4143	BARRS4PT	1	30	10.0	45.9			21	215
								4164	ONETA7PT	1	23	-143.2	-113.6	1.079LK		35	500
4140	RIVSD4PT	23	1.035	-9.8	100.0	0.0	0.0										
		1			55.4R	0.0	0.0	3134	WELEETK4	1	15	64.7	-10.4			58	110
								3948	BEE 4	1	22	148.8	39.2			63	237
								4114	WEKWA4PT	1	23	-1.4	-0.7			1	215
								4116	JENKS4PT	1	30	15.2	6.6			7	215
								4124	B111 4PT	1	30	-39.9	-16.9			15	287
								4139	RIVSD7PT	1	23	-169.3	7.9	1.025LK		33	500
								4145	TPS 4PT	1	23	18.1	6.0			9	215
								4208	ORU W4PT	1	30	-15.1	10.5			5	344
								4212	ORU E4PT	1	23	-5.4	13.2			4	344
								4269	OKMUL4PE	1	23	84.4	0.1			38	215
4114	WEKWA4PT	23	1.035	-9.8	0.0	1.0	0.0										
		1			0.0	0.2	0.0	3128	KEYSTON4	1	15	42.8	-9.9			27	160
								4112	WEKWA7PT	1	23	-127.4	-12.9	1.025LK		25	500
								4140	RIVSD4PT	1	23	1.4	-2.0			1	215
								4172	SSPRS4PT	1	23	63.3	14.3			27	229
								4180	WEDTP4PT	1	23	39.4	7.7			17	229
								4210	TNTAP4PT	1	23	-20.5	2.6			9	229
4174	TULSN4PT	23	1.035	-8.8	0.0	7.0	0.0										
		1			0.0	1.3	0.0	4196	HARVE4PT	1	23	36.9	8.2			23	160
								4197	N46W 4PT	1	23	15.2	1.9			9	160
								4198	CHER 4PT 138	1	23	-3.0	14.9			8	174
								4203	OWSAN4PT	1	23	-5.7	2.1			3	186
								4210	TNTAP4PT	1	23	27.8	-4.3			15	186
								4211	TULSN7PT	1	23	-124.2	-24.0	1.025LK		24	500
								4216	BARNS4PB	1	23	55.0	-0.8			25	215
								4224	NEASN4PB	1	23	-8.8	0.8			4	215
4147	CATSA4PT	23	1.027	-8.5	0.0	8.6	0.0										
		1			0.0	1.7	0.0	3313	CATSA5GR	1	21	-50.1	37.1	1.000LK		40	150
								3313	CATSA5GR	2	21	-50.6	37.6			41	150
								4128	LYNNE4PT	1	23	43.8	-15.3			26	174
								4151	TCEMT2PT	1	23	15.7	-4.8	1.000UN		32	50
								4161	E211P4PT	1	23	27.0	-24.7			20	174
								4194	AGR W4PT	1	23	1.6	-6.6			5	141
								4198	CHER 4PT 138	1	23	5.5	-16.7			10	174
								4202	OWASS4PT	1	23	-1.4	-8.2			6	145

FROM BUS	NAME	AREA ZONE	VOLT PU/KV	ANGLE	GEN MW/MVAR	LOAD MW/MVAR	SHUNT MW/MVAR	TO BUS	NAME	CKT	AREA	MW	MVAR	TRANSFORMER RATIO	ANGLE	RATING %I	MVA
4163	ONETA4PT	23	1.048	-8.8	0.0	16.6	0.0										
		1			0.0	3.4	0.0	4125	B101S4PT	1	30	40.0	18.9			15	287
								4126	B101N4PT	1	30	43.0	24.0			22	215
								4142	BARR 4PT	1	30	35.2	21.3			18	215
								4143	BARRS4PT	1	30	10.2	45.9			21	215
								4164	ONETA7PT	1	23	-145.0	-113.5	1.079LK		35	500
4140	RIVSD4PT	23	1.035	-10.1	100.0	0.0	0.0										
		1			56.4R	0.0	0.0	3134	WELEETK4	1	15	64.3	-10.3			57	110
								3948	BEE 4	1	22	148.5	39.2			63	237
								4114	WEKWA4PT	1	23	-1.7	-0.7			1	215
								4116	JENKS4PT	1	30	16.2	6.7			8	215
								4124	B111-4PT	1	30	-39.9	-16.8			15	287
								4139	RIVSD7PT	1	23	-171.9	8.2	1.025LK		33	500
								4145	TPS 4PT	1	23	18.8	6.0			9	215
								4208	ORU W4PT	1	30	-14.6	10.6			5	344
								4212	ORU E4PT	1	23	-3.6	13.4			4	344
								4269	OKMUL4PE	1	23	84.0	0.1			38	215
4114	WEKWA4PT	23	1.035	-10.0	0.0	1.0	0.0										
		1			0.0	0.2	0.0	3128	KEYSTON4	1	15	42.5	-10.0			26	160
								4112	WEKWA7PT	1	23	-128.2	-12.9	1.025LK		25	500
								4140	RIVSD4PT	1	23	1.7	-2.0			1	215
								4172	SSPRS4PT	1	23	64.1	14.3			28	229
								4180	WEDTP4PT	1	23	39.8	7.7			17	229
								4210	TNTAP4PT	1	23	-20.7	2.7			9	229
4174	TULSN4PT	23	1.035	-9.0	0.0	7.0	0.0										
		1			0.0	1.3	0.0	4196	HARVE4PT	1	23	37.0	8.2			23	160
								4197	N46W 4PT	1	23	15.2	1.9			9	160
								4198	CHER 4PT 138	1	23	-2.6	14.9			8	174
								4203	OWSAN4PT	1	23	-5.7	2.0			3	186
								4210	TNTAP4PT	1	23	28.0	-4.3			15	186
								4211	TULSN7PT	1	23	-124.9	-24.0	1.025LK		25	500
								4216	BARNS4PB	1	23	54.8	-0.8			25	215
								4224	NEASN4PB	1	23	-8.8	0.8			4	215
4147	CATSA4PT	23	1.027	-8.7	0.0	8.6	0.0										
		1			0.0	1.7	0.0	3313	CATSA5GR	1	21	-51.0	37.3	1.000LK		41	150
								3313	CATSA5GR	2	21	-51.5	37.7			41	150
								4128	LYNNE4PT	1	23	45.6	-15.4			27	174
								4151	TCEMT2PT	1	23	15.6	-4.8	1.000UN		32	50
								4161	E21TP4PT	1	23	28.0	-24.9			21	174
								4194	AGR W4PT	1	23	1.3	-6.6			5	141
								4198	CHER 4PT 138	1	23	5.0	-16.7			10	174
								4202	OWASS4PT	1	23	-1.7	-8.2			6	145

FROM BUS	NAME	AREA ZONE	VOLT PU/KV	ANGLE	GEN MW/MVAR	LOAD MW/MVAR	SHUNT MW/MVAR	TO BUS	NAME	CKT	AREA	MW	MVAR	TRANSFORMER RATIO	ANGLE	RATING XI	MVA
4163	ONETA4PT	23 1	1.048	-8.8	0.0 0.0	16.6 3.4	0.0 0.0	4125	B101S4PT	1	30	39.9	18.9			15	287
								4126	B101N4PT	1	30	43.3	24.0			22	215
								4142	BARR 4PT	1	30	34.9	21.3			18	215
								4143	BARRS4PT	1	30	9.9	45.9			21	215
								4164	ONETA7PT	1	23	-144.6	-113.5	1.079LK		35	500
4140	RIVSD4PT	23 1	1.035	-10.0	100.0 56.3R	0.0 0.0	0.0 0.0	3134	WELEETK4	1	15	64.4	-10.3			57	110
								3948	BEE 4	1	22	148.5	39.2			63	237
								4114	WEKWA4PT	1	23	-1.6	-0.7			1	215
								4116	JENKS4PT	1	30	16.1	6.7			8	215
								4124	B111-4PT	1	30	-39.8	-16.8			15	287
								4139	RIVSD7PT	1	23	-171.3	8.2	1.025LK		33	500
								4145	TPS 4PT	1	23	18.6	6.0			9	215
								4208	ORU W4PT	1	30	-15.7	10.6			5	344
								4212	ORU E4PT	1	23	-3.4	13.4			4	344
								4269	OKMUL4PE	1	23	84.1	0.1			38	215
4114	WEKWA4PT	23 1	1.035	-9.9	0.0 0.0	1.0 0.2	0.0 0.0	3128	KEYSTON4	1	15	42.5	-9.9			26	160
								4112	WEKWA7PT	1	23	-128.1	-12.9	1.025LK		25	500
								4140	RIVSD4PT	1	23	1.6	-2.0			1	215
								4172	SSPRS4PT	1	23	63.9	14.3			28	229
								4180	WEDTP4PT	1	23	39.7	7.7			17	229
								4210	TNTAP4PT	1	23	-20.6	2.7			9	229
4174	TULSN4PT	23 1	1.035	-8.9	0.0 0.0	7.0 1.3	0.0 0.0	4196	HARVE4PT	1	23	37.0	8.2			23	160
								4197	N46W 4PT	1	23	15.2	1.9			9	160
								4198	CHER 4PT 138	1	23	-2.7	14.9			8	174
								4203	OWSAN4PT	1	23	-5.7	2.0			3	186
								4210	TNTAP4PT	1	23	27.9	-4.3			15	186
								4211	TULSN7PT	1	23	-124.7	-24.0	1.025LK		25	500
								4216	BARNS4PB	1	23	54.9	-0.8			25	215
								4224	NEASN4PB	1	23	-8.8	0.8			4	215
4147	CATSA4PT	23 1	1.027	-8.7	0.0 0.0	8.6 1.7	0.0 0.0	3313	CATSA5GR	1	21	-50.8	37.2	1.000LK		41	150
								3313	CATSA5GR	2	21	-51.3	37.6			41	150
								4128	LYNNE4PT	1	23	45.3	-15.4			27	174
								4151	TCEMT2PT	1	23	15.7	-4.8	1.000UN		32	50
								4161	E21TP4PT	1	23	27.7	-24.8			21	174
								4194	AGR W4PT	1	23	1.4	-6.6			5	141
								4198	CHER 4PT 138	1	23	5.1	-16.7			10	174
								4202	OWASS4PT	1	23	-1.6	-8.2			6	145

PTI INTERACTIVE POWER SYSTEM SIMULATOR--PSS/E   THU, JUL 31 1986 15:51
12-85 1988 APR 100 BASE   GROUP B
GB88APR, SPRING, NO.2, CASE10

FROM BUS	NAME	AREA ZONE	VOLT PU/KV	ANGLE	GEN MW/MVAR	LOAD MW/MVAR	SHUNT MW/MVAR	TO BUS	NAME	CKT	AREA	MW	MVAR	TRANSFORMER RATIO	ANGLE	RATING %I	MVA
4163	ONETA4PT	23	1.048	-8.8	0.0	16.6	0.0										
		1			0.0	3.4	0.0	4125	B101S4PT	1	30	40.2	18.9			15	287
								4126	B101N4PT	1	30	43.9	24.0			22	215
								4142	BARR 4PT	1	30	35.2	21.3			18	215
								4143	BARRS4PT	1	30	9.1	46.0			21	215
								4164	ONETA7PT	1	23	-145.1	-113.5	1.079LK		35	500
4140	RIVSD4PT	23	1.035	-10.1	100.0	0.0	0.0										
		1			56.7R	0.0	0.0	3134	WELEETK4	1	15	64.3	-10.3			57	110
								3948	BEE 4	1	22	148.4	39.2			63	237
								4114	WEKWA4PT	1	23	-1.7	-0.6			1	215
								4116	JENKS4PT	1	30	16.5	6.7			8	215
								4124	B111-4PT	1	30	-40.1	-16.8			15	287
								4139	RIVSD7PT	1	23	-172.1	8.3	1.025LK		33	500
								4145	TPS 4PT	1	23	18.9	6.1			9	215
								4208	ORU W4PT	1	30	-15.4	10.6			5	344
								4212	ORU E4PT	1	23	-2.7	13.4			4	344
								4269	OKMUL4PE	1	23	83.9	0.1			38	215
4114	WEKWA4PT	23	1.035	-10.0	0.0	1.0	0.0										
		1			0.0	0.2	0.0	3128	KEYSTON4	1	15	42.4	-9.9			26	160
								4112	WEKWA7PT	1	23	-128.4	-12.8	1.025LK		25	500
								4140	RIVSD4PT	1	23	1.7	-2.0			1	215
								4172	SSPRS4PT	1	23	64.2	14.3			28	229
								4180	WEDTP4PT	1	23	39.9	7.7			17	229
								4210	TNTAP4PT	1	23	-20.8	2.7			9	229
4174	TULSN4PT	23	1.035	-9.0	0.0	7.0	0.0										
		1			0.0	1.3	0.0	4196	HARVE4PT	1	23	36.9	8.2			23	160
								4197	N46W 4PT	1	23	15.2	1.9			9	160
								4198	CHER 4PT 138	1	23	-2.7	14.9			8	174
								4203	OWSAN4PT	1	23	-5.8	2.0			3	186
								4210	TNTAP4PT	1	23	28.1	-4.3			15	186
								4211	TULSN7PT	1	23	-124.7	-24.0	1.025LK		25	500
								4216	BARNS4PB	1	23	54.8	-0.8			25	215
								4224	NEASN4PB	1	23	-8.9	0.8			4	215
4147	CATSA4PT	23	1.027	-8.7	0.0	8.6	0.0										
		1			0.0	1.7	0.0	3313	CATSA5GR	1	21	-50.9	37.3	1.000LK		41	150
								3313	CATSA5GR	2	21	-51.4	37.7			41	150
								4128	LYNNE4PT	1	23	46.2	-15.4			27	174
								4151	TCEMT2PT	1	23	15.6	-4.8	1.000UN		32	50
								4161	E21TP4PT	1	23	27.0	-24.8			21	174
								4194	AGR W4PT	1	23	1.4	-6.6			5	141
								4198	CHER 4PT 138	1	23	5.2	-16.7			10	174
								4202	OWASS4PT	1	23	-1.6	-8.2			6	145

2

VITA

Ward Thomas Jewell

Candidate for the Degree of

Doctor of Philosophy

Thesis: THE EFFECTS OF MOVING CLOUD SHADOWS ON ELECTRIC UTILITIES WITH DISPERSED SOLAR PHOTOVOLTAIC GENERATION

Major Field: Electrical Engineering

Biographical:

Personal Data: Born May 13, 1957, in Tulsa, Oklahoma, to Joseph and Catherine Jewell. Married to Ginna Krietmeyer on December 29, 1979. Two children, Jeremy Nathan, born July 7, 1984, and Joshua Isaac, born May 17, 1986.

Education: Graduated from Thomas A. Edison High School, Tulsa, Oklahoma, in May, 1975; received Bachelor of Science Degree in Electrical Engineering from Oklahoma State University in May, 1979; received Master of Science Degree from Michigan State University in August, 1980; completed requirements for the Doctor of Philosophy Degree at Oklahoma State University in December, 1986.

Professional Experience: Research Associate, Oak Ridge National Laboratory, Oak Ridge, Tennessee, October, 1980, to January, 1984; Instructor, School of Electrical and Computer Engineering, Oklahoma State University, January, 1984 to present.